FINAL REPORT

AIR FORCE OFFICE OF SCIENTIFIC RESEARCH

for

-C-

CONTRACT F 44620-68-0086

RESEARCH IN ATMOSPHERIC ACOUSTICS

SMU No. 80-36

Southern Methodist University
Dallas, Texas 75222
for
Department of Geological Sciences

13 July 1971

E. Herrin (ltr)
Eugene Herrin, Professor
Principal Investigator
A.C. 214-363-5611. ext. 602

DISCLAIMER NOTICE

THIS DOCUMENT IS THE BEST QUALITY AVAILABLE.

COPY FURNISHED CONTAINED A SIGNIFICANT NUMBER OF PAGES WHICH DO NOT REPRODUCE LEGIBLY.

UNCLASSIFIED
Security Classification

DOCUMENT CONTROL DATA - R & D

(Security classification of title, body of abstract and indexing annotation must be entered when the overall report is classified)

1. ORIGINATING ACTIVITY (Corporate author)
Southern Methodist University
Dept. of Geological Sciences
Dallas, Texas 75222

2a. REPORT SECURITY CLASSIFICATION
UNCLASSIFIED

2b. GROUP

3. REPORT TITLE

RESEARCH IN ATMOSPHERIC ACOUSTICS

4. DESCRIPTIVE NOTES (Type of report and inclusive dates)
Scientific Final

5. AUTHOR(S) (First name, middle initial, last name)
Eugene T. Herrin
John A. McDonald
Gordon G. Sorrells
Eduard J. Douze
Zolton A. Der

6. REPORT DATE
13 July 1971

7a. TOTAL NO. OF PAGES
150

7b. NO. OF REFS
51

8a. CONTRACT OR GRANT NO.
Contract No. F 44620-68-0086-C

b. PROJECT NO.
AO 1152-5

c. 62701D

d.

9a. ORIGINATOR'S REPORT NUMBER(S)

9b. OTHER REPORT NO(S) (Any other numbers that may be assigned this report)

10. DISTRIBUTION STATEMENT

Approved for public release, distribution unlimited

11. SUPPLEMENTARY NOTES
TECH OTHER

12. SPONSORING MILITARY ACTIVITY
Air Force Office of Scientific Research
1400 Wilson Boulevard (NPG)
Arlington, Virginia 22209

13. ABSTRACT

This final report consists of eight published papers. They can be grouped under the following headings:

1. An engineering description of the digital system used for acquiring most of the infrasonic & seismic data used in this program.
2. Studies of atmospheric turbulence spectra, acoustic waves from atmospheric disturbances & means of reducing infrasonic "noise."
3. The relationships between long seismic noise & atmospheric pressure changes due to turbulence & due to infrasonic waves.

2

DD FORM 1 NOV 65 1473

UNCLASSIFIED
Security Classification

FINAL REPORT

Order Number: ARPA 1152, Amendment 5

Project Code Number: 62701 D

Name of Contractor: Southern Methodist University

Date of Contract: 4 March 1970

Amount of Contract: $118,642.00

Contract Number: F44620-68-0086

Contract Termination Date: 4 March 1971

University Account No. 80-36

Principal Investigator: Eugene Herrin

Title of Work: Research in Atmospheric Acoustics

INTRODUCTION

This study of infrasonic signals and noise was undertaken in cooperation with our research group in seismology. Digital data acquisition equipment was used to record both infrasonic and long period seismic data, and the data processing programs for our XDS 925 system were common to both kinds of studies. The seismic systems mentioned in this report were provided by the Long Range Seismic Measurements Program (Project VELA UNIFORM) under a cooperative agreement between Southern Methodist University and Teledyne-Geotech. Out of this work has come an extensive library of computing programs, considerable experience in the handling of synoptic infrasonic and seismic information and the background knowledge needed to pursue further research in the acquisition, processing and interpretation of infrasonic data. The major technical accomplishments of this study are described in the 8 papers which comprise the following chapters of this report.

CONTENTS

The papers forming the contents of this final report have either been published, are in press or were presented at a professional scientific meeting.

THE STRUCTURE OF ATMOSPHERIC TURBULENCE AND ITS APPLICATION TO THE DESIGN OF PIPE ARRAYS

John A. McDonald

E. J. Douze

Eugene Herrin

(In press, Geophysical Journal R. A. S.)

Dallas Geophysical Laboratory
Southern Methodist University
Dallas, Texas 75222

S

SUMMARY

Turbulent boundary layers at the surface of the earth limit the detection of infrasonic waves with periods greater than one second. Pipe arrays designed to improve the signal-to-noise ratios of infrasonic waves usually assume that the background noise due to this turbulent boundary layer is incoherent between the array inlets. The power at various points on a surface was measured; coherences between these points were determined and they were found to be significant in the period range 1 to 100 sec. Such coherent noise must be considered when pipe arrays are designed.

INTRODUCTION

Infrasonic waves of periods greater than one second travel long distances due to low absorption and are, therefore, important in studies of the structure of the atmosphere. The detection of such waves is limited, however, by the presence of a turbulent boundary layer at the surface of the earth. The effects of such turbulent noise can be reduced by using multiple sampling pipe arrays as inlets to the pressure measuring transducers (Daniels 1959). A lack of statistical data on the nature of this turbulent boundary layer has hampered the design of pipe arrays. There have been investigations into the variations of turbulence with altitude (e.g. Davenport 1961) but few data are available for determinations of the horizontal structure of turbulence in the period range common to the periods of infrasonic waves.

The objective of the research presented here was to determine the power due to turbulence on a flat surface and then to find the coherence between these points as a function of distance of separation, confining the observations and results to the period range 1-100 sec. This information was then used to design pipe arrays with optimum signal-to-noise ratios.

In our studies we used as the source of turbulence the steady prevailing wind of high summer in North Texas. Velocities were determined from cross-spectra and these clearly indicated that the turbulence travelled at the velocity of the wind as determined by an anemometer. The coherence fell rapidly with increasing distance and we concluded that the power levels were associated with the wind derived turbulence and not with propagating signals.

EXPERIMENTAL CONDITIONS

Priestley (1966) has performed one of the few investigations of the structure of atmospheric turbulence in the period range 1 to 100 sec. The present investigation was intended, initially, to repeat and extend that of Priestley, but, as will be shown later, different criteria were used in the selection of the data.

At the height of summer in North Texas the weather conditions afford air flows which are stable in velocity and direction. During the period June through August when the data were collected the prevailing wind was of almost constant velocity from the north-north-west. A site was chosen on the campus of the University of Texas at Dallas which provided virtually uninterrupted passage of air flow from the prevailing direction. All major obstructions were a hundred or more meters to the south of the pressure detecting transducers.

The recording trailer was placed about 80m east-south-east of the transducers, and the wind speed and direction were measured at the trailer at a height of 7m above the ground.

EXPERIMENTAL SYSTEM

The transducers used for measuring the pressure variations were NBS, Model N3 designed and built by the National Bureau of Standards. These microphones have been explained in principle by Priestley (1966) and in detail by Herrin et al. (1971). The electrical analog of the transducer is shown in figure 1.

The data from these transducers were digitized and recorded on punched paper tape at a rate of 5 samples per second. The sampling rate and the length of rolls of paper tape restricted the data samples to maximum of about 40 minutes.

The input to the system can be a pipe array or a single tube, the length and internal diameter of which determine its resistance. In the present research the input resistance was chosen so that the time constant of its combination with the fore-volume approximated to that used by Priestley (1966). To ensure that the sampling point was remote from any turbulence due to the microphone can, 50 ft. of thick walled garden hose was attached to each inlet, the open end of the hose was then the effective inlet to the microbarograph system. The overall system response is shown in figure 2.

Samples of data were taken with the three inlets tied together and in the same plane; coherence measurements were very nearly 1.0 over the period range of interest. Phase measurements indicated that the three microphones could be considered to be identical within the limits of experimental error.

DATA ACQUISITION & PROCESSING

Data were taken with the wind blowing along the line of microbarograph inlets and for the wind blowing perpendicular to the line of inlets. The wind speed and direction were not recorded continuously but measurements were taken at a number of times during a run. During a typical run the wind speed was sampled at 30 second intervals, resulting in a mean speed of 2.68m/sec with a standard deviation of 1.07m/sec.

The data were processed on an XDS 925 computer. The punched paper tapes were transferred to magnetic tape and a computer program was written to enable the latter to be viewed in analog form on a display oscilloscope. If digitizing errors were seen to seriously affected the data, the data were rejected. If an error was minor, such as an occasional drop-out, another program removed them and wrote an error free edited tape. The latter was used as the input to the Spectra and cross-spectra programs.

Although auto-and cross-correlations may be calculated before transformation into the frequency domain, the fast Fourier transform (Cooley & Tukey, 1965) provides a more efficient method. The spectra may be estimated by transforming the digital time series into the frequency domain and then smoothing the data in a suitable manner.

The method used in this research is outlined below and is described in detail by Welch (1967).

The data are divided into M segments, each segment being identified by a subscript from 1 to M. Each segment consisting of K data points, is transformed into the frequency domain by the use of the fast Fourier transform

$$S_m(f) = \sum_{k=0}^{K-1} t_m(k) \exp\left\{\frac{-2\pi i k f}{K}\right\}.$$

The spectral estimates are then computed by averaging over the number of segments (M)

$$\hat{P}_{mn}(f) = \frac{1}{M} \sum_{j=1}^{M} S_{mj}(f) . S_{nj}^{*}(f),$$

where the P_{nn} are the estimates of the spectra of the multiple time series and the P_{mn} are the cross-spectra. The star indicates the complex conjugate.

It can be shown that the bias in the estimates of P_{mn} (f) depend directly on the time lag between sensors caused by the

travel time of the noise. The time segment chosen to be transformed must be large compared to the probable time lag and in the present analysis the lag did not exceed 5 percent of the total segment. It should be noted that this problem is not caused by the method used; when the cross-spectra are computed by the indirect method the cross-correlation must be calculated for lags well beyond the peak in the cross-correlation.

The number of segments used determines the reliability of the results, for example, averaging over 10 segments is equivalent to taking 10 percent lags using the auto-correlation method. The number of segments used in the present research varied between 12 and 20 depending on the amount of data that were available. The length of the data samples were limited by the physical length of a roll of paper tape. This in turn limited the analysis to periods of less than about 100 secs.

The relative power of the background noise for two different wind velocities is shown in figure 3. It will be seen that the power increased by a factor of approximately 10 when the wind velocity almost doubled, and that this increase in power is independent of the period. It is not known if this simple relationship

extends to a greater range of wind velocities as data were not obtained for higher wind velocities. Figure 4 shows the coherence of the noise and its relationship to the microphone spacings for wind parallel to the line of the microphones. The coherence, $K_{mn}(f)$, is defined in this paper as,

$$K_{mn}(f) = \frac{|C_{mn}(f) + jQ_{mn}(f)|^2}{P_{mm}(f) \cdot P_{nn}(f)},$$

where $C_{mn}(f)$ is the cospectral density,

$$C_{mn}(f) = Re\,(P_{mn}(f)),$$

and $Q_{mn}(f)$ is the guadrature spectral density

$$Q_{mn}(f) = -Im\,(P_{mn}(f))$$

(Robinson, 1967). The $P_{mm}(f)$ are then the spectral densities and $P_{nm}(f)$ the cross spectral densities.

In figures 4 and 5 the coherence is not plotted when the values fall below the expected zero coherence level.

It will be seen that the coherence decreases rapidly for increasing separation of the microphones and the decrease is even more rapid when the microphones are perpendicular to the direction of the wind (fig. 5). Apparently the turbulent cells that are the source of the wind-generated noise change very rapidly as they migrate downwind.

Priestley (1966) also studied the spatial organization of the noise for periods of less than 100 sec. A comparison of the two sets of data shows that in both cases the coherence of the noise falls off rapidly at shorter periods; however, Priestley shows a less rapid decrease in coherence with increasing distance of separation. At a separation of 30m or more we find that the coherence at a period of 10 sec. is essentially zero, while Priestley still shows a measurable coherence of greater than 0.2. In general, the overall shapes of the curves are similar but Priestley shows a greater coherence at all spacings and at all periods.

The difference in the results appears to come about because of a difference in methods used to select the data. Priestley (1969, personal communication) monitored the wind speed and direction until very stable conditions were obtained. In our work data were taken during periods when the wind conditions were reasonably constant. Thus the results presented by Priestley (1966) may well constitute an upper bound on the spatial coherences to be expected from wind generated infrasonic noise, while the coherences presented in this paper are more representative of average field conditions.

The phase angles obtained from individual cross-spectra are a measure of the velocity at which the coherent fraction of the

noise travelled between inlets. Knowing the distance between inlets the apparent velocity of the noise can thus be calculated. Table 1 shows an example of the results obtained with the wind vector parallel to and perpendicular to the direction between inlets. At those periods where the coherence fell below 0.1 the velocity could not be calculated and the appropiate space has been left blank in the table. The results show that the noise is travelling at the same velocity as the wind for the inlets parallel to the wind vector. The velocities calculated perpendicular to the wind vector show the expected large apparent velocities. The large variations in velocity are caused primarily by fluctuations in the spectral estimates. A few degrees of change in the estimated phase angle is sufficient to cause the variations.

These measurements indicate that the infrasonic noise field was almost entirely wind-generated. However, other types of noise may sometimes be present, and they may be dependent on the locality and season.

In the period range 1-100 sec wind-generated disturbances are the dominant cause of background noise and the noise power is directly related to the wind velocity. Other sources of noise can be identified only under rather unusual circumstances. For example

microbaroms, similar in period to the well known 6 to 8 sec microseisms, can sometimes be identified, (e.g. Donn, and Posmentier, 1969). But almost always the operational sensitivity of a microbarograph system is limited by wind-generated noise.

In review and long after this paper was first written, it has been suggested that the data presented in figures 4 and 5 may be partially invalid due to a statistical uncertainty in the stationarity of them. Recent research for a paper now in preparation has indicated that the spectra are repeatable for similar wind speeds. The spectra shown in figure 6 are from longer data samples than those in figures 4 and 5 but we feel that the stationarity is proven.

PIPE ARRAYS

Pipe arrays have been used extensively in conjunction with microbarographs to improve the signal-to-noise ratio for acoustic-gravity waves (Daniels, 1959), under the assumption that the background noise is incoherent between the inlets. With this assumption and with a perfectly coherent signal, a signal-to-noise improvement equal to the square root of the number of inlets should be obtained. The experiments discussed in the preceding section indicate that some coherence in the background noise may exist between inlets in the period range 1 to 100 seconds; therefore, this coherence must be considered when the noise reducing properties of a pipe array are determined.

Except for the delay caused by the travel time in the pipe, the pipe array provides, at a single infrasonic microphone, the direct sum of sample points spread over a considerable area. Should the dimensions of the pipe array become an appreciable fraction of the signal wave-length; however, response to the signal is degraded. Thus, the maximum dimension of the pipe array is controlled by the shortest wave lengths of interest. On the other hand, if the pipe array is made small enough so that it does not degrade the shorter period signals, it will not be very effective

in improving the signal-to-noise ratio because of the high coherence of the noise.

In order to determine the response of different pipe arrays, a computer program was written to calculate the signal-to-noise ratio improvement. The signal was assumed to be perfectly coherent across the pipe array, and its amplitude was affected only by the time delays between inlets caused by the finite travel time of the wave and by the travel time within the pipe from the inlet to the microphone. A noise model was constructed based on the observed coherences and phase angles from field experiments which were presented in the preceding section of this paper.

The coherences between inlets for a longitudinal orientation to the wind vector can be expressed as

$$Coh_L(f, d) = \exp -2\alpha(f)\, d,$$

and for a transverse orientation as

$$Coh_T(f, d) = \exp -2\beta(f)\, d,$$

where d is the inlet spacing and f is the frequency. Basically the same expressions were used and theoretically justified by Priestley (1966). The value of the constants α and β were determined by a best least squares fit. The cross spectra can then

be expressed as

$$P_{mn}(f) = \exp -(\alpha d_x \cos\theta + \beta d_x \sin\theta) \cdot \exp -(2\pi i f d_x \cos\theta / v), \quad (1)$$

θ being the orientation with respect to the wind vector and v the wind velocity. The first exponential describes the effect of the loss of coherence between inlets and the second the effect of the time delay between inlets caused by the turbulence travelling at the wind velocity (Table 1). Equation 1 thus describes the normalized cross-spectra between inlets. By "normalized" we mean reduced to unit power in the auto-spectra. Knowing the auto and cross-spectra the complete spectral matrix can be computed. The array response is then simply the sum over all the inlets (n)

$$P_{total}(f) = \sum_{n=1}^{n} \sum_{m=1}^{m} P_{mn}(f).$$

It must be emphasized that the model is an idealized one using wind-generated noise. Ideally, the frequency-wave number spectrum for the pipe array should be computed, but because of the large number of inlets this approach is impractical.

The signal-to-noise ratios for a large number of pipe arrays were computed, and some typical examples are shown in figures 7, 8 and 9. Signal-to-noise ratio is defined as the maximum signal amplitude divided by the root mean square of the noise amplitude. Two important features are immediately evident from figure 7. Irrespective

of wind direction the signal is significantly degraded at periods below about 5 seconds, and this degradation effectively controls the signal-to-noise ratio. At perioc greater than 10 seconds the signal wave-length is large enough to eliminate any signal degradation and the signal-to-noise ratio is controlled by the high-in phase coherence of noise between inlets 5m apart.

In figure 6 can be seen the effectiveness of inlet spacing for three different signal periods. As would be expected the larger spacings are more suitable for the longer periods.

Figure 5 shows a comparison of pipe arrays of different configurations but of the same total overall length. It is evident that the dimensions of the pipe array control the signal-to-noise ratio, and not the overall pipe length. The larger is more effective at long periods and the smaller is more effective at shorter periods.

CONCLUSIONS

It is important that typical infrasonic noise fields should be considered in the design of pipe arrays. The data selection criteria used by Priestley (1966) tends to produce data that are more coherent than may be found in general. In the short period region (1-10 secs) optimal pipe arrays can be designed for the improvement of signal-to-noise ratios. As the wind generated noise is reduced with respect to the signal amplitude, the limiting noise may be due to 6 to 8 second microbaroms. Pipe arrays will have essentially no effect on this type of noise.

It would appear that the turbulence which is the cause of the background noise consists of turbulent cells of all dimensions. They contribute to the noise in relation to their size, the bigger cells causing the appreciable coherence at longer periods while the smaller cells contribute to the shorter period noise.

ACKNOWLEDGEMENTS

John L. Lobdell and Nancy Cunningham were responsible for the systems programming, Rick Arnett assisted with the field work and their help is greatly appreciated. The NBS transducers used in the experiments were on loan from the National Bureau of Standards. The research was carried out during the tenure of a National Aeronautics and Space Administration Traineeship by one of us (J. A. M.), and was supported by the Air Force Office of Scientific Research under Contract No. F44620-68-C-0086.

REFERENCES

Cooley, J. S. and J. W. Tukey, An algorithm for the machine calculation of complex Fourier series, Math. Computation, 19, 297-301, 1965.

Daniels, F. P., Noise reducing line microphone for frequencies below 1 cps. J. Acoust. Soc., 31, 4, 529-531, 1959.

Davenport, A. G., The spectrum of horizontal gustiness near the ground in high winds, Quart. J. Roy. Met. Soc., 87, 372, 194-211, 1961

Donn, W. L. and E. S. Posmentier, Infrasonic waves from the marine storm of April 7, 1966, J. Geophys. R., 72, 8, 2053-2061, 1967.

Herrin, E., J. A. McDonald and G. G. Sorrells, Data Acquistion Paper (Title to be determined; to be submitted for this edition of Geophysical Journal).

Priestley, J. T., Correlation studies of pressure fluctuations on the ground beneath a turbulent boundary layer, NBS Report 8942, U.S. Dept. of Commerce, National Bureau of Standards, 1966.

Robinson, E. A., Multichannel time series analysis with digital computer programs, Holden-Day, 298 p., 1967.

Welch, P. D., The use of fast Fourier transforms for the estimation of power spectra: a method based on time averaging over short modified periodograms, Trans. IEEE AU-15, 2, 70-73, 1967.

FIGURE CAPTIONS

1. Electrical analog of the transducer assembly.
2. Response of the microbarograph system.
3. The relative power of the background noise as a function of period and of wind velocity.
4. Coherence of the noise for wind parallel to the line of microbarographs.
5. Coherence of the noise for wind perpendicular to the line of microbarographs.
6. Illustrating the stationarity of the noise for three different 3-hour time periods with similar wind speeds.
7. Signal degradation and signal-to-noise ratio for a linear pipe array of length 300m with the transducer in the center and inlets at 5m intervals.
8. The effect of different inlet spacings for a linear array of length 150m with the transducer at one end.
9. A comparison between pipe arrays of the same total lengths but different configurations; inlets at 5m intervals.

TABLE CAPTION

1. Measured apparent velocities of the turbulent noise.

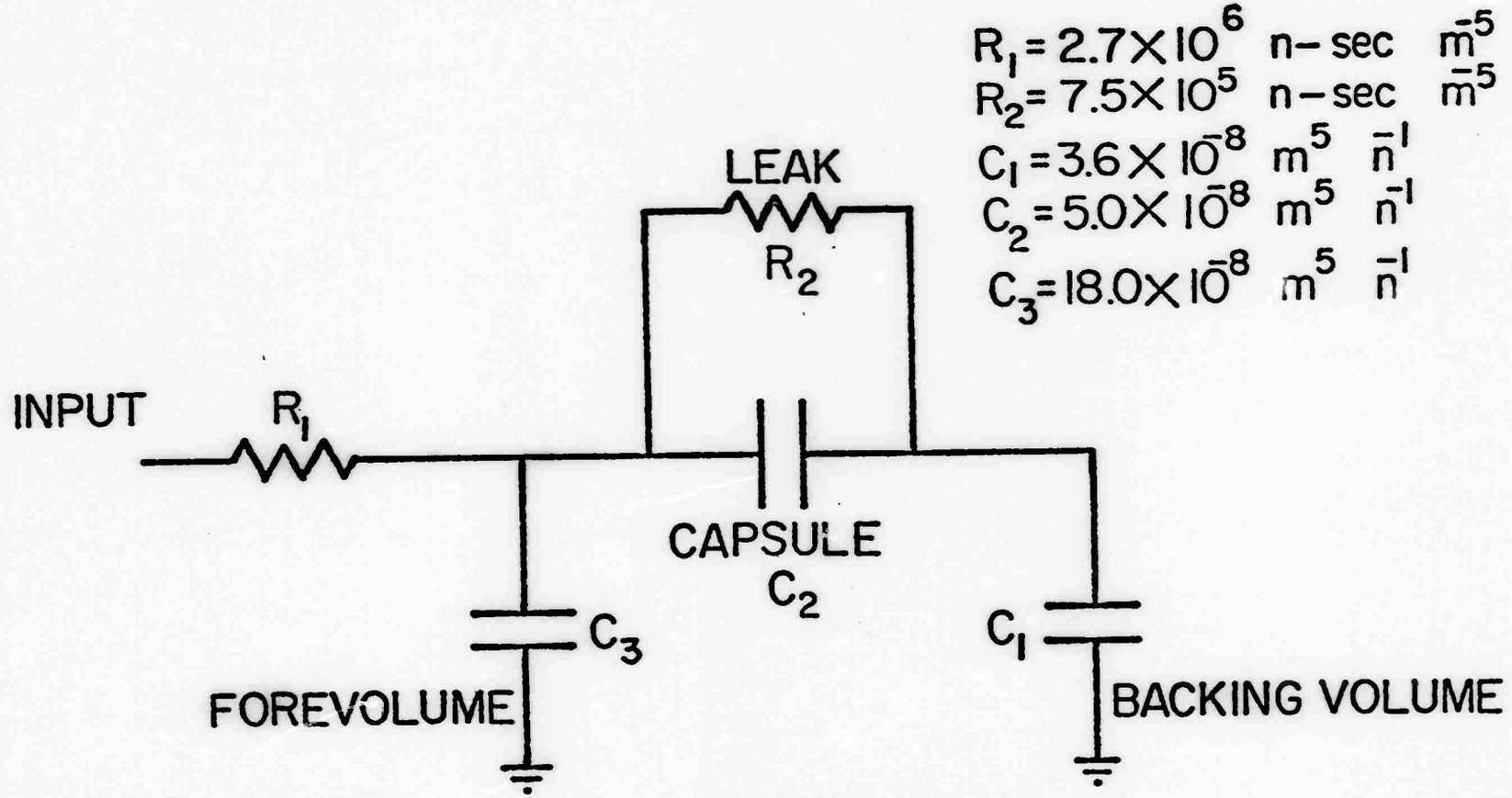
$R_1 = 2.7 \times 10^6$ n-sec m^{-5}
$R_2 = 7.5 \times 10^5$ n-sec m^{-5}
$C_1 = 3.6 \times 10^{-8}$ m^5 n^{-1}
$C_2 = 5.0 \times 10^{-8}$ m^5 n^{-1}
$C_3 = 18.0 \times 10^{-8}$ m^5 n^{-1}
LEAK
R_2
INPUT
R_1
CAPSULE
C_2
C_3
FOREVOLUME
C_1
BACKING VOLUME

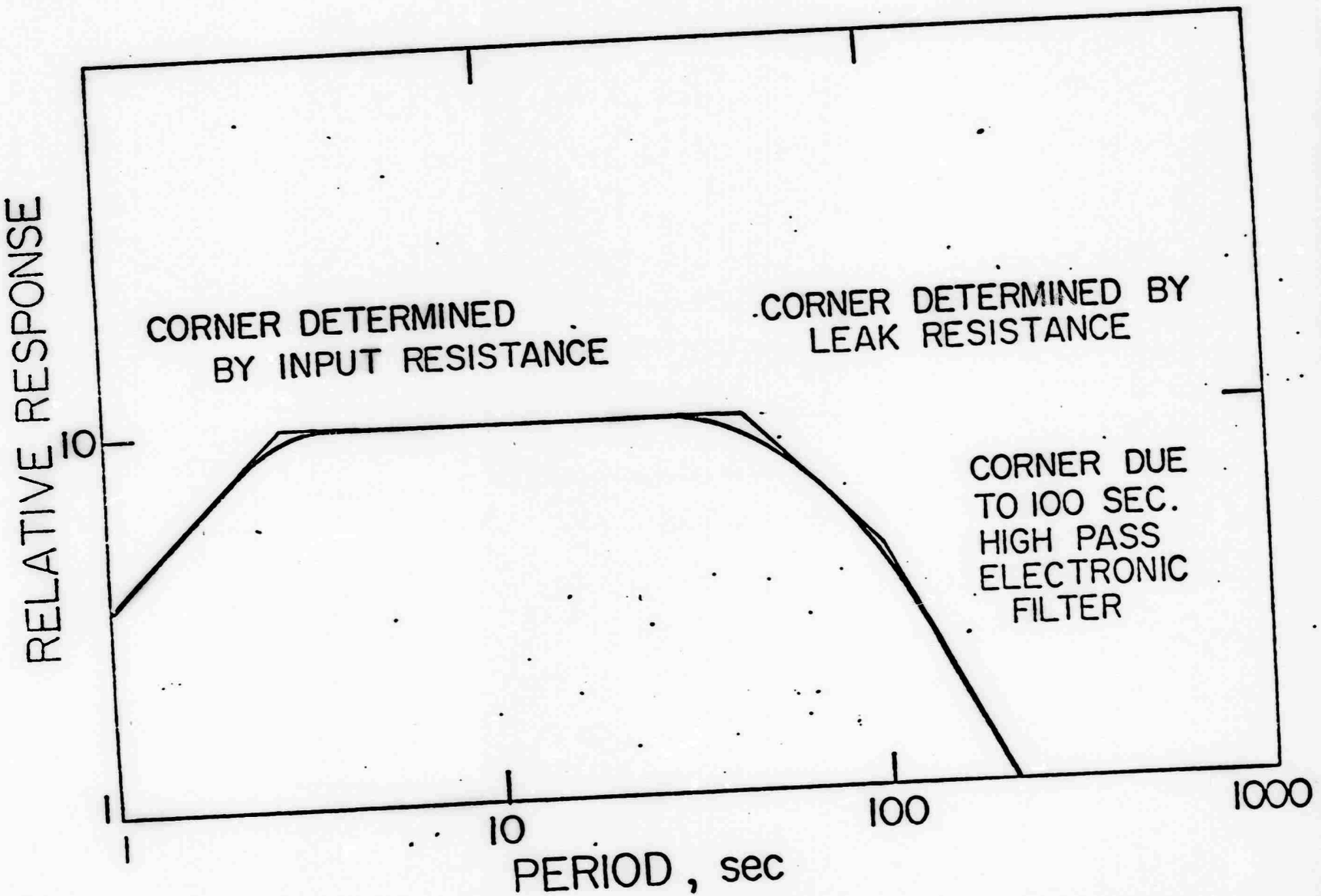
RELATIVE RESPONSE
10
1
CORNER DETERMINED BY INPUT RESISTANCE
CORNER DETERMINED BY LEAK RESISTANCE
CORNER DUE TO 100 SEC. HIGH PASS ELECTRONIC FILTER
1
10
100
1000
PERIOD, sec

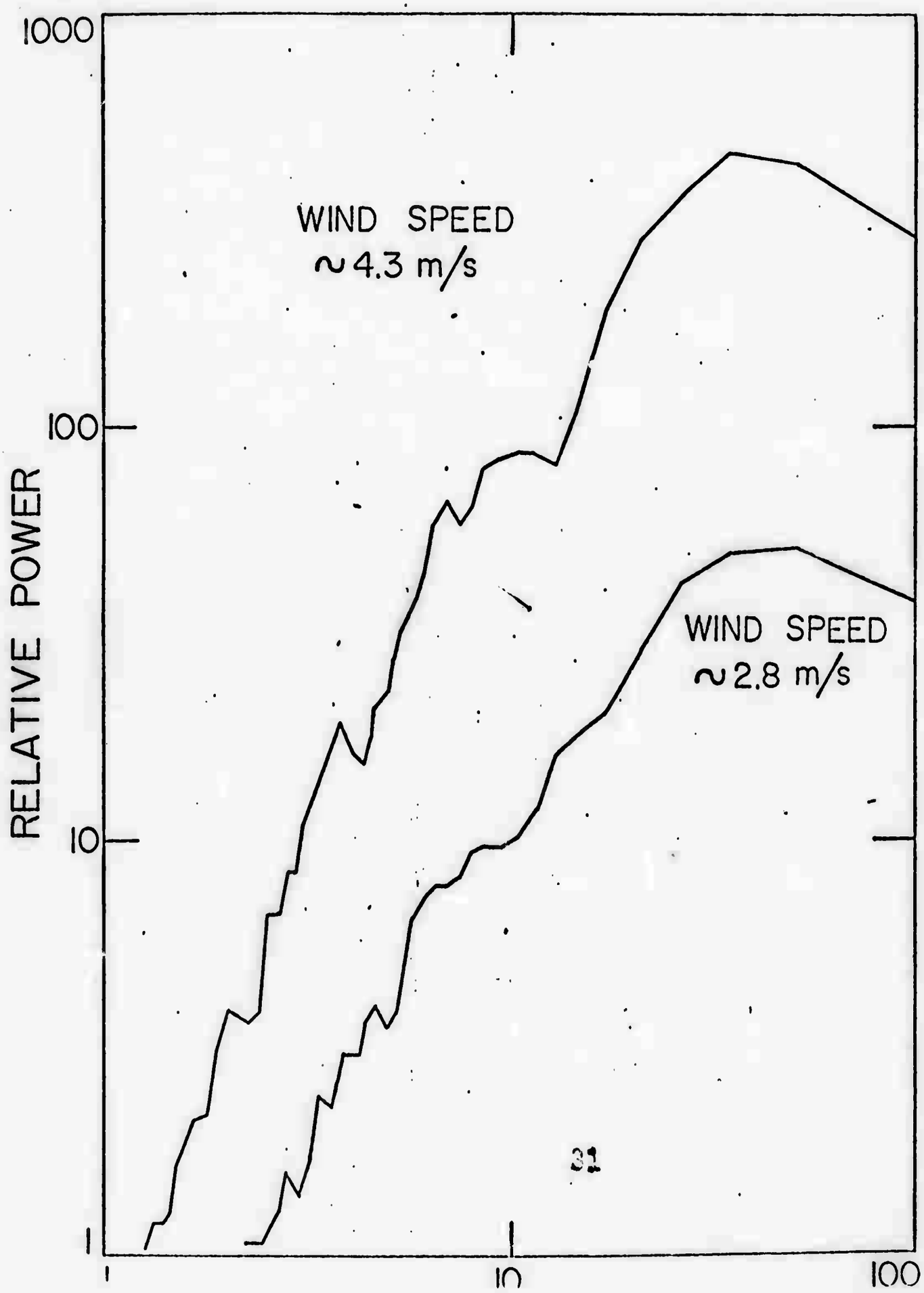
1000
100
10
1
RELATIVE POWER
WIND SPEED
≈4.3 m/s
WIND SPEED
≈2.8 m/s
1
10
100

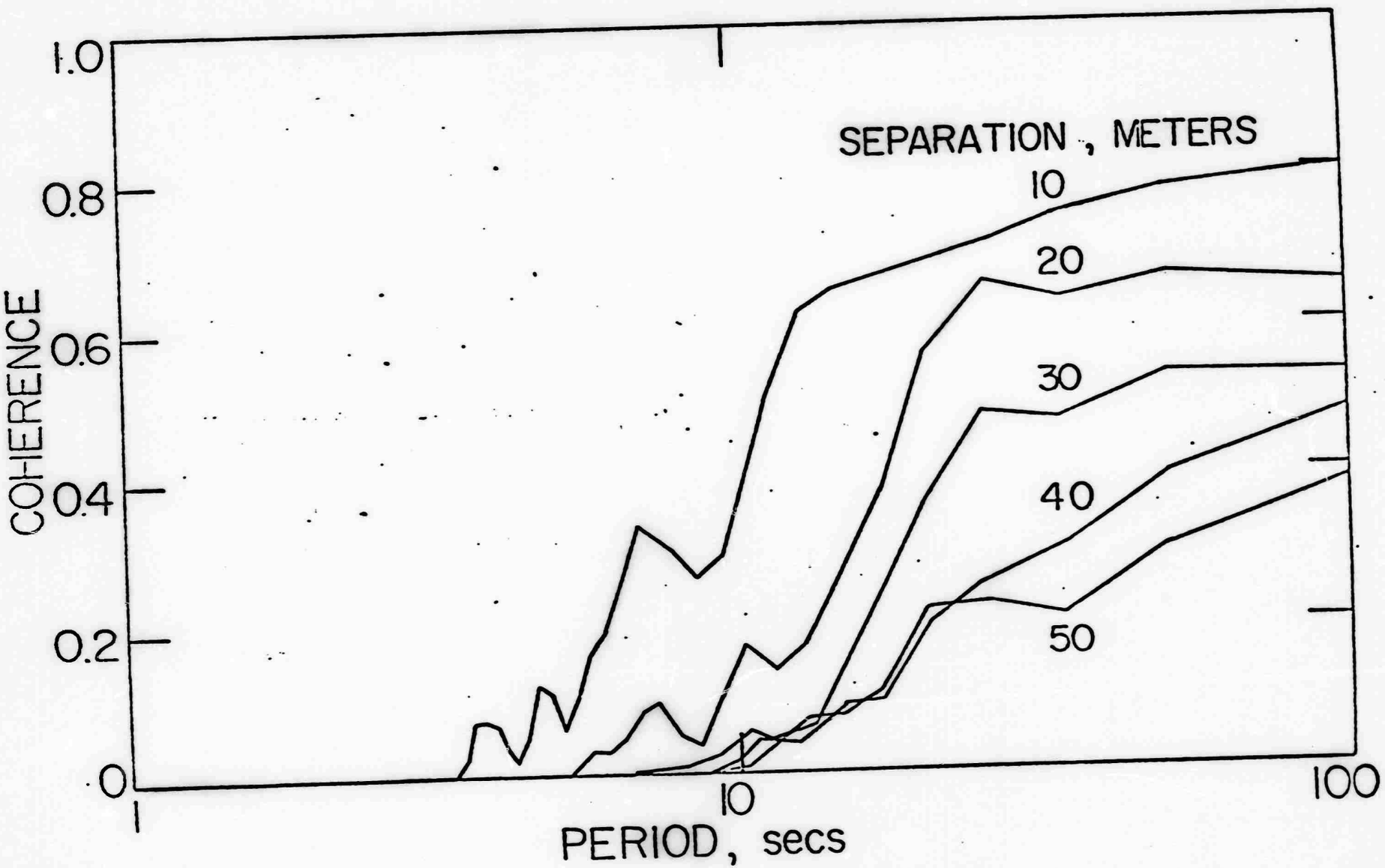
1.0
0.8
0.6
0.4
0.2
0
COHERENCE
SEPARATION , METERS
10
20
30
40
50
1
10
100
PERIOD, secs

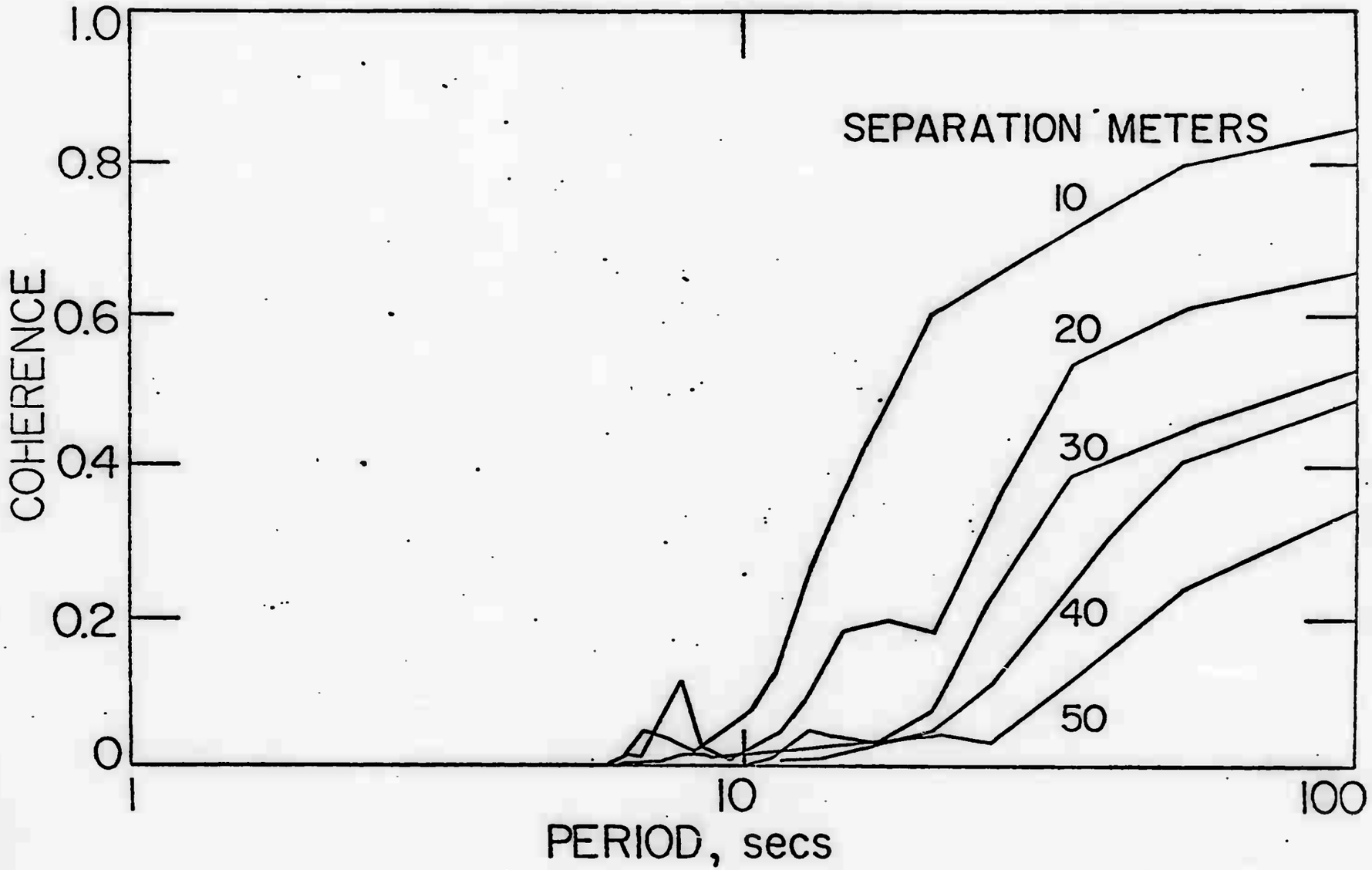
1.0
0.8
0.6
0.4
0.2
0
COHERENCE
SEPARATION METERS
10
20
30
40
50
1
10
100
PERIOD, secs

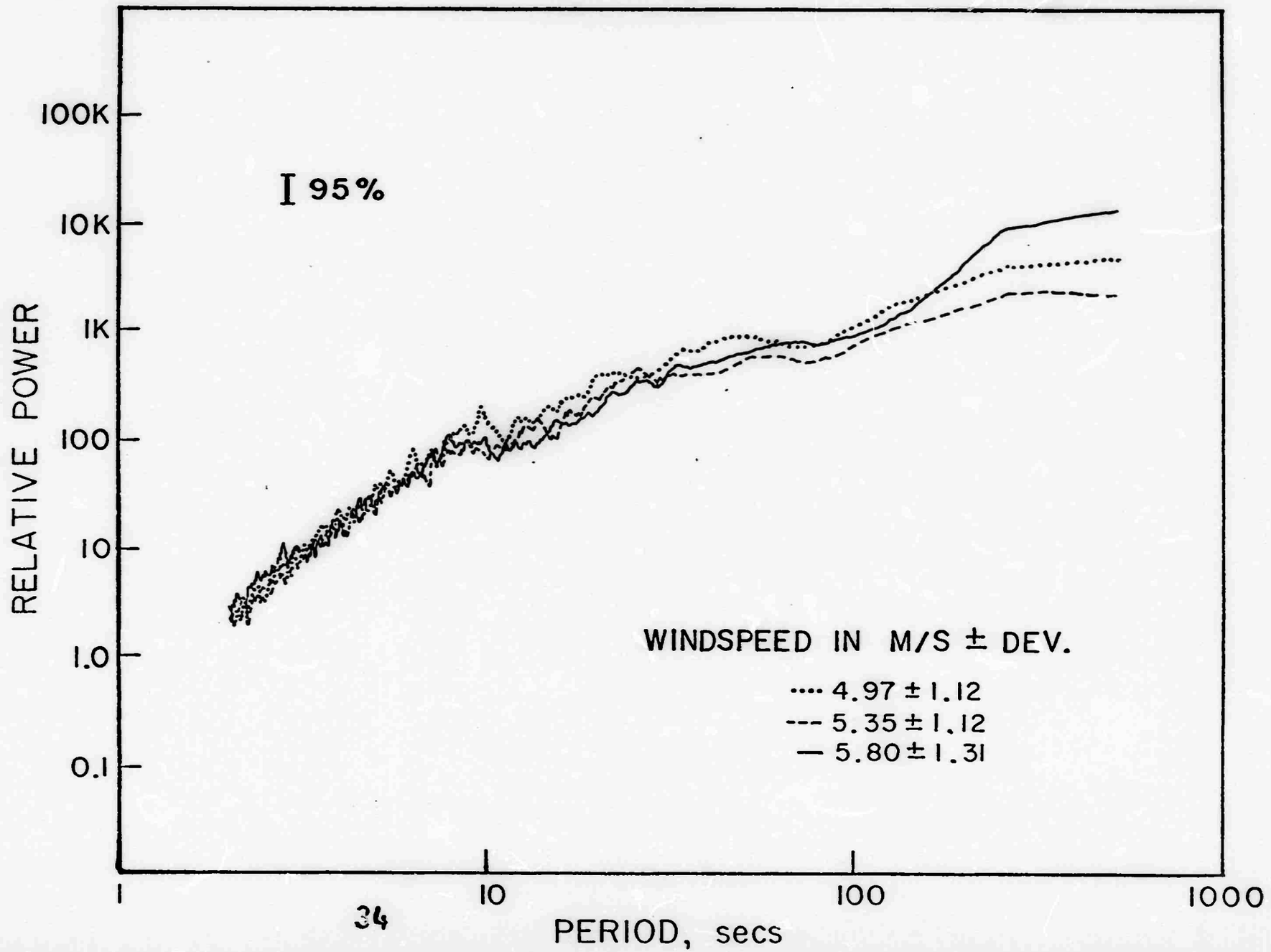
100K
10K
1K
100
10
1.0
0.1
RELATIVE POWER
I 95%
WINDSPEED IN M/S ± DEV.
···· 4.97 ± 1.12
--- 5.35 ± 1.12
— 5.80 ± 1.31
1
10
100
1000
PERIOD, secs

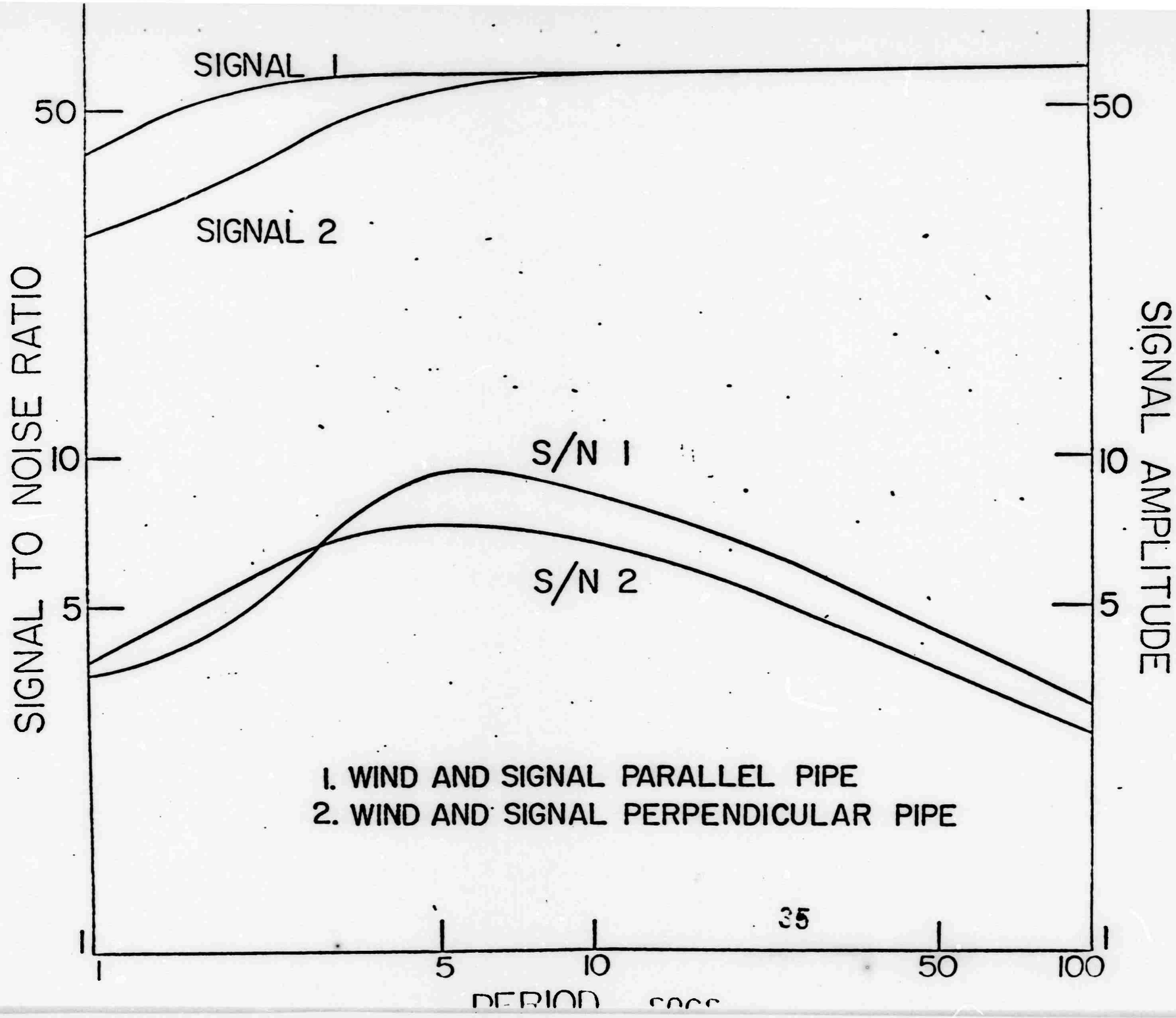
SIGNAL 1
SIGNAL 2
S/N 1
S/N 2
50
10
5
1
SIGNAL TO NOISE RATIO
SIGNAL AMPLITUDE
1. WIND AND SIGNAL PARALLEL PIPE
2. WIND AND SIGNAL PERPENDICULAR PIPE
35
1
5
10
50
100
PERIOD SECS

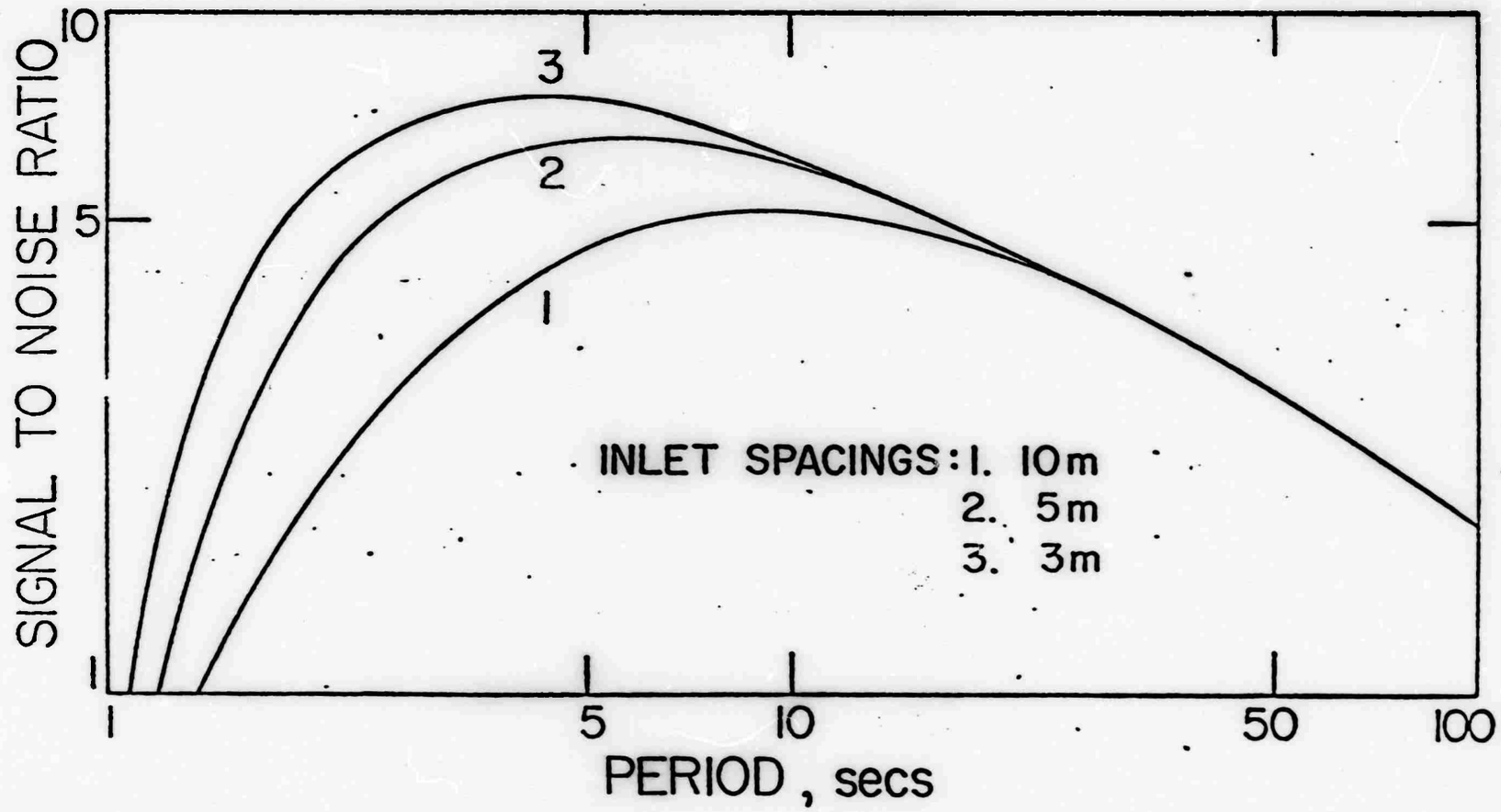
SIGNAL TO NOISE RATIO
10
5
1
3
2
1
INLET SPACINGS: 1. 10m
2. 5m
3. 3m
1
5
10
50
100
PERIOD, secs

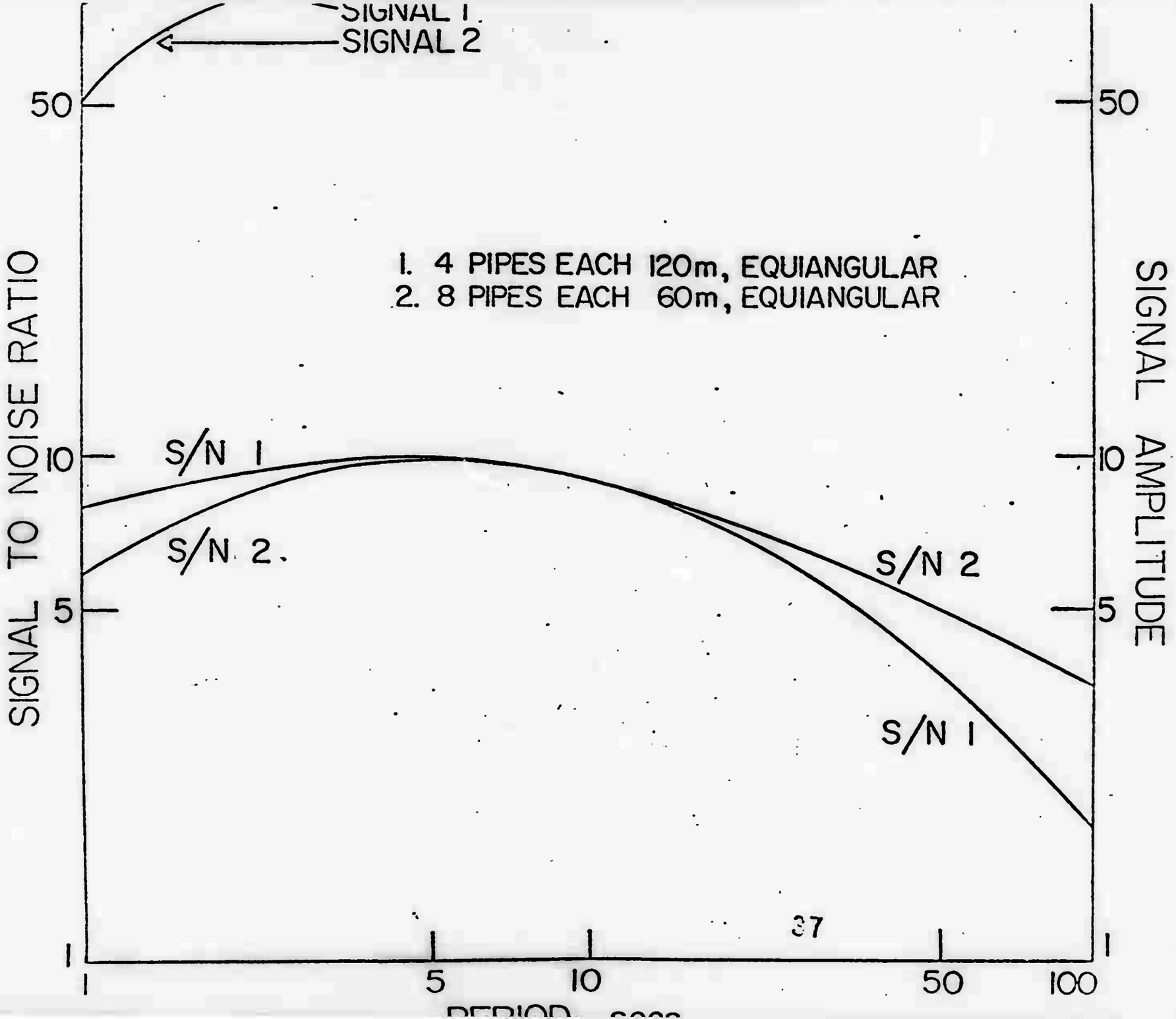
SIGNAL 1
SIGNAL 2
1. 4 PIPES EACH 120m, EQUIANGULAR
2. 8 PIPES EACH 60m, EQUIANGULAR
S/N 1
S/N 2
S/N 2
S/N 1
SIGNAL TO NOISE RATIO
SIGNAL AMPLITUDE
50
10
5
1
50
10
5
1
1
5
10
50
100
37

Pipe array orientation	Parallel to wind direction			Perpendicular to wind direction		
Wind velocity	2.5-4.0 m/sec.			4.0-6.0 m/sec.		
Inlet separation	10m	20m	30m	10m	20m	30m
Period	Apparent Velocities, m/sec.					
102.4	2.4	2.6	3.6	10.0	20.8	98.1
51.2	3.6	3.8	3.9	7.1	24.3	49.2
34.13	4.2	3.8	3.8	8.3	71.4	28.8
25.60	3.9	3.8	4.2	28.1	97.3	40.5
20.48	3.9	4.1	4.4	25.0	101.2	
17.07	4.2	4.2	4.3	15.1		
14.63	4.0	4.0		19.2		
12.80	3.8	3.6		23.4		
11.38	3.6	3.7				
10.24	3.6	4.0				
9.31	3.6					
8.53	3.5					
7.88	3.5					
7.31	3.6					
6.83	3.5					
6.40	3.2					
6.02	3.2					
5.69	3.4					

VERY LONG PERIOD WAVES ASSOCIATED WITH ATMOSPHERIC DISTURBANCES

John A. McDonald
Eugene Herrin

(Text of a paper delivered to the

American Geophysical Union, 10 December 1970)

Dallas Geophysical Laboratory
Southern Methodist University
Dallas, Texas 75222

ABSTRACT

(EOS, Trans. AGU, 51, 760, 1970)

Data have been collected in digital form from a triangular microbarograph array with sides approximately 5 km in length. This array was operated in East Texas during the spring of the year; a period of maximum atmospheric turbulence. The array was particularly well situated for the prevalent tornado paths to the west and north, hurricanes to the east and south and spring thunderstorms typical to the area. Data were recorded over a wide band of period; from the order of units to the order of hundreds of seconds. Filtering and decimation of the individual channels and beam forming of the array data indicate that very long period waves may be associated with these violent atmospheric disturbances. However, acoustic waves are dominated by large amplitude waves of lower velocities probably associated either with the jet stream or with large cells of atmospheric turbulence.

INTRODUCTION

A microbarograph array was operated in East Texas for the period January through August 1970. The array data are being used to study:

a) Propagating atmospheric acoustic signals,

b) Earth motions due to turbulence and due to acoustic waves,

c) Atmospheric effects due to violent disturbances in the atmosphere.

During the period of the operation of this array various important atmospheric events accurred, such as:

a) the Lubbock tormado,

b) the Oklahoma city tornado

c) Hurricane Celia

d) the passage of many frontal systems.

In this presentation we indicate that we have recently started to search for acoustic waves associated with severe weather disturbances. This research is being pursued with the plan of trying to understand the mechanisms which generate such waves.

Our array in East Texas was in a particularly good locality and operated in a very suitable time period for violent atmospheric disturbances. The association of patterns of acoustic waves with such "events" is still tenuous. However, our preliminary results

indicate that energy propagating at acoustic velocities can be detected after the passage of a frontal system. The use of a small array for such an analysis will be shown here.

RESULTS

The first figure shows the array at Grand Saline; the small array should be disregarded. The array had legs of approximately 5 km with the stations designated CH 2, CH 7 and CH 8. The base station (CH 2) was located at the Morton Co. Salt Mine. The microbarographs were operated without pipe arrays.

The short period end of the response at 2 secs. was determined by the input leak resistance, and the corner at about 45 sec. (figure 2) by a capillary leak in the capsule. The excursions in the y-direction have been calculated in counts/μbar in order to obtain an absolute value for the amplitude of the waves.

Figure 3 shows data taken from the ESSA daily weather maps for the days of 20 and 21 April 1970, when a frontal system passed through the area of Grand Saline, Texas. One would guess that the front passed through the town in the early hours of 21 April 1970.

We show in figure 4 five channels of digital data displayed in analog form. Three represent microbarograph data from CH 2, CH 7, CH 8 (see figure 1), one shows the variation of wind velocity (in m/sec) and the other the variation of wind direction with time. The abscissa represent almost 12 hours of data which have been

decimated by a factor of 10; thus, the bar in the figure represents 2000 sec.

The frontal system can be seen to arrive at 0200 Z accompanied by a wind shift.

The data from the microbarograph array were searched for energy with acoustic velocities before the arrival of the front; during the passage of the front and after the passage of the front.

Figure 5 shows the output from a beam steer program during the frontal passage. In this program signals are brought into coincidence by time shifting and the relative increase in the amplitude of the summed channels is detected when coincidence is achieved. The average power in a beam is compared with the sum of the power of the individual channels; if the ratio of these powers increases above the value for uncorrelated noise a signal is said to have been detected. In this particular program time is averaged by means of a recursive filter. In figure 5 it will be seen that the passage of the front (0200 Z) is accompanied by energy of acoustic velocity (at ~320 m/s). The beam steer output for the two hours beginning at 0342 Z can be seen in figure 6. Energy can still be seen to be travelling at acoustic velocities from about the arc from which the front travelled. A similar

analysis prior to the arrival of the front showed no significant energy at acoustic velocities.

In figure 7 can be seen the definition of coherence used in this study. The phase lag or lead is then the arc-tangent of the ratio:

$$\frac{\text{Quadrature spectral density}}{\text{cospectral density}}$$

or the ratio of the imaginary to the real parts of the cross spectral density.

Using these formulae the coherences and phase lags were calculated during the frontal passage and are shown in figure 8. The high coherences and systematic phase differences over the 5 km of these very long period energy movements should be noted.

CONCLUSIONS

The results presented here and other data indicate that energy travelling at acoustic velocities can be related to frontal systems. But at the present time we would not like to speculate on the nature of the generating mechanism.

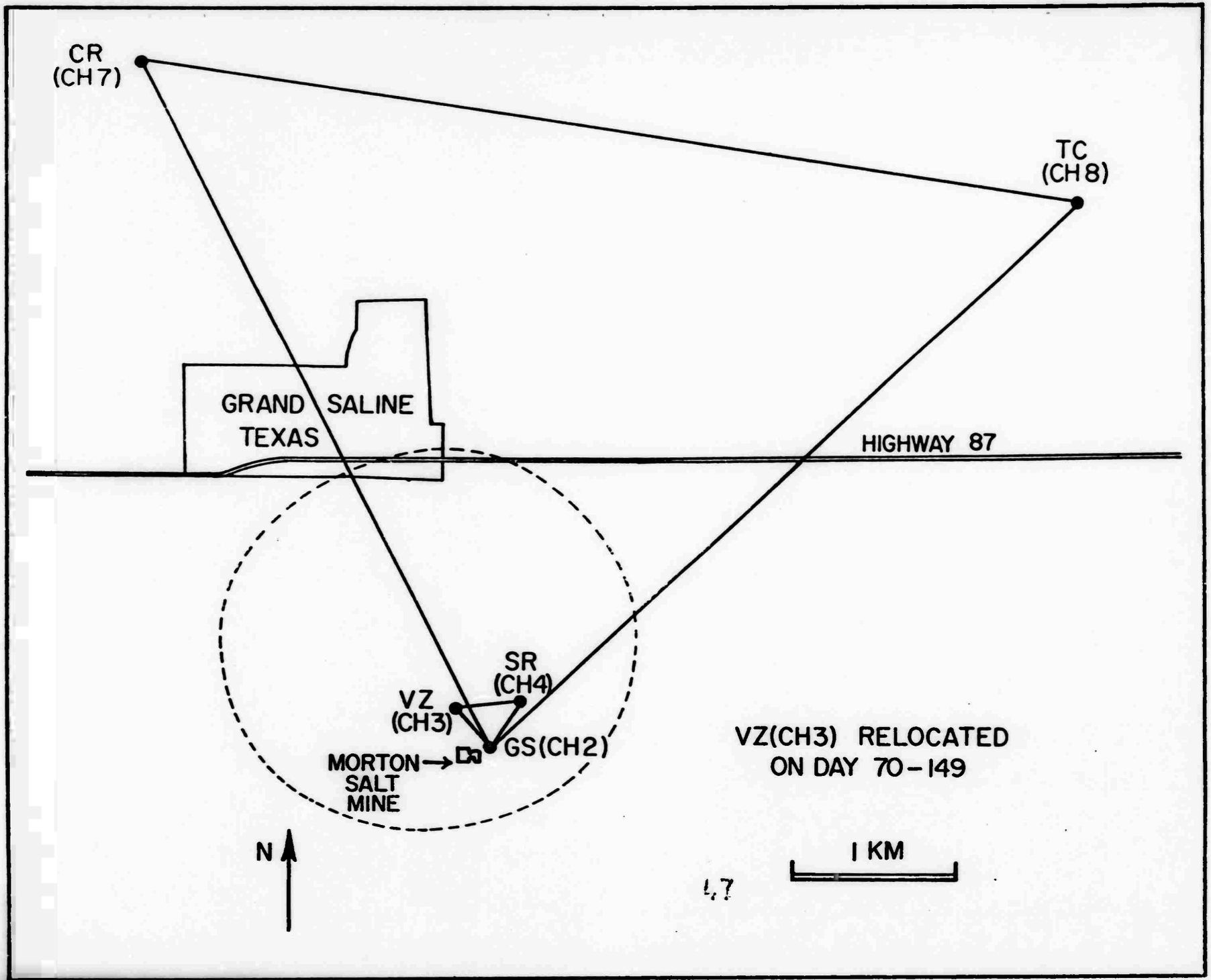
CR
(CH7)
TC
(CH8)
GRAND SALINE
TEXAS
HIGHWAY 87
SR
(CH4)
VZ
(CH3)
GS(CH2)
MORTON
SALT
MINE
N
VZ(CH3) RELOCATED
ON DAY 70-149
1 KM

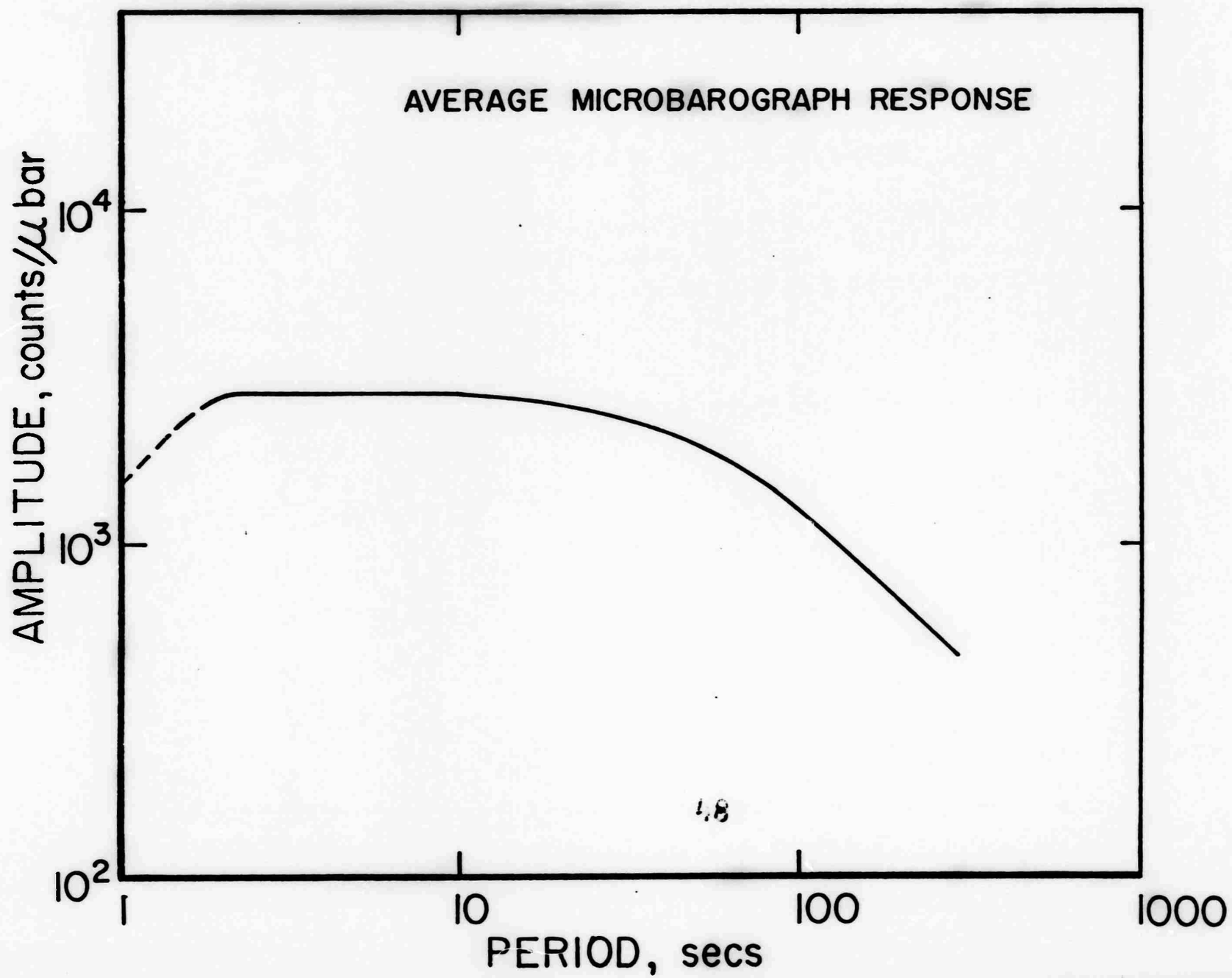
AVERAGE MICROBAROGRAPH RESPONSE
AMPLITUDE, counts/μ bar
10⁴
10³
10²
1
10
100
1000
PERIOD, secs

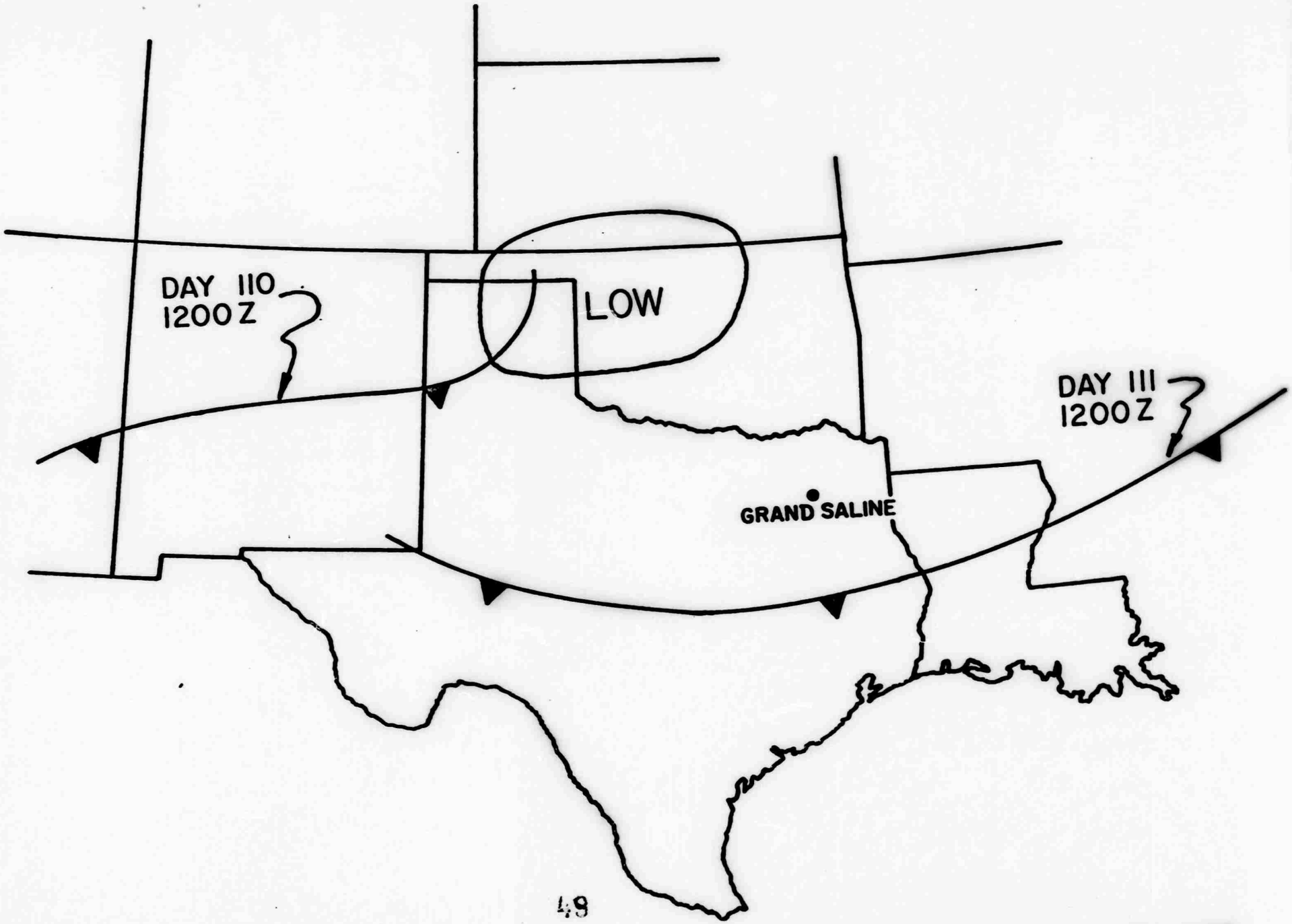

FROM ESSA DAILY WEATHER MAPS

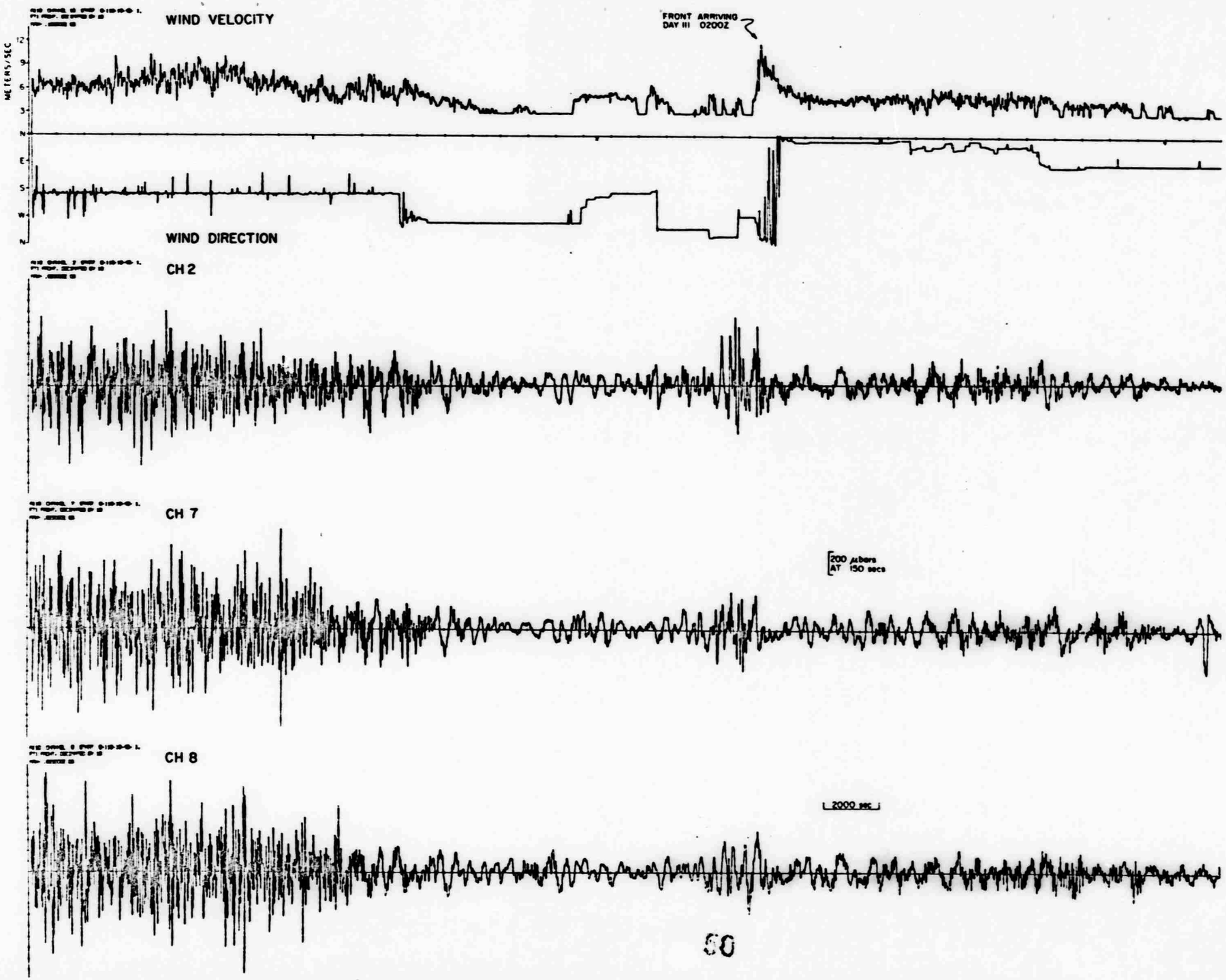
WIND VELOCITY
FRONT ARRIVING
DAY III 0200Z
METERS/SEC
12
9
6
3
N
E
S
W
N
WIND DIRECTION
CH 2
CH 7
200 Mbars
AT 150 secs
CH 8
2000 sec

DAY 111

AZIMUTH, degrees

90 50 10 330 290 250 210 170 130

ZULU TIME

0145 0200 0215 0230 0245 0300 0315 0330

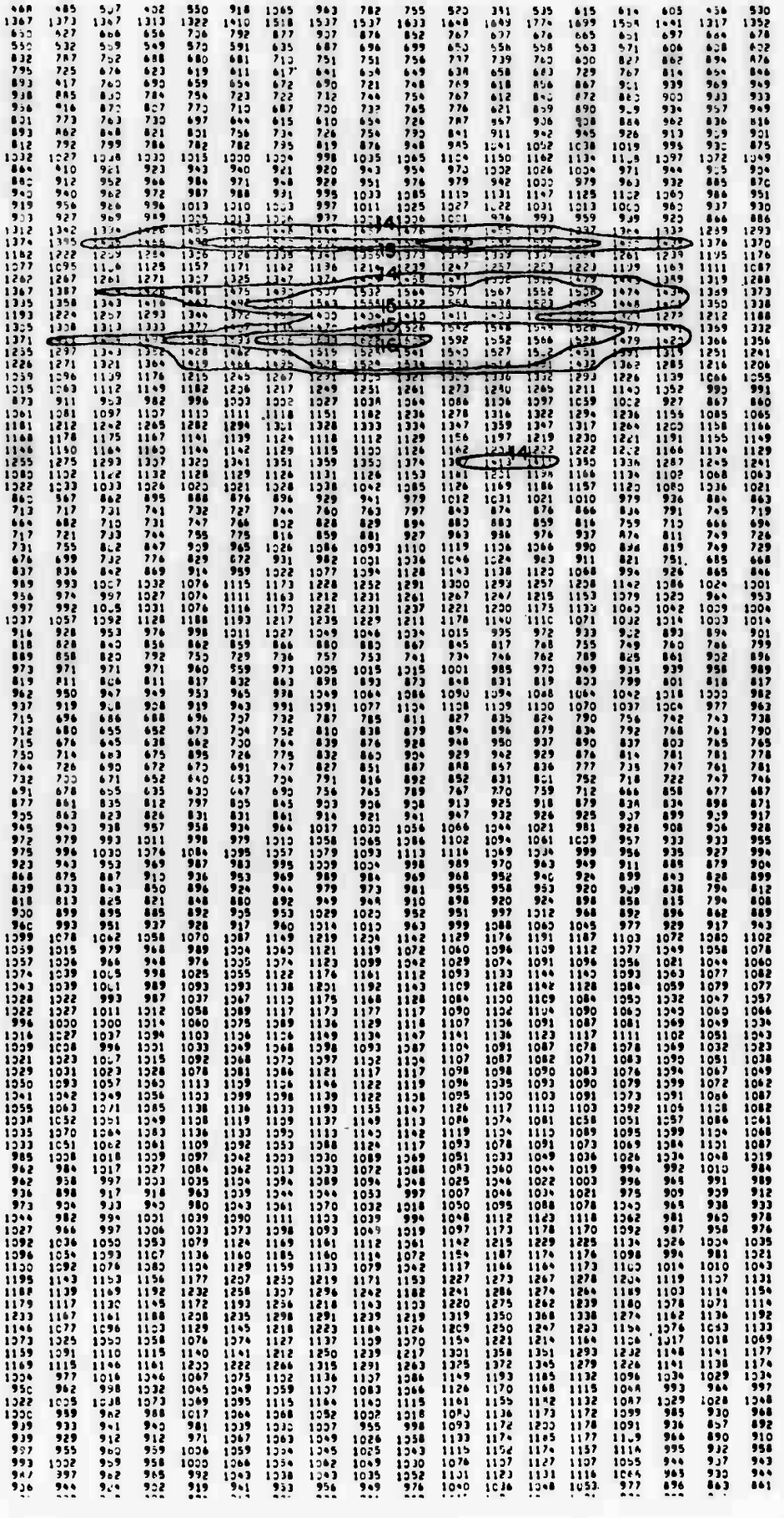

DAY 111

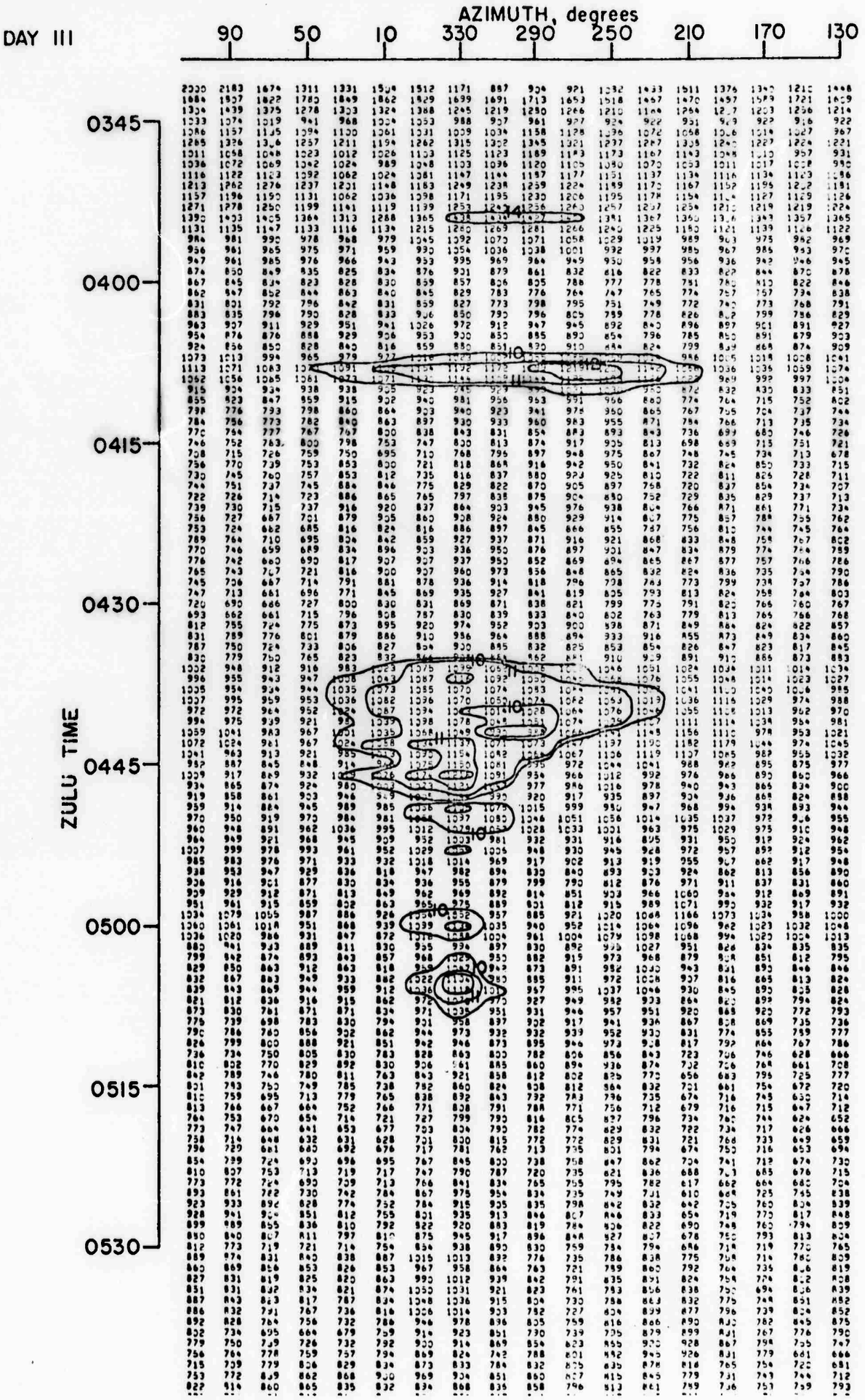
AZIMUTH, degrees
90
50
10
330
290
250
210
170
130
ZULU TIME
0345
0400
0415
0430
0445
0500
0515
0530

COHERENCE SQUARED

$$C_{ij}(f) = \frac{[P_{ij}(f)]^2}{P_i(f)P_j(f)}$$

WHERE $P_{ij}(f)$ IS THE CROSS-SPECTRAL DENSITY BETWEEN CHANNEL i AND CHANNEL j, $P_i(f)$ AND $P_j(f)$ ARE THE SPECTRAL DENSITY ESTIMATES.

COHERENCE & PHASE RELATIONSHIPS OVER APPROX. 5 km

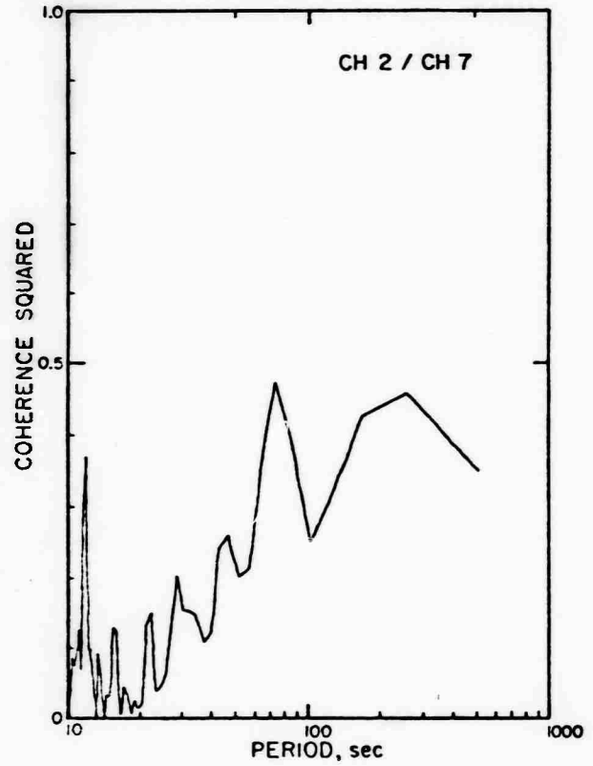

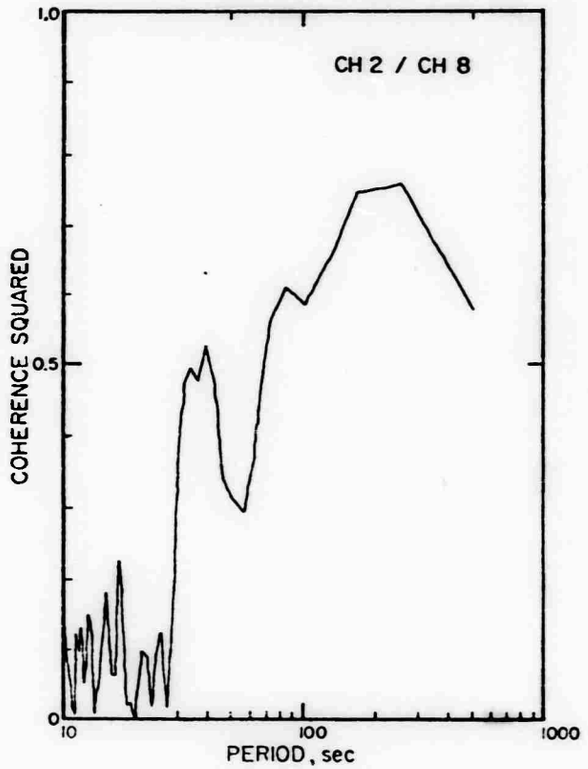

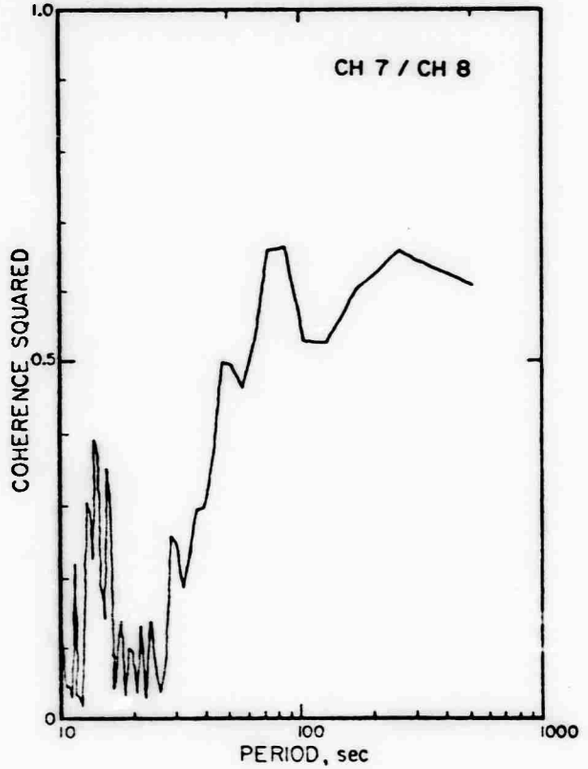

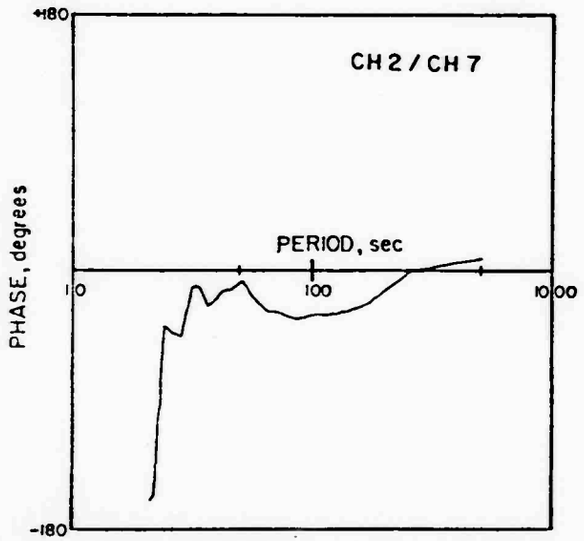

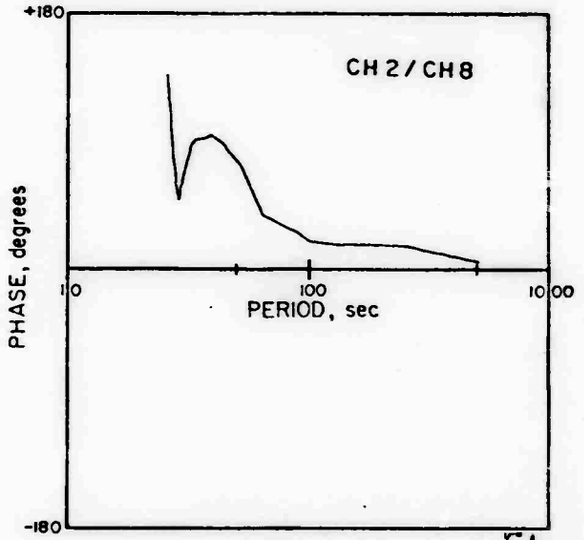

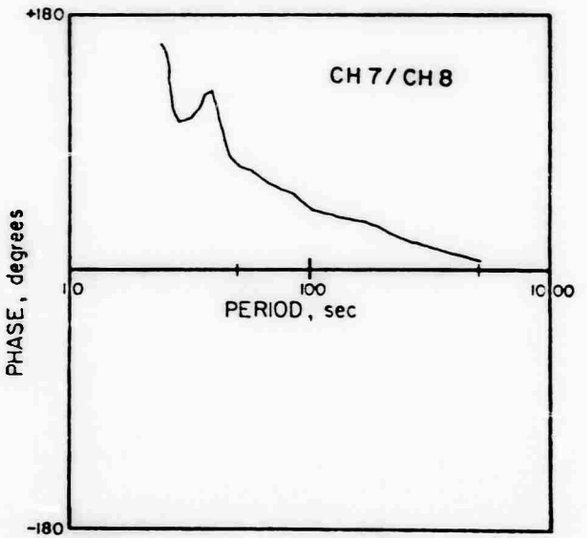

THE RESPONSE OF THE EARTH TO LOCAL CHANGES IN ATMOSPHERIC PRESSURE

G. G. Sorrells

John A. McDonald

Eugene Herrin

(Paper delivered to the American Geophysical Union 9 December 1970)

55

Dallas Geophysical Laboratory
Southern Methodist University
Dallas, Texas 75222

ABSTRACT

(EOS, Trans. AGU, 51, 777, 1970)

Observations have been made of the long period seismic and atmospheric pressure fields at the surface of the earth and at a depth of 183 m in a mine. In the period range 20-100 sec. and during intervals of moderate atmospheric turbulence the seismic noise field at the surface is highly correlated with the changes in atmospheric pressure. In contrast there is little correlation between the seismic noise field in the mine and these pressure changes unless they are moving with acoustic velocities. These observed seismic disturbances are not related to buoyancy in the seismometer but are due to the response of the earth to changes in the atmospheric pressure.

GROUND MOTIONS ASSOCIATED WITH ACOUSTIC WAVES

G. G. Sorrells

John A. McDonald

Eugene Herrin

(Nature Physical Science, 229, 14-16, 1971)

57

Dallas Geophysical Laboratory
Southern Methodist University
Dallas, Texas 75222

GROUND MOTIONS ASSOCIATED WITH ACOUSTIC WAVES

On July 4, 1970, a signal travelling with acoustic velocity was observed at a 5 km triangular microbarograph array at Grand Saline in East Texas. There is a computer program which can search any given arc for a signal of any given velocity. At a particular velocity, data from the elements of the array are brought into coincidence by time shifting. The correlator detects a relative increase in the summed signals at coincidence, and it compares the power in a beam to the sum of the powers of the individual elements. If this ratio increases significantly above the value for the uncorrelated noise, a signal is said to have been detected. The advantage of this particular program is that the use of a recursion filter[1] instead of a conventional convolution filter reduces considerably the data processing time required. The program was run on data from the three elements of the array for the time period during which the signal was observed. Fig. 1 shows the output from the program and a signal can be seen clearly beginning at approximately 0140 GMT with an azimuth of 220°.

Two three-component, long period seismographs are in operation at the same location. One system is at the surface and the other almost directly below the first in a salt mine at a depth of 183 m. These seismographs have their long period response electronically amplified to produce the overall response shown in Fig. 2.

Crary and Ewing[2] have shown that the buoyant response of ther vertical seismograph to changes in the atmospheric pressure can be an important source of long period seismic noise. It is also known that small variations in temperature can cause considerable long period noise. Extreme care was taken during the installation of the seismic system to reduce these effects to a minimum. The surface seismometers are heavily insulated and the mine seismometers are in a thermally stable environment. The vertical seismometers were sealed in rigid steel cases with time constants of several hours. These seismometers were placed in sealed vaults with time constants ranging from 10 to 26 h. Tests showed that external pressure variations of about 100 μbar at a period of 200 s produced pressure variations within the vault which were of the same order as the system noise of the microbarograph (~0.02 μbar).

The mine, which has only one entrance, acts as a low pass filter to surface pressure variations. The time constant of the mine is greater than 4 min. Nevertheless seismic disturbances which were practically identical were recorded both at the surface and in the mine during the passage of the acoustic wave. The coherences between the base station microbarograph and the surface and mine vertical seismographs, which are shown in Fig. 3, indicate that at periods from 20 to 100 s the seismic disturbance is closely related to the acoustic wave. In view of the precautions taken during the installation of the seismographs, we believe that the disturbance recorded by the seismographs represents true Earth motion.

It has been shown[3-5] that although the energy transfer between the atmosphere and the Earth is very slight a disturbance in one medium can cause motions in the other. Bolt[6] observed a dispersed acoustic signal from the Great Alaskan Earthquake some 2 h 40 min after the earthqueake. The signal resembled the acoustic waves generated by nuclear explosions.

Our results are in general agreement with unpublished theoretical studies by G.G.S. of the response of the Earth to slowly moving plane pressure waves. These studies show that in a half-space of reasonably competent rock, a pressure wave moving at

330 ms^{-1} would generate a vertical displacement at the surface of the Earth of 10 to 15 mμ per μbar in the period range from 20 to 100 s. These studies also show that the amplitudes of the seismic disturbance recorded at a depth of 183 m should be within 5 per cent of the amplitudes recorded at the surface.

C2

REFERENCES

1. Shanks, J. L., Geophys., 32, 31 (1967).
2. Crary, A. P., and Ewing, M., Trans. Amer. Geophys. Union, 33, 499 (1952).
3. Press, F., and Ewing, M., Geophys., 16, 416 (1951).
4. Jardetzky, W. S., and Press, F., Bull. Seismol. Soc. Amer., 42, 135 (1952).
5. Ewing, M., and Press, F., Trans. Amer. Geophys. Union, 34, 95 (1953).
6. Bolt, B. A., Nature, 202, 1095 (1964).

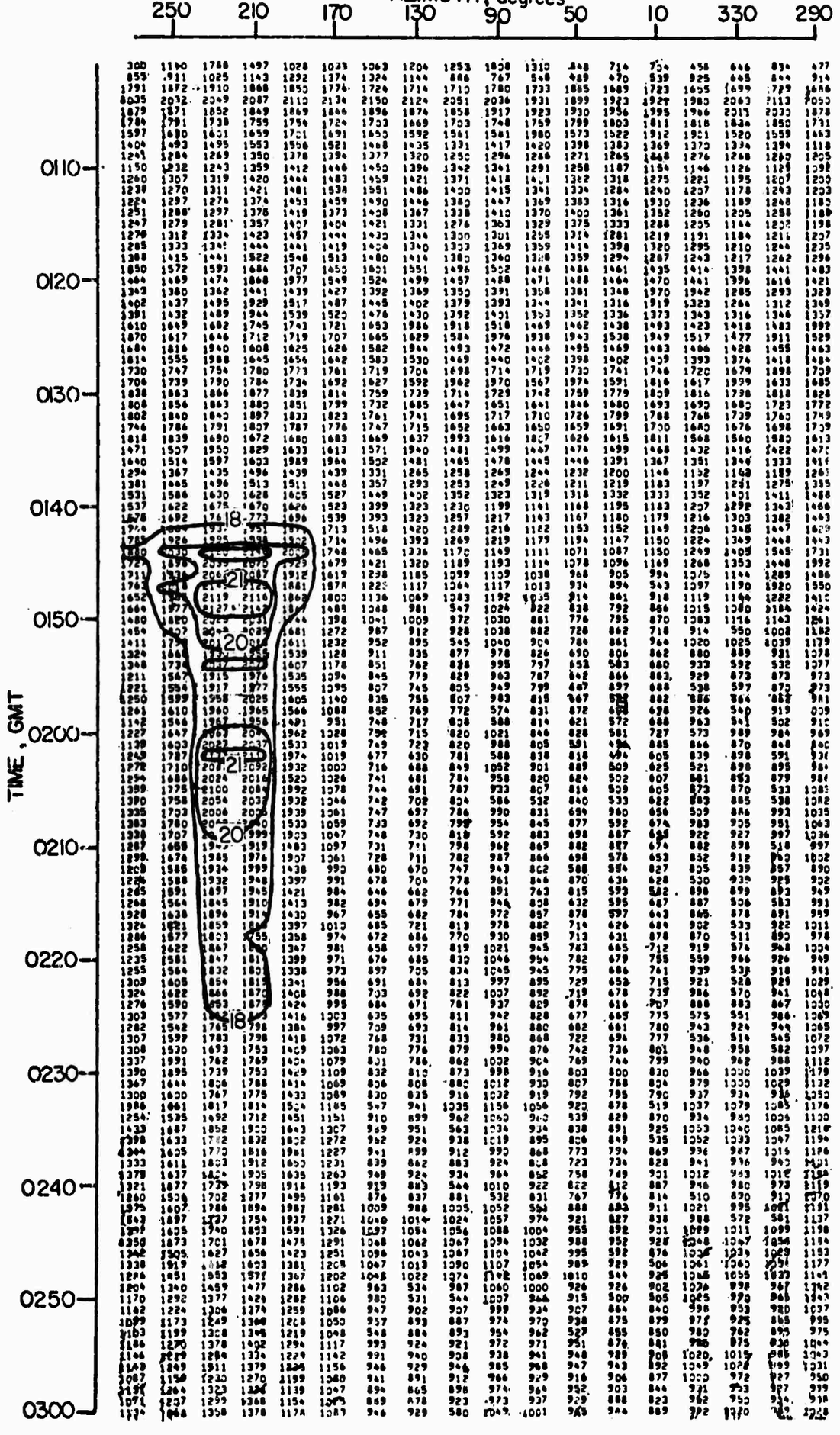
AZIMUTH, degrees
250
210
170
130
90
50
10
330
290
TIME, GMT
0110
0120
0130
0140
0150
0200
0210
0220
0230
0240
0250
0300
18
21
20
21
20
18

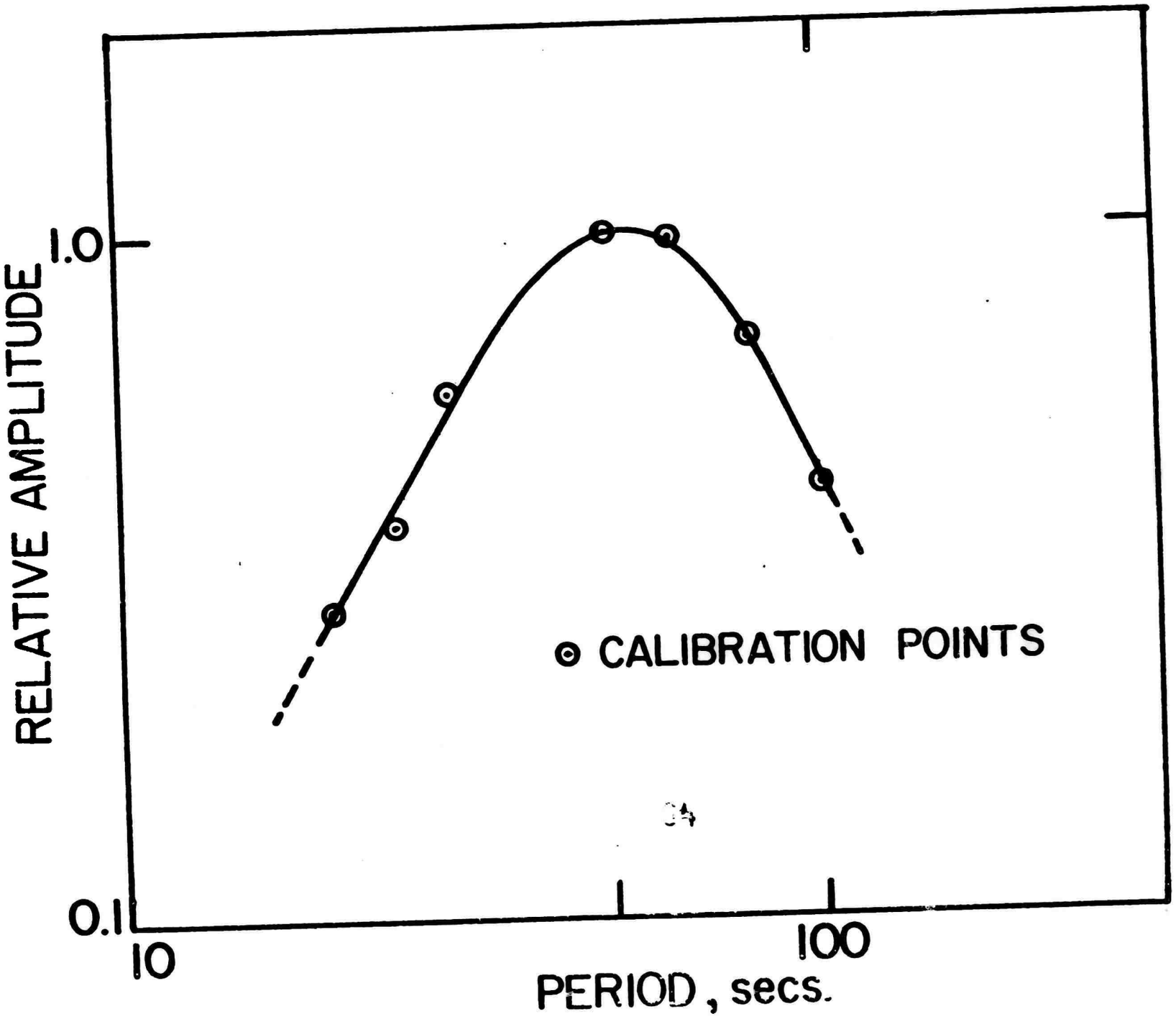
RELATIVE AMPLITUDE
1.0
0.1
10
100
PERIOD, secs.
⊙ CALIBRATION POINTS

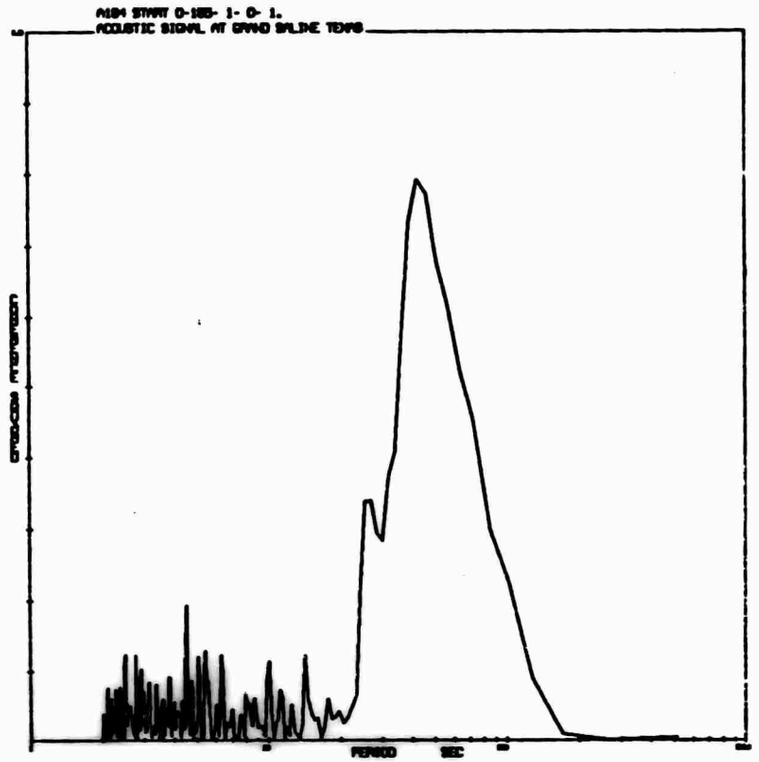
A184 START 0-185- 1- 0- 1.
ACOUSTIC SIGNAL AT GRAND SALINE TEXAS
PERIOD SEC

(a)

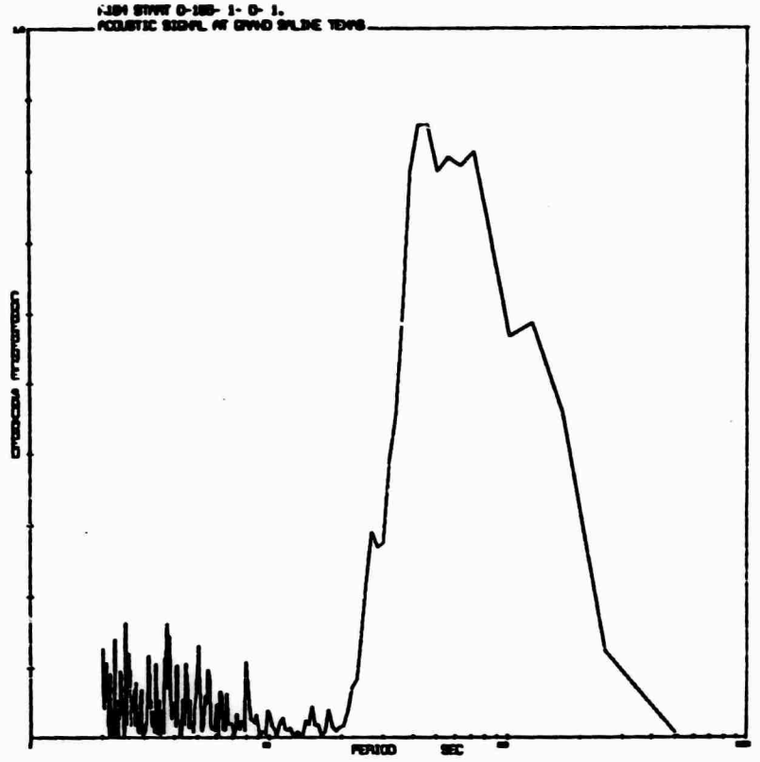
A184 START 0-185- 1- 0- 1.
ACOUSTIC SIGNAL AT GRAND SALINE TEXAS
PERIOD SEC

(b)

THE RESPONSE OF THE EARTH TO LOCAL ATMOSPHERIC PRESSURE CHANGES

G. G. Sorrells*

Z. A. Der†

(Text of Paper delivered to the Seismolgical Society of America, 26 March 71, Riverside, California)

* Dallas Geophysical Laboratory
Southern Methodist University
Dallas, Texas 75222

† Teledyne-Geotech
3401 Shiloh Road
Garland, Texas 75040

ABSTRACT

(GSA Abstracts with Programs, 3, 198, 1971)

Experimental frequency response of the earth to local atmospheric pressure changes have been calculated from data collected at a combined infrasonic and seismic observatory operated temporarily in the vicinity of Grand Saline, Texas. Theoretical frequency responses computed for reasonable earth models of the structure in the vicinity of the recording site compare favorably with the experimental observations. The implications of the results with regard to the detection of long-period seismic signals and to the measurement of shallow earth structure are discussed.

67

INTRODUCTION

When the wind blows across the surface of the earth it can cause relatively large perturbations in the local atmospheric pressure field. Since the earth is not a perfectly rigid body it will deform in response to these pressure changes. An experiment to measure the magnitude of the response of the earth to wind generated pressure changes was jointly conducted at the Morton Salt Co. mine near Grand Saline, Texas, by the Dallas Geophysical Laboratory of Southern Methodist University and Teledyne Geotech of Garland, Texas. Details concerning the sensing and recording systems used at the site are given by Herrin et al (1971). The basic sensing equipment consisted of two sets of three-component long-period seismographs with responses peaked between 50 and 60 seconds, an anemometer, and six microbarographs.

The seismographs were installed at the surface and in the mine at a depth of 183 meters; while the microbarographs were distributed in a 5 km array with the base microbarograph and the anemometer located 60 meters south of the surface seismic installation. All data were transmitted to a TC-200 digital acquisition system housed in a recording trailer, sampled at 1 second intervals, and stored on digital tapes. This particular report will be concerned with the data recorded by the surface and mine vertical seismograph and the base microbarograph during calm and windy periods.

PRESENTATION OF RESULTS

Calm Period. Power spectral density and coherence estimates calculated from data recorded during a 3-hour interval when the mean wind speed was less than or equal to 3 meters/sec are displayed in figures 1-a and b. The spectral density estimates have been corrected for their respective frequency responses.

The anticipated spread of the estimates at the 90% confidence level is shown by the vertical bar in the lower right hand corner of figure 1-a.

As shown by the dotted curve in figure 1-a the variations in the local atmospheric pressure field are quite low. In the period range 20-100 seconds, the RMS amplitude is only about 0.5 μbars. That is, during this interval and within this period range the mean change in the local atmospheric load is about 5 parts in 10^7. The solid and dashed curves shown in this figure are the spectral estimates of the seismic noise recorded in the mine and at the surface. Notice that they are, for all practical purposes, identical. The existence of the prominent gap in the spectra which occurs roughly between the periods of 20 and 100 seconds has been shown by Molnar et al (1969) to be potentially important to the detection and identification of surface waves generated by low magnitude earthquakes and underground nuclear explosions. Within this particular period range the noise level is relatively low, the RMS amplitude being only about 15-17 mμ. This means that systems with responses peaked somewhere between 40 and 60 seconds can potentially be operated with relatively high magnifications.

The squares of the estimated coherence between the seismic noise recorded at the surface and in the mine is shown by the solid curve in figure 1-b. The relatively high values between 8 and 20 seconds are not surprising since most of the noise within this period range is known to consist of fundamental mode Rayleigh waves with wavelengths much longer than the vertical distance between the two locations. Notice, however, that the range of significant coherence exte out to periods on the order of 200 seconds. This result demonstrates the important point that the detection threshold for surface waves is not system noise limited. The source of by far the greater part of the noise beyond the classical microseism band is unknown at the present time. Despite the relative low coherence between local atmospheric pressure changes and the seismic noise

recorded at both locations we feel that a substantial fraction of this noise could be pressure generated and we are presently investigating this possibility through field experiments near Canton, Texas.

Windy Period. Power spectral density and coherence estimates calculated from a 3-hour interval in which the mean wind speed was 9.4 meters/sec are shown in figure 2. As shown by the dotted curve in figure 2-a the wind blowing across the surface of the earth causes relatively large fluctuations in the local atmospheric pressure field. In the period range 20-100 seconds the RMS pressure amplitude is 16.7 μbars or about 28 dB greater than RMS pressure amplitude calculated from data recorded during the calm period. It will be observed that the increase in the amplitude of the pressure changes is accompanied by an increase in the seismic noise recorded at the surface relative to that recorded in the mine. During this interval the RMS amplitude of the surface noise increased to 65.2 mμ while the RMS amplitude of the mine noise is only slightly greater than that recorded during a calm period. The solid curve in figure 2-b is the square of the estimated coherence between the seismic noise recorded at the surface and in the mine. Notice that the coherence is quite low in comparison to similar measurements made during the calm period. The loss of coherence plus the increased noise observed at the surface implies that during windy periods, noise is added to the surface spectrum but not to the mine spectrum. As shown by the dashed curve in this figure the principal sources of this noise in the period range 20-100 seconds are the local variations in atmospheric pressure caused by the wind. In contrast, the coherence between local atmospheric pressure and the seismic noise recorded in the mine is negligible below 300 seconds indicating that this particular source does not contribute significantly to the mine spectrum in the period range of present interest. The spectrum of the surface seismic noise caused by atmospheric pressure changes is compared

to the total spectrum in figure 2-c. Power levels which drop below the dashed line are not significantly different from zero at the 95% confidence level. From this comparison it can be seen that in the period range 20-100 seconds all but about 3 dB of the surface noise is caused by local atmospheric pressure changes.

DISCUSSION OF RESULTS

It is obvious from the results presented in the previous paragraphs that during windy periods local atmospheric pressure variations can cause a substantial fraction of the noise recorded by long-period vertical seismographs located at the surface of the earth. The two most likely explanations for this noise are that either the seismometer is responding buoyantly to pressure changes acting directly on the mass or the elastic deformations of the earth caused by local atmospheric pressure changes are large in comparison to the noise from other sources. The evidence concerning buoyancy has been considered in some detail in a previous paper (Sorrells et al, 1971) and has led us to conclude that it contributes only a negligible amount of power to the noise field at periods less than 100 seconds. The evidence concerning elastic deformations of the earth is discussed below.

Elastic Deformations. There is considerable experimental evidence which indicates that the pressure field caused by the wind is spatially organized and tends to propagate at the mean wind speed. On the strength of this evidence Sorrells (1971) suggested that to a first approximation the wind-generated pressure field could be considered to be a plane wave propagating at the speed and in the direction of the mean wind. A computer program has been developed which calculates the displacement frequency response of a layered elastic half space to a slowly moving plane pressure wave (Sorrells et al, 1971). This program

has been used to calculate the responses of two earth models which approximate the structure at and about the Grand Saline Salt dome. Model 1 which approximates the structure at the salt dome is shown in figure 3-a. The salt dome itself is assumed to be infinitely extended in the horizontal dimension and is represented by the semi-infinite layer in this model. The second layer represents the salt dome cap which is remarkably thin at Grand Saline, while the upper layer represents the poorly consolidated Tertiary sediments overlying the dome. With the exception of the P and S velocities of the upper layer, the properties of this model are reasonably well established. There is, however, a considerable uncertainty associated with the estimates of these quantities. Sonic log data from a nearby well shows the P wave velocity to be 1.9 km/sec at a depth of 183 meters. We would anticipate the velocity above this level to be somewhat lower. Cores from test holes in the immediate vicinity of the recording site show that the upper layer consists primarily of sandy clay with interbedded sand lenses. Measurements reported by Press (1966) indicate that P wave velocities could be as low as 900 meters/sec. We have assumed a value of 1.3 km/sec; however, it could be as high as 1.5 km/sec or as low as 1.1 km/sec without substantially changing the calculated response. The shear wave velocity in the upper layer was assumed to be 0.475 km/sec because that value provided a theoretical response which agreed reasonably well with the experimental data at periods less than 30 seconds. As we shall see, however, the velocity could be as low as .400 km/sec or as high as .550 km/sec.

Since the salt dome is in fact limited in horizontal extent it is necessary to consider the sediments surrounding the dome as well. Model 2 which is shown in figure 3-b, approximates the structure in this region. Down to a depth of 88 meters it is the same as that used in Model 1. Below that depth the P wave velocities and thicknesses were taken from a sonic log which was made approximately 5 miles

northwest of the recording site. The S wave velocities were calculated from P wave data under the assumption that Poisson's ratio was 0.33. Likewise densities were calculated from the P wave data assuming a linear relationship between the two quantities.

An estimate of the actual response function $|H(\omega)|$ is given by

$$|H(\omega)| = \frac{|\hat{R}_m(\omega)|}{|\hat{R}_z(\omega)|} \frac{|\hat{G}_{zm}(\omega)|}{\hat{G}_m(\omega)}$$

where $|\hat{R}_m(\omega)|$ and $|\hat{R}_z(\omega)|$ are respectively the estimated frequency response functions of the microbarograph and the vertical seismograph; $\hat{G}_{zm}(\omega)$ is the cross power spectral density estimate of the outputs of the two systems and $\hat{G}_m(\omega)$ is the power spectral density estimate of the output of the microbarograph. An example of a response calculated from windy period data recorded at the surface is compared to the theoretical responses of models 1 and 2 in figure 3-c. Notice that at periods less than about 30 seconds the response of models 1 and 2 are virtually identical. While there is considerable scatter in the experimental data in this period range, its basic trend is satisfactorily approximated by the predicted response. The shape of the response curve below 30 seconds is determined largely by the structure in the uppermost 80 meters. The observed scatter suggests that the structure within this zone may be considerably more complex than was assumed in constructing the models. The two dashed curves which form the envelop enclosing the experimental data are the responses obtained from model 1 when the shear wave velocity in the first layer is changed to 400 meters/sec and 550 meters/sec. These probably represent the limits on the value the shear wave velocity can assume in the upper layer.

Observe that at periods greater than 30 seconds the experimental data favors model 1. This is encouraging since the recording site is located above the salt dome and the wavelengths involved are less than the diameter of the dome ($\sim$ 3 km). Notice, however, that there is a systematic divergence between the observed data and the model 1 response at periods greater than about 50 seconds (wavelengths $\sim$ 470 meters). We feel that this reflects the influence that the sediments surrounding the dome excercise on the observed response. This influence should increase with increasing wavelength until at wavelengths large compared to the diameter of the dome the observed response should closely resemble the model 2 response. Indeed we have found (Sorrells et al, 1971) that the observed response to the pressure field caused by acoustic waves with wavelengths greater than 12 km is in good agreement with the model 2 response. The apparent absence of pressure generated noise in the mine can be explained by comparing the responses of model 1 at the surface and at a depth of 183 meters. It will be observed that at periods less than 100 seconds the amplitudes of the pressure generated noise recorded in the mine should be at least a factor of 7 below those recorded at the surface.

On the basis of the results presented in this figure we conclude that during windy periods most of the noise recorded at the surface within the period range 20-100 seconds is earth motion in response to the local atmospheric pressure variations caused by the wind.

The Response of Other Geologic Media to the Wind Generated Pressure Field. The relatively good agreement between observed and calculated responses implies that we may use the theory with some confidence to predict the pressure generated contribution to the long-period noise field recorded by a vertical seismograph located in other geologic media. In figure 4 we compare the experimental response

obtained at the surface at Grand Saline with theoretical surface responses calculated for a granitic half space and for a granitic half space overlain by a two-meter thick low velocity zone. The parameters used in the calculations are listed in table 1. These models were selected for examination because they represent the general type of geologic environment that experience has led us to associate with a "quiet" seismic installation. Observe that the predicted response for both media are well below the Grand Saline response. This implies that earth motion caused by the wind generated pressure field will be significantly lower at surface installations on these media than that observed at Grand Saline. In fact, it can be shown that given atmospheric conditions identical to those observed during the windy period at Grand Saline the pressure generated noise at sites located on granites should be negligible in comparison to noise from other sources. This implies that through the careful selection of an appropriate geologic medium it should be possible to obtain noise levels at surface installations which are comparable to those obtained in mines. It is well to recall at this point that our discussion has been restricted to the noise recorded by the vertical seismograph. Because of the sensitivity of the horizontal seismograph (Rodgers, 1968) to tilts, the wind generated pressure field will cause substantial noise on horizontal seismograms; even those which are recorded in competent geologic media (Sorrells, 1971).

CONCLUSIONS

From the results presented previously we conclude that deformations of the earth in response to the wind generated pressure field can contribute significantly to the noise recorded by a vertical seismograph in the period range 20-100 seconds. The occurrence of this noise can strongly limit the use of vertical seismographs located at the surface to detect surface waves from small magnitude events. The noise will be most severe on the surface of geologic regimes characterised

by a low velocity surficial layer. Apparently this layer does not have to be very thick in order for the noise to occur. In regions of this type both theory and experiment indicate that the pressure-generated noise can be eliminated by installing the seismographs at depths on the order of several hundred meters. In regions where high velocity material extends to the surface the theory indicates that the contribution of earth motion caused by the wind-generated pressure field to the noise recorded by a vertical seismograph should be negligible at periods less than 100 seconds in comparison to earth noise from other sources even if the seismograph is located at the surface. This implies that it may be possible to obtain relatively low noise levels on long-period vertical seismographs at very shallow depths providing that care is exercised in the selection of the site geology. Experiments to verify this particular inference are obviously desirable.

REFERENCES

Herrin, Eugene and John McDonald (1971), A digital system for the acquisition and processing of geoacoustic data: (submitted to Geophys. Jour. Roy. Astron. Soc.)

Molnar, P. J., J. Savino, L. Sykes, R. Liebermann, G. Hade, P. Pomeroy (1969), Samll earthquakes and explosions in western North America recorded by new high-gain long-period seismographs: Nature, v. 224, p. 1268-1273.

Rodgers, P. N. (1968), The response of the horizontal pendulum seismometer to Rayleigh and Love waves, tilt and the free oscillations of the earth: Bull. Seis. Soc. Am., v. 58, p. 1385-1406.

Sorrells, G. G. (1971), A preliminary investigation into the relationship between long-period seismic noise and local fluctuations in the atmospheric pressure field: Geophys. Jour. Roy. Astron. Soc. (in press).

Sorrells, G. G., J. A. McDonald, Z. A. Der, and Eugene Herrin (1971), Earth motion caused by local atmospheric pressure changes: (submitted to Geophys. Jour. Roy. Astron. Soc.).

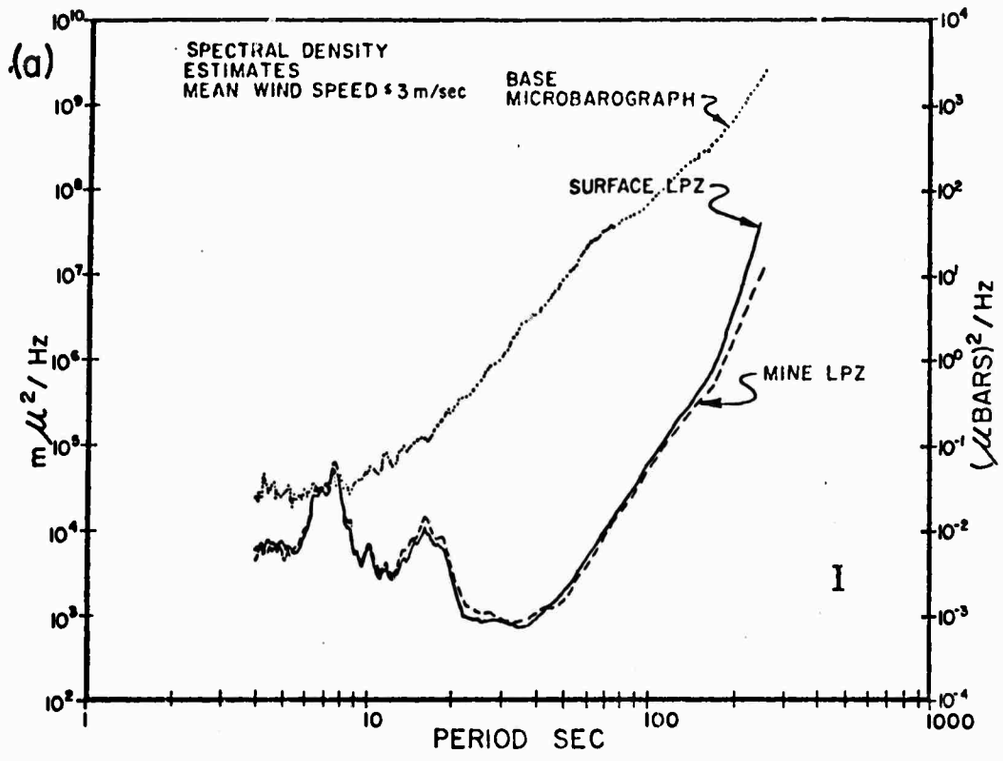
(a)
SPECTRAL DENSITY
ESTIMATES
MEAN WIND SPEED ≤ 3 m/sec
BASE
MICROBAROGRAPH
SURFACE LPZ
MINE LPZ
I
mμ²/Hz
(μBARS)²/Hz
PERIOD SEC
1
10
100
1000

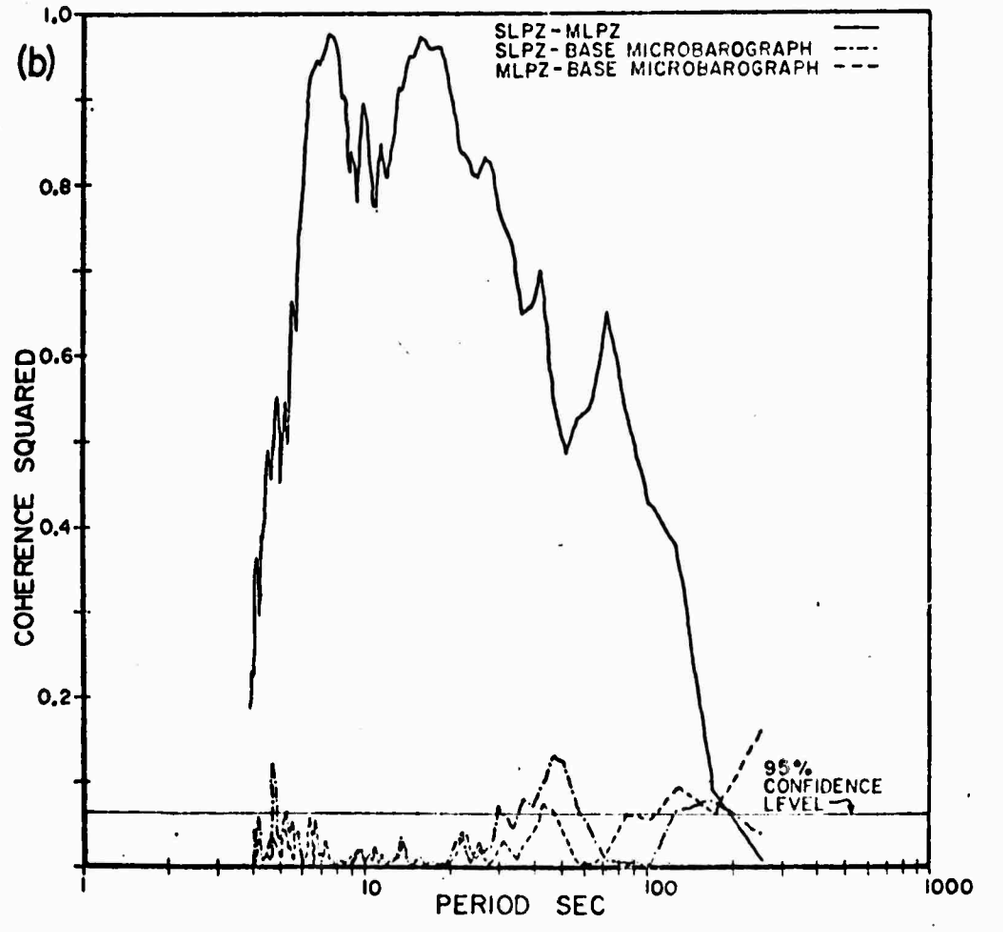
(b)
SLPZ-MLPZ
SLPZ-BASE MICROBAROGRAPH
MLPZ-BASE MICROBAROGRAPH
95%
CONFIDENCE
LEVEL
COHERENCE SQUARED
0.2
0.4
0.6
0.8
1.0
PERIOD SEC
1
10
100
1000

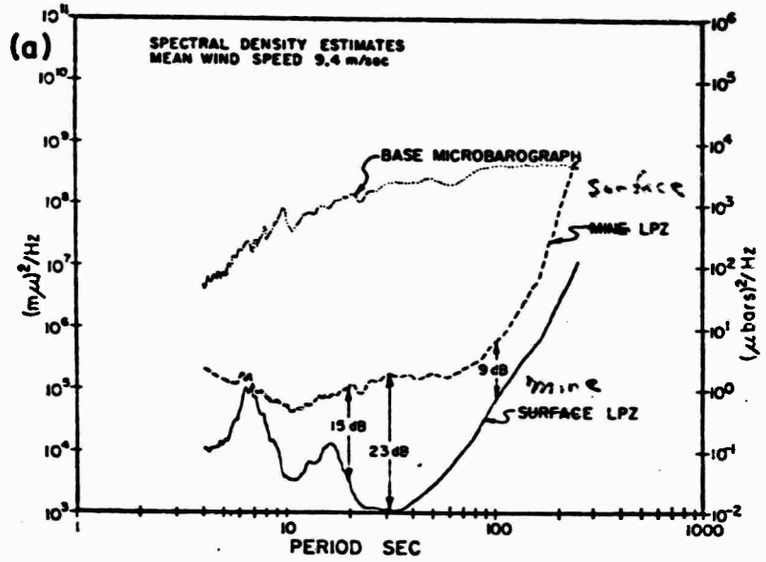
(a)
SPECTRAL DENSITY ESTIMATES
MEAN WIND SPEED 9.4 m/sec
BASE MICROBAROGRAPH
Surface
MLPZ
mine
SURFACE LPZ
9dB
15dB
23dB
(mμ)²/Hz
(μbars)²/Hz
PERIOD SEC

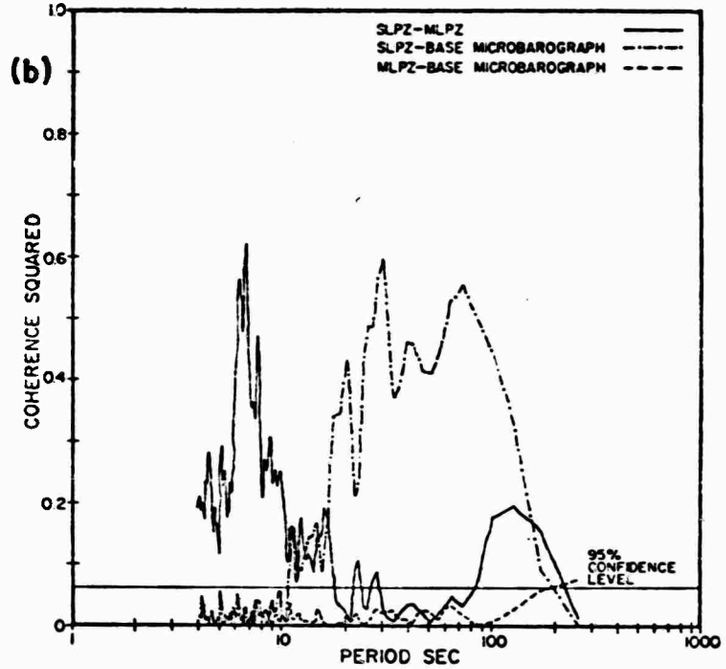
(b)
SLPZ-MLPZ
SLPZ-BASE MICROBAROGRAPH
MLPZ-BASE MICROBAROGRAPH
COHERENCE SQUARED
95% CONFIDENCE LEVEL
PERIOD SEC

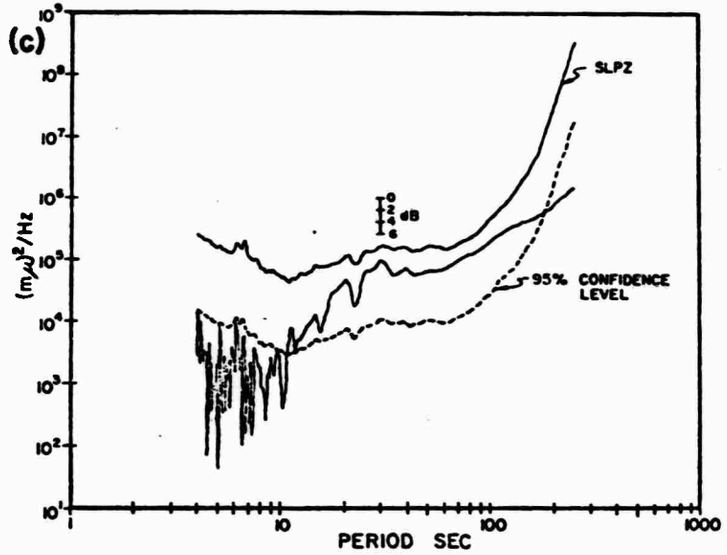
(c)
SLPZ
9dB
95% CONFIDENCE LEVEL
(mμ)²/Hz
PERIOD SEC

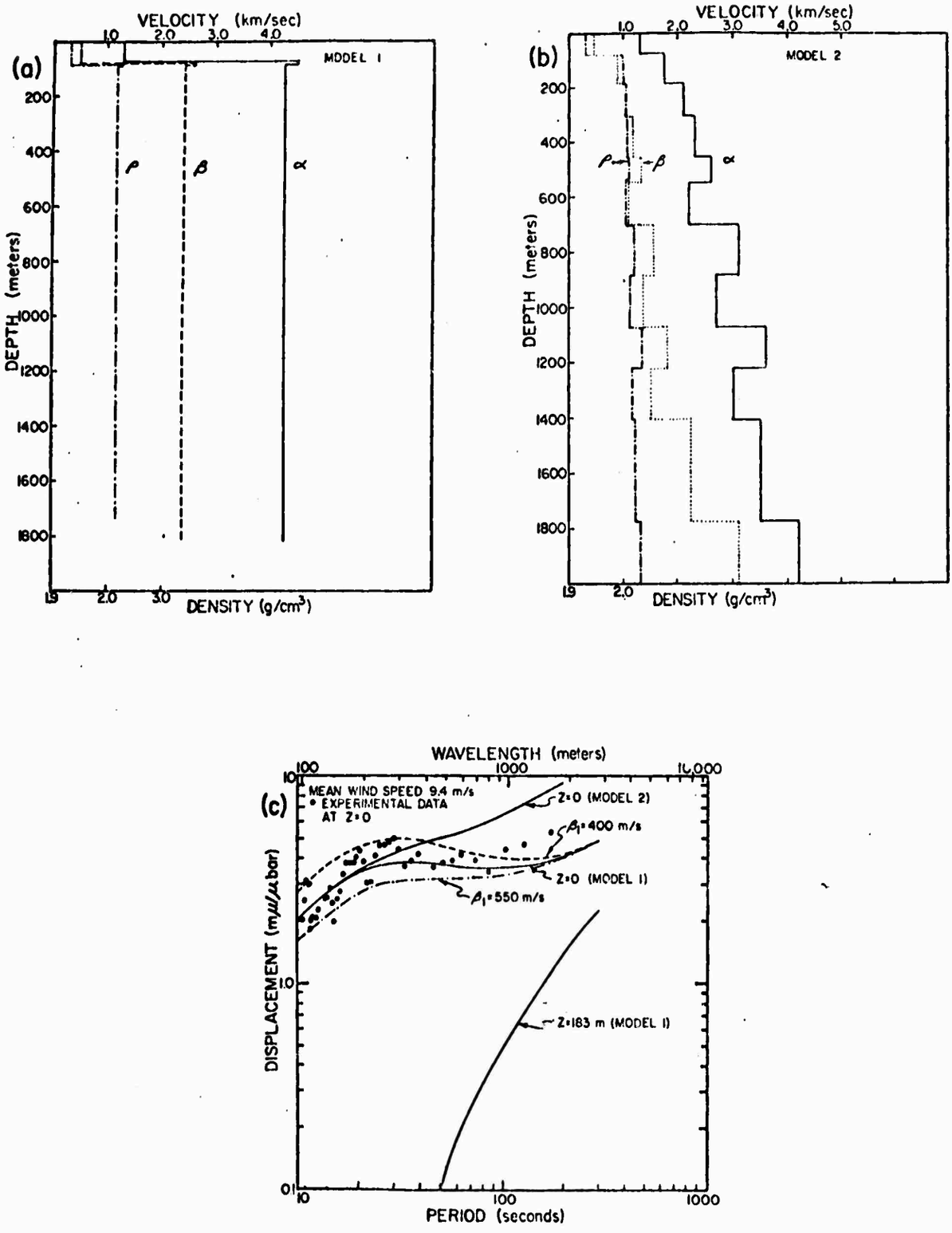
(a)
VELOCITY (km/sec)
1.0
2.0
3.0
4.0
MODEL 1
ρ
β
α
DEPTH (meters)
200
400
600
800
1000
1200
1400
1600
1800
1.9
2.0
3.0
DENSITY (g/cm³)
(b)
VELOCITY (km/sec)
1.0
2.0
3.0
4.0
5.0
MODEL 2
ρ
β
α
DEPTH (meters)
200
400
600
800
1000
1200
1400
1600
1800
1.9
2.0
DENSITY (g/cm³)
(c)
WAVELENGTH (meters)
100
1000
10,000
MEAN WIND SPEED 9.4 m/s
• EXPERIMENTAL DATA AT Z=0
Z=0 (MODEL 2)
β₁=400 m/s
Z=0 (MODEL 1)
β₁=550 m/s
Z=183 m (MODEL 1)
DISPLACEMENT (mμ/μbar)
10
1.0
0.1
10
100
1000
PERIOD (seconds)

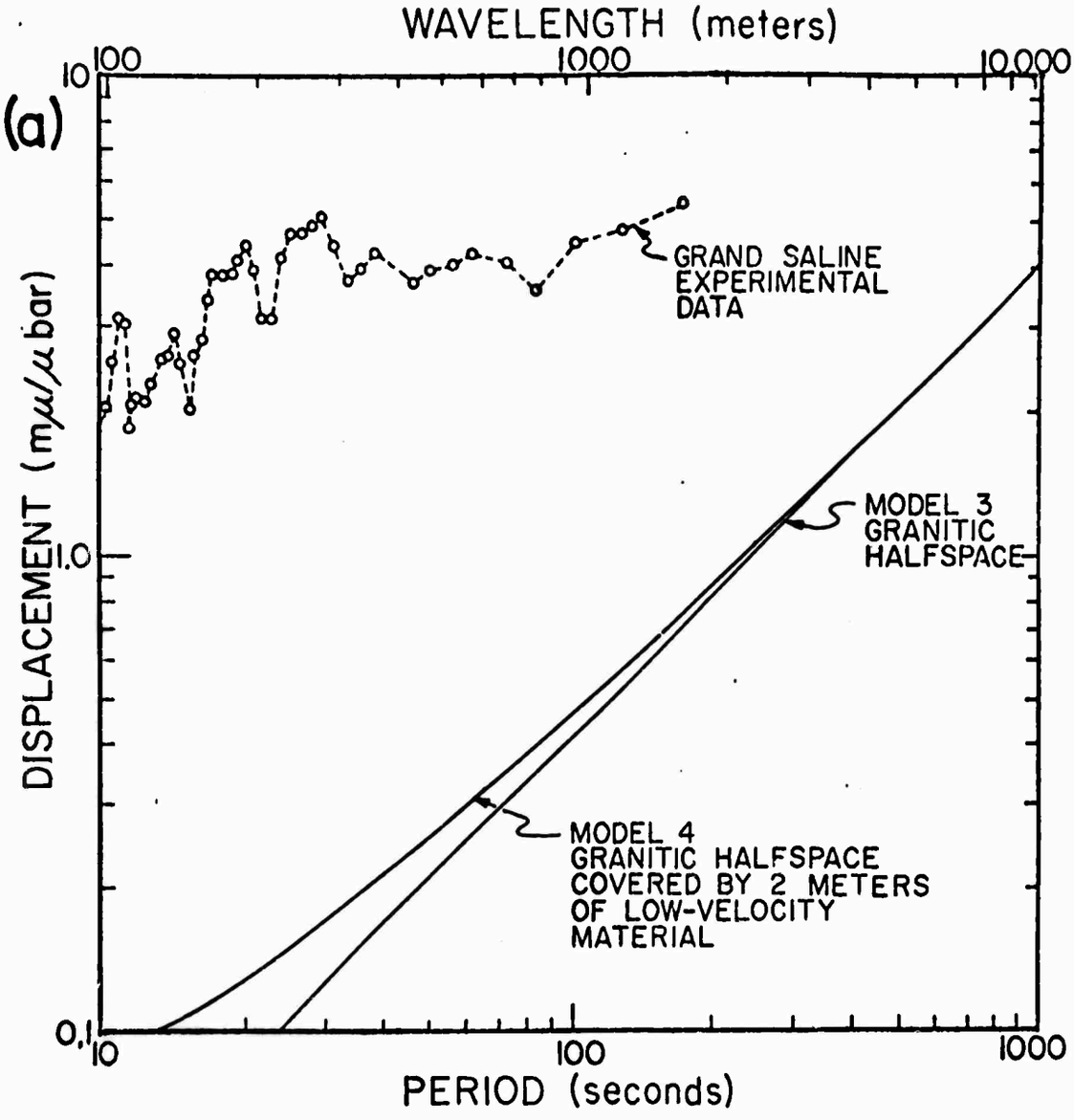

TABLE 1

Model No.	Layer No.	Thickness (meters)	P velocity (km/sec)	S velocity (km/sec)	density (g/cm^3)
3	1	∞	5.56	3.15	2.63
4	1	2	1.5	.5	1.9
	2	∞	5.56	3.15	2.63

A Preliminary Investigation into the Relationship between Long Period Seismic Noise and Local Fluctuations in the Atmospheric Pressure Field.

Gordon G. Sorrells

(In press, Geophysical Journal R. A. S.)

Teledyne-Geotech
3401 Shiloh Road
Garland, Texas 75040

and

Dallas Geophysical Laboratory
Southern Methodist University
Dallas, Texas 75222

Abstract

The displacement response of an elastic halfspace to a plane pressure wave is examined in order to establish the conditions under which sources of this type can contribute significantly to the long period seismic noise field. The study is restricted to pressure waves which propagate at spaces well below the seismic wave velocities characteristic of the halfspace. The numerical studies indicate that pressure waves with amplitudes of 100 μbars or more can contribute significantly to the long period vertical background observed at the surface provided that the detectors are located on sections of alluvial fill or poorly to moderately indurated sandstones and shales whose thicknesses are greater than about a kilometer. These same waves can also create significant tilt noise on long period horizontal seismographs located at or near the surface, regardless of the rock type. The seismic disturbances created by pressure waves decays rapidly away from the surface. Therefore, it appears that it may be possible to eliminate the effects of atmospherically generated noise by placing the detectors at moderate depths.

A Preliminary Investigation into the Relationship between Long Period Seismic Noise and Local Fluctuations in the Atmospheric Pressure Field

INTRODUCTION

In a recent article Capon, (1969), suggested that a significant fraction of the long period seismic noise field observed at the Montana LASA could be generated by local fluctuations in the atmospheric pressure field acting upon the surface of the earth. This hypothesis is examined in the paragraphs below in order to establish the conditions under which it is valid. For the purposes of this preliminary investigation it shall be assumed that the atmospheric pressure field consists of a system of plane waves which propagate at speeds well below the seismic wave speeds characteristic of the medium and that the medium can be approximated by a homogeneous, isotropic, elastic half space. Arbitrary pressure fields and the response of layered media to such fields will be considered at a later date if the outcome of this preliminary investigation justifies the study of more sophisticated models.

THEORY

Let x and z denote cartesian coordinates in directions parallel and normal to the surface of an elastic half space. Let the plane z = 0 coincide with the surface of the half space and take z positive into the medium and x positive to the right of an arbitrarily chosen origin. If a pressure field of the form p(x,t) is imposed upon the surface of the half space then, as shown by Dunkin and Corbin, 1970, the components of the displacement field generated by the disturbance are given generally by

$$U(x,z,t) = \frac{1}{4\pi^2}\int_{-\infty}^{\infty}\int_{-\infty}^{\infty} P(k,\omega) R_u(k,\omega) e^{i\omega t} e^{-ikx}\, dk\, d\omega \qquad (1)$$

$$W(x,z,t) = \frac{1}{4\pi^2}\int_{-\infty}^{\infty}\int_{-\infty}^{\infty} P(k,\omega) R_w(k,\omega) e^{i\omega t} e^{-ikx}\, dk\, d\omega \qquad (2)$$

where U and W are the displacement components in the x and z directions respectively; R_u and R_w are the corresponding medium responses, and P(k,w) is complex frequency wave number spectrum of the source function which is defined by

$$P(k,\omega) = \int_{-\infty}^{\infty}\int_{-\infty}^{\infty} p(x,t) e^{-i\omega t} e^{ikx}\, dx\, dt \qquad (3)$$

In the case of a homogeneous and isotropic elastic half space which is characterized by a compressional wave velocity α, a shear wave velocity β and a density ρ, the medium response functions are (Ewing, Jardetsky & Press, 1957).

$$R_u(k,\omega,z) = -\frac{i}{\mu}\,\frac{k\left[(2k^2-k_\beta^2)e^{-\nu z} - 2\nu\nu' e^{-\nu' z}\right]}{(2k^2-k_\beta^2)^2 - 4k^2\nu\nu'} \qquad (4)$$

$$R_w(k,\omega,z) = -\frac{1}{\mu}\,\frac{\nu\left[(2k^2-k_\beta^2)e^{-\nu z} - 2k^2 e^{-\nu' z}\right]}{(2k^2-k_\beta^2)^2 - 4k^2\nu\nu'} \qquad (5)$$

$$k_\beta^2 = \frac{\omega^2}{\beta^2} \tag{6}$$

$$\gamma^2 = k^2 - \frac{\omega^2}{\alpha^2} \tag{7}$$

$$\gamma'^2 = k^2 - k_\beta^2 \tag{8}$$

$$\mu = \beta^2 \rho \tag{9}$$

Suppose that the pressure field is a plane wave which travels at a speed c, where $c << \beta$.

The complex frequency wave number spectrum of this particular field is given by

$$P(k,\omega) = \int_{-\infty}^{\infty}\int_{-\infty}^{\infty} P(t-\tfrac{x}{c})\, e^{-i\omega t}\, e^{ikx}\, dt\, dx \tag{10}$$

The right side of equation 10 may be integrated to yield

$$P(k,\omega) = 2\pi\, P(\omega)\, \delta(k-\tfrac{\omega}{c}) \tag{11}$$

Now using equation 11 to replace the appropriate terms in equations 1 and 2 and performing the indicated integration over the variable k yields

$$U(x,z,t) = \frac{1}{2\pi}\int_{-\infty}^{\infty} P(\omega)\, R_u(\omega,\tfrac{\omega}{c},z)\, e^{i\omega(t-\frac{x}{c})}\, d\omega \tag{12}$$

$$W(x,z,t) = \frac{1}{2\pi}\int_{-\infty}^{\infty} P(\omega)\, R_w(\omega,\tfrac{\omega}{c},z)\, e^{i\omega(t-\frac{x}{c})}\, d\omega \tag{13}$$

A further simplification is possible. Since it has been assumed that c is much less than the elastic wave velocities of the medium a satisfactory expression for the medium responses in equations 12 and 13 can be obtained by expanding these functions in powers of $\frac{c}{\alpha}$ and $\frac{c}{\beta}$ and neglecting all terms in which these ratios are raised to powers greater than 2. To this degree of

approximation it can be shown that the components of displacement given by equations 12 and 13 become

$$U(x,z,t) = \frac{ic}{4\pi\mu}\int_{-\infty}^{\infty}\frac{P(\omega)}{|\omega|}\left(\frac{\alpha}{\lambda+\mu}-\frac{|\omega|}{c}z\right)e^{-\frac{|\omega|}{c}z}e^{i\omega(t-\frac{x}{c})}\,d\omega \quad (14)$$

$$W(x,z,t) = -\frac{c}{4\pi\mu}\int_{-\infty}^{\infty}\frac{P(\omega)}{|\omega|}\left(\frac{\lambda+2\mu}{\lambda+\mu}+\frac{|\omega|}{c}z\right)e^{-\frac{|\omega|}{c}z}e^{i\omega(t-\frac{x}{c})}\,d\omega \quad (15)$$

Equations 14 and 15 describe a seismic disturbance which propagates at the same rate as the imposed pressure field. It may be readily verified that this disturbance is identical in form to that created by a static load p(x) imposed upon the surface of the half space (cf, Sneddon, 1951). Furthermore, it is important to note that in this particular case there is no energy transport by the normal seismic waves (i.e., waves traveling at speeds α or β or the Rayleigh wave velocity). To an observer moving at the same speed as the load, the disturbance would remain fixed and would be identical to that created by a static load.

DISCUSSION

Let us restrict our attention to one sinusoidal component of the pressure disturbance. If this component has a pressure amplitude of P_o microbars, a frequency of oscillation ω_o $\frac{\text{radians}}{\text{sec}}$ and propagates a speed of c_o meters/sec it is clear from equations 14 and 15 that the associated displacement components will be

$$U(x,z,t) = \frac{i c_o P_o}{2\mu} \frac{\left(\frac{\mu}{\lambda+\mu} - \frac{|\omega_o| z}{c_o}\right) e^{-\frac{|\omega_o|}{c_o} z} e^{i\omega_o\left(t - \frac{x}{c_o}\right)}}{|\omega_o|} \tag{16}$$

$$W(x,z,t) = -\frac{c_o P_o}{2\mu} \frac{\left(\frac{\lambda+2\mu}{\lambda+\mu} + \frac{|\omega_o| z}{c_o}\right) e^{-\frac{|\omega_o|}{c_o} z} e^{i\omega_o\left(t - \frac{x}{c_o}\right)}}{|\omega_o|} \tag{17}$$

which at the surface reduce to

$$U(x,0,t) = \frac{i c_o P_o}{2(\lambda+\mu)} \frac{e^{i\omega_o\left(t - \frac{x}{c_o}\right)}}{|\omega_o|} \tag{18}$$

$$W(x,0,t) = -\frac{c_o P_o (\lambda+2\mu)}{2\mu(\lambda+\mu)} \frac{e^{i\omega_o\left(t - \frac{x}{c_o}\right)}}{|\omega_o|} \tag{19}$$

Equations 18 and 19 have been used to compute the amplitude of the displacement components for the models whose elastic properties are listed in table I. For the purposes of these computations it is assumed that $P_o = 1$, $c_o = 5$ and that ω_o takes on values between $\frac{\pi}{10}$ and $\frac{\pi}{50}$. The corresponding period range is from 20 to 100 seconds. The results are displayed in figures 1 through 4, where the vertical and horizontal components of displacement are plotted as a function of period.

Model 1 is clearly an extreme case and was included to show the worst possible conditions. As shown in figure 1 this model is quite sensitive to small changes in atmospheric pressure. For instance, in the period range 20-40 seconds, the average vertical displacement is 80 mμ for a pressure amplitude of 1 μbar. In the same range the average horizontal displacement is 10 mμ/μbar. These results imply that one of the reasons that long-period installations located on thick sections of alluvial fill are generally characterized by high noise levels is that the unit is quite sensitive to small changes in atmospheric pressure.

Models 2a-2b have velocities and densities characteristic of many sandstone shale sequences found in the mid-continent and Gulf Coast regions of the United States. Model 2b differs from 2a only in that the shear wave velocity has been increased to 1 km/sec. The curves shown in figure 2 indicate that the pressure sensitivity of these models is considerably lower than the unconsolidated sediments model.

In the period range 20-40 seconds the average vertical displacement is about 1 mμ/μbar for model 2a and 0.6 mμ/μbar for model 2b. However, if we assume pressure amplitudes on the order of 100 μbars, the corresponding vertical displacements of the surface would be 100 and 60 mμ for models 2a and 2b. Now, in general, the vertical seismic background observed at periods greater than 25 seconds is somewhere on the order of 100-200 mμ. Thus pressure waves with

of 100 μbars or more can generate a significant fraction of the seismic background at periods greater than 25 sec, if the installations happens to be located on a thick section of moderately to poorly indurated sandstones and shales. By thick, it is meant that the dimensions of section are much larger than the wavelength of the disturbance. For the periods and speeds considered above the corresponding wavelengths would be less than 200 meters. Consequently, these results could be applied to sections whose dimensions are as small as a kilometer. It is important to note that the shallow structure beneath the Montana LASA is quite similar to that used in model 2b at least down to depths of about 1.5 km (cf, Glover and Alexander, 1968). Thus, it appears reasonable to expect that, at the Montana LASA, atmospherically generated seismic noise can contribute significantly to the vertical long period noise spectrum, as suggested by Capon (1969).

The situation is quite different for the more competent rocks which are represented by models 3 and 4. As shown in figures 3 and 4, the sensitivity of these models to atmospheric pressure fluctuations has been reduced by about an order of magnitude relative to the sandstone-shale models considered previously. Therefore, in rocks of this type, displacements caused by atmospheric loading cannot contribute significantly to the long-period seismic noise background unless the pressure amplitudes are on the order of a millibar or more.

The previous paragraphs have been concerned with the displacements at the surface of the earth caused by a plane pressure wave. These waves also produce tilts, which can be a major source of noise on the long-period horizontal seismograph system. The tilts produced by a plane pressure wave may be determined in the following way.

Let $\theta(x,z,t)$ be the angle of tilt measured from the horizontal.

Then $\text{Tan}\ \theta = \frac{\partial W}{\partial x}$

or using eq. 17

$$\text{Tan}\ \theta = \frac{i P_0}{2\mu}\left(\frac{\lambda+2\mu}{\lambda+\mu} + \frac{|\omega_0|}{c_0}z\right) e^{-\frac{|\omega_0|}{c_0}z}\, e^{i\omega_0\left(t-\frac{x}{c_0}\right)} \qquad (20)$$

Since θ is generally small

$$\text{Tan}\ \theta \approx \theta$$

Consequently at z = 0

$$\theta \approx \frac{i P_0}{2\mu}\,\frac{\lambda+2\mu}{\lambda+\mu}\, e^{i\omega\left(t-\frac{x}{c_0}\right)} \qquad (21)$$

Thus at the surface the amplitude of the tilt is dependent only upon the elastic constants of the medium and the pressure amplitude and is independent of frequency. The tilts associated with a 1 μbar pressure amplitude in each of the 4 models described above is listed in table 2.

It can be seen from this table the tilts at the surface are quite small. However, because of the tilt sensitivity of the long-period horizontal seismometer, even these small tilts can produce large apparent horizontal displacements. Rodgers (1968) has shown that the apparent horizontal displacements caused by tilt is given

by

$$U_\theta = \frac{g T^2}{4\pi^2} \Theta \qquad (22)$$

where U_θ is the apparent horizontal displacement; g is the local value of gravity and T is the period of the oscillation. U_θ was computed for models 1 through 4 using the values of Θ listed in table 2 and g = 980 $\frac{cm}{sec^2}$. The resulting values are plotted as a function of increasing period in figure 5. The apparent displacements are surprisingly large. A pressure change as small as one μbar in the period range from 20 to 40 seconds can generate 340 to 1200 mμ of noise at the surface of a half space characterised by the parameters of model 1. In the same period range, the noise caused by a one μbar pressure change at the surface of a half space characterised by the elastic parameters of model 2a would increase from about 5 mμ at 20 seconds to 18 mμ at 40 seconds. At the surface of the more competent units which are represented by models 3 and 4 a one-μbar pressure change would generate less than a mμ of noise. However, it is interesting to note that even in the most competent unit pressure variations of the order 100 μbars can generate as much as 100 mμ of noise. It would appear, therefore, that during intervals of moderate turbulence the apparent horizontal displacements caused by pressure related tilts will contribute significantly to the long period noise field observed by a horizontal seismograph, regardless of the properties of the medium.

2.3 ATTENUATION WITH DEPTH

An interesting feature of the half space response to slowly moving plane pressure waves is the rate at which the disturbance decays away with depth. Let $G_w(z)$ denote the ratio of the vertical displacement at a depth z to the vertical displacement at the surface. Then from eqs. 17 and 19

$$G_w(z) = \frac{\left(\frac{\lambda+2\mu}{\lambda+\mu} + \frac{|\omega_0|}{c_0}z\right)}{\frac{\lambda+2\mu}{\lambda+\mu}} e^{-\frac{|\omega_0|}{c_0}z} \qquad (23)$$

Similarly, if $G_u(z)$ denotes the ratio of the horizontal displacement at depth z to the horizontal displacement at the surface, then from equations 16 and 18

$$G_u(z) = \frac{\left(\frac{\mu}{\lambda+\mu} - \frac{|\omega_0|}{c}z\right)}{\frac{\mu}{\lambda+\mu}} e^{-\frac{|\omega_0|}{c}z} \qquad (24)$$

If we let $G_\theta(z)$ define a similar ratio for the tilts it is clear from eqs. 20 and 21 that

$$G_\theta(z) = G_w(z) \qquad (25)$$

$G_w(z)$ is plotted as a function of z in figure 6 for the cases where $c = 5$, $\frac{\lambda+2\mu}{\lambda+\mu} = 1.0$ and 1.5, and for periods 20, 40, and 60 secs. Generally, the results show that the attenuation with depth is weakly dependent on the elastic properties of the medium. The values 1.0 and 1.5 span the practical range of values that the ratio $(\lambda + 2\mu)/(\lambda + \mu)$ can assume for rocks, with the higher values being associated with the more competent rocks. It can be seen from the curves in this figure that the differences in attenuation with depth between poorly consolidated and competent rocks is only 2 dB.

Furthermore, the seismic disturbance will decay rapidly with increasing depth. For example, at a depth of 100 meters (328 ft.), the amplitude of a 20-second period sinusoid would be 40 dB below the amplitude observed at the surface. At the same depth, waves with periods of 40 and 60 seconds would be reduced by about 11 and 6 dB, respectively. However, in order to obtain a 40 dB reduction of the noise generated by atmospheric pressure variations over the period range from 20 to 60 seconds, the detectors would have to be placed at least 300 meters deep.

These results suggest that in regions where local atmospherically generated seismic noise can be anticipated to be significant at the surface (i.e., in regions of thick sandstone-shale sequences or alluvial fill) much of this type of noise can be eliminated by placing the detector at moderately shallow depths.

One further point requires emphasis. Recently there has been considerable interest in extending the response of long-period systems to cover a pass band from 30 to 100 seconds (cf. Pomeroy et al, 1969). From eqs. 16 and 17 it is seen that the displacement response of the half space increases linearly with increasing period. Furthermore, eq. 22 shows that the tilt response of the horizontal seismograph system will increase as the square of the period. Consequently, on the basis of these results, one can anticipate that atmospherically generated seismic noise will place severe restrictions on the magnifications that can be obtained with ultra long-period systems which are operated near the surface.

CONCLUSIONS

The basic purpose of this initial study was to determine the conditions under which the displacements and tilts generated by plane pressure waves can contribute significantly to the long-period noise field. On the basis of the results presented in the previous paragraphs it appears that the vertical displacements generated by these waves can contribute significantly to the long-period noise field provided that

a. the installation is located at or near the surface of a section of alluvial fill or poorly to moderately indurated sanstones and shales which is at least 1 km thick, and

b. the pressure amplitudes are of the order of 100 μbars or greater.

Pressure waves with amplitudes of the order of 100 μbars will also create significant tilt noise on long-period horizontal seismograph systems located at or near the surface, regardless of the rock type. However, the noise will be much less severe on competent units.

The results also show that the seismic disturbances created by plane pressure waves will decay rapidly with depth. Furthermore, the rate of decay is virtually independent of the rock type. The implications are that the contribution of atmospherically generated noise to the long-period background can be virtually eliminated for periods less than a minute by placing the detectors

at depths on the order of 300 meters.

Finally, it appears that atmospherically generated noise will be more severe on ultra long-period systems than on presently operating systems.

These results are considered to be sufficiently significant to warrant the study of the response of more complex media to more realistic pressure fields. Consequently, numerical techniques to compute the response of layered media to arbitrary pressure fields are being developed.

BIBLIOGRAPHY

Capon, J., 1969, Investigation of long period noise at LASA, Jour. Geophys. Res. Vol. 74, No. 12, p. 3182-3193.

Dunkin, J. W. and D. G. Corbin, 1970, Deformation of a layered elastic halfspace by uniformly moving line loads, Bull. Seis. Soc. Am., Vol. 60, No. 1, pp. 167-191.

Ewing, W. M., W. S. Jardetzky, and F. Press, 1957, Elastic waves in layered media. McGraw Hill Book Co., New York, p. 380.

Glover, P. and S. S. Alexander, 1968, Lateral variations in crustal structure beneath the Montana LASA, Seismic Data Laboratory Rpt. No. 205, p. 20.

Pomeroy, Paul W., G. Hade, J. Savino, and R. Chander, Preliminary results from high gain wide band long period electromagnetic seismograph systems, Jour. Geophys. Res. Vol. 74, No. 12, p. 3295 - 3298.

Rodgers, P. W., 1968, The response of the horizontal pendulum seismometer to Rayleigh and Love waves, tilt, and free oscillations of the earth, Bull. Seis. Soc. Am., Vol. 58, No. 5, p. 1385 - 1406.

Sneddon, I. N., 1951, Fourier Transforms; McGraw Hill Co., New York, p. 542.

Table 1. Parameters of the models used to compute vertical and horizontal components of displacement

Model No.	α km/sec	β km/sec	ρ g/cm^3	Geology
1	0.3	0.1	1.6	Unconsolidated sediments
2a	2.9	0.7	2.3	Sedimentary rock
2b	2.9	1.0	2.3	Sedimentary rock
3	4.8	2.8	2.3	Sedimentary rock
4	5.8	3.25	2.85	Granites

Table 2. Tilts caused by a plane pressure wave with a 1 μbar amplitude

Model No.	Tilt (radians)
1	3.5×10^{-9}
2	4.6×10^{-11}
3	3.5×10^{-12}
4	2.2×10^{-12}

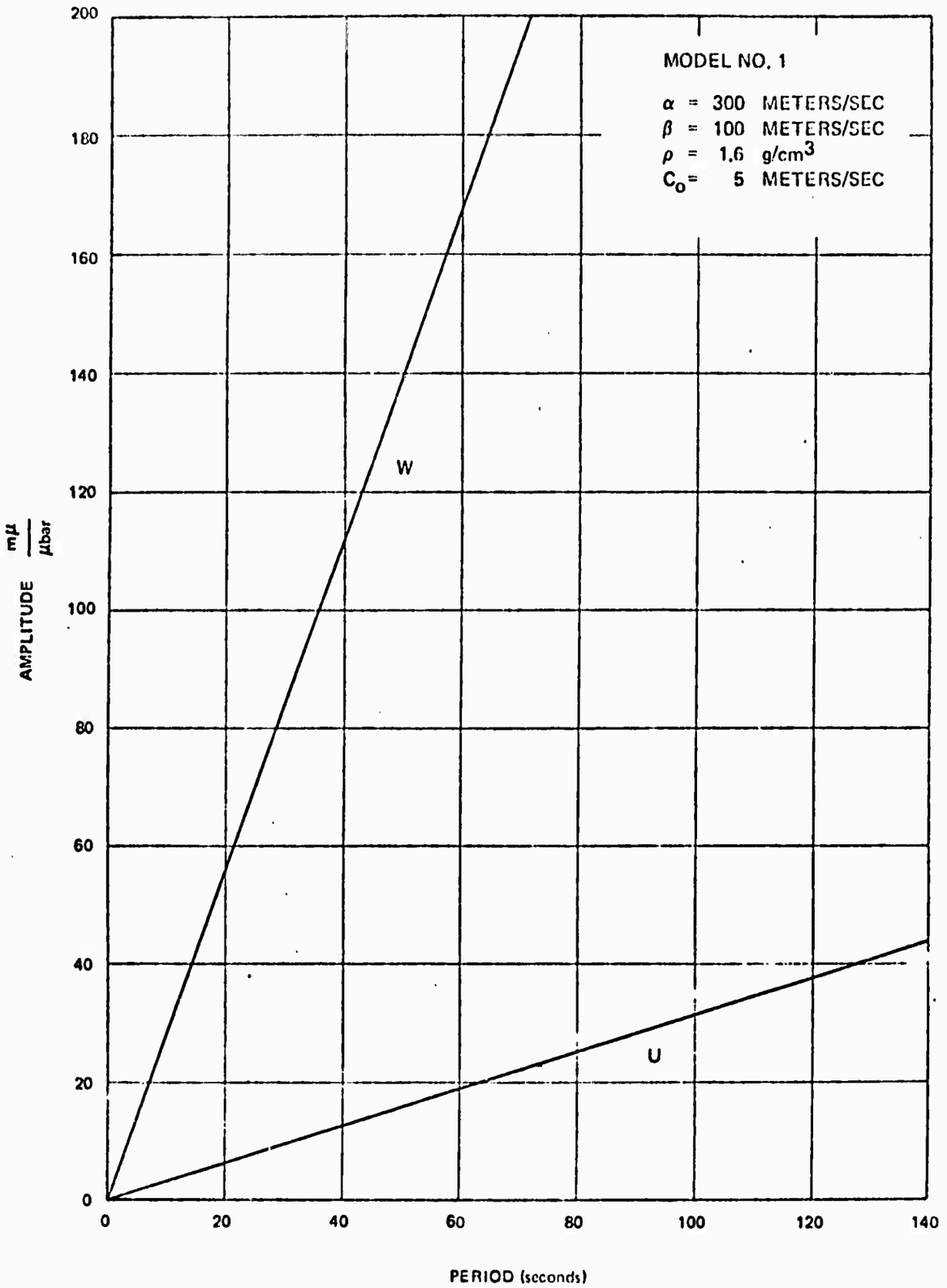

Figure 1. Surface displacement response of a half space consisting of unconsolidated sediments.

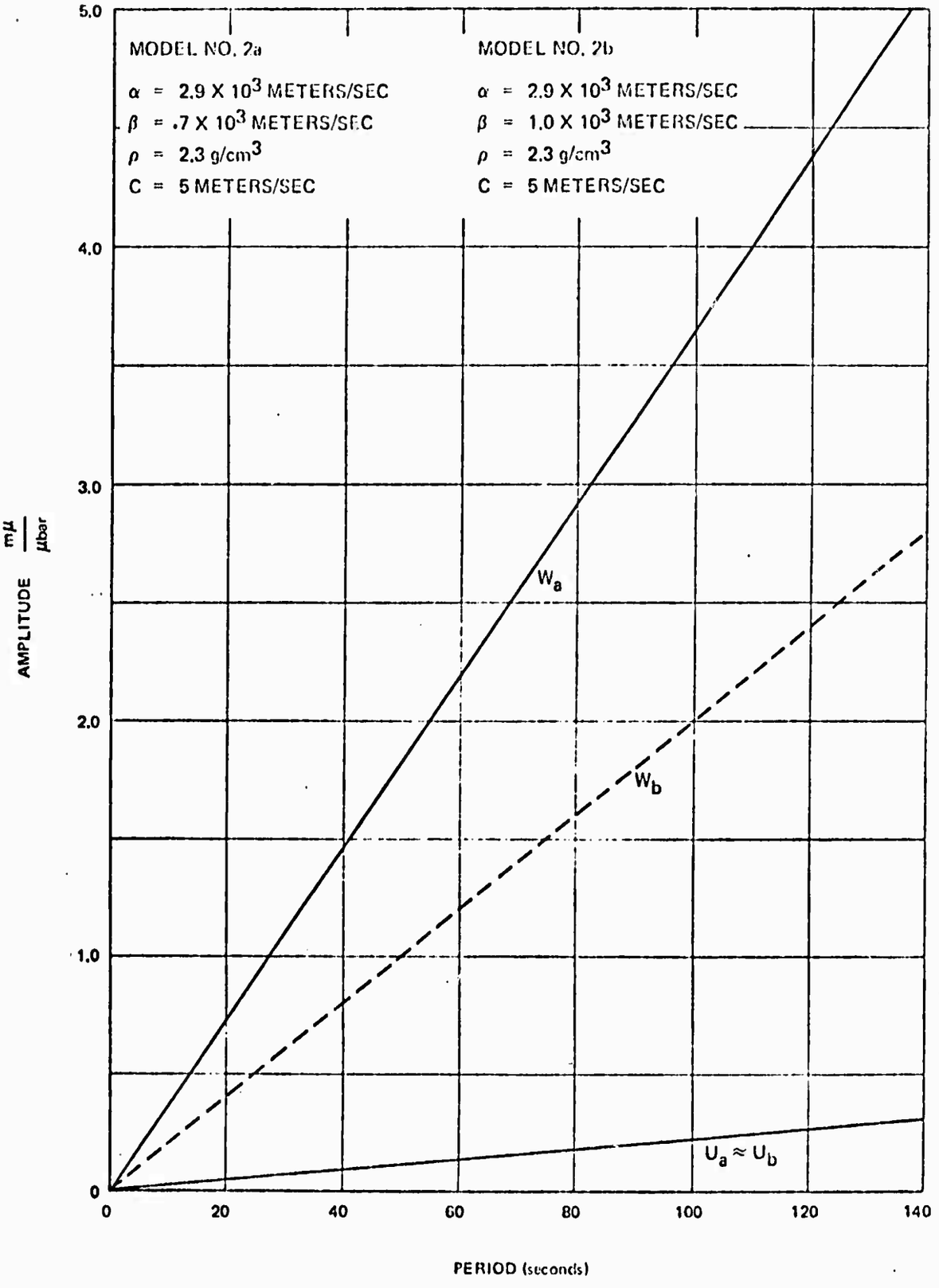

Figure 2. Surface displacement response of a weak sandstone shale half space

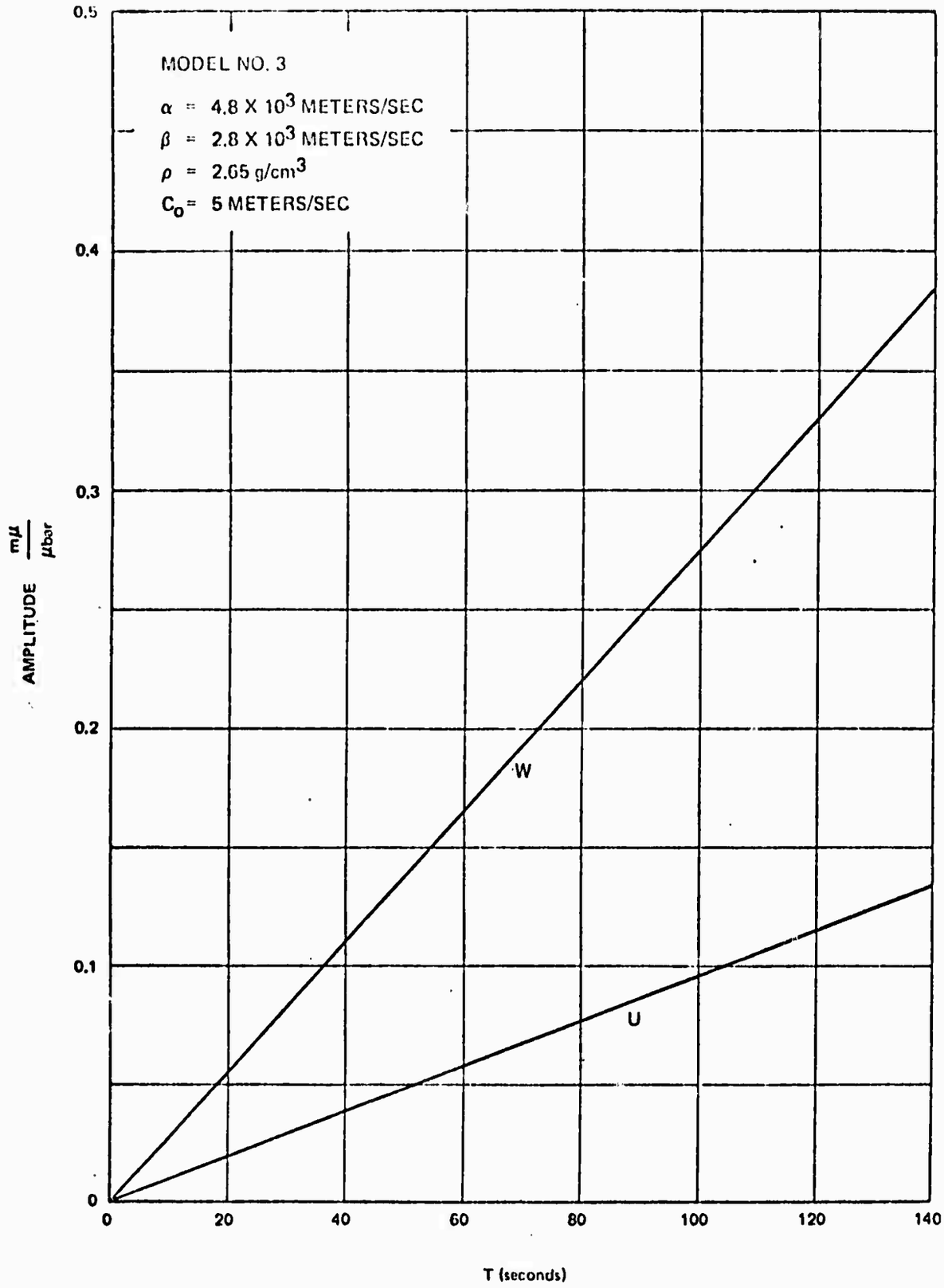

Figure 3. Surface displacement response for a competent sedimentary rock half space

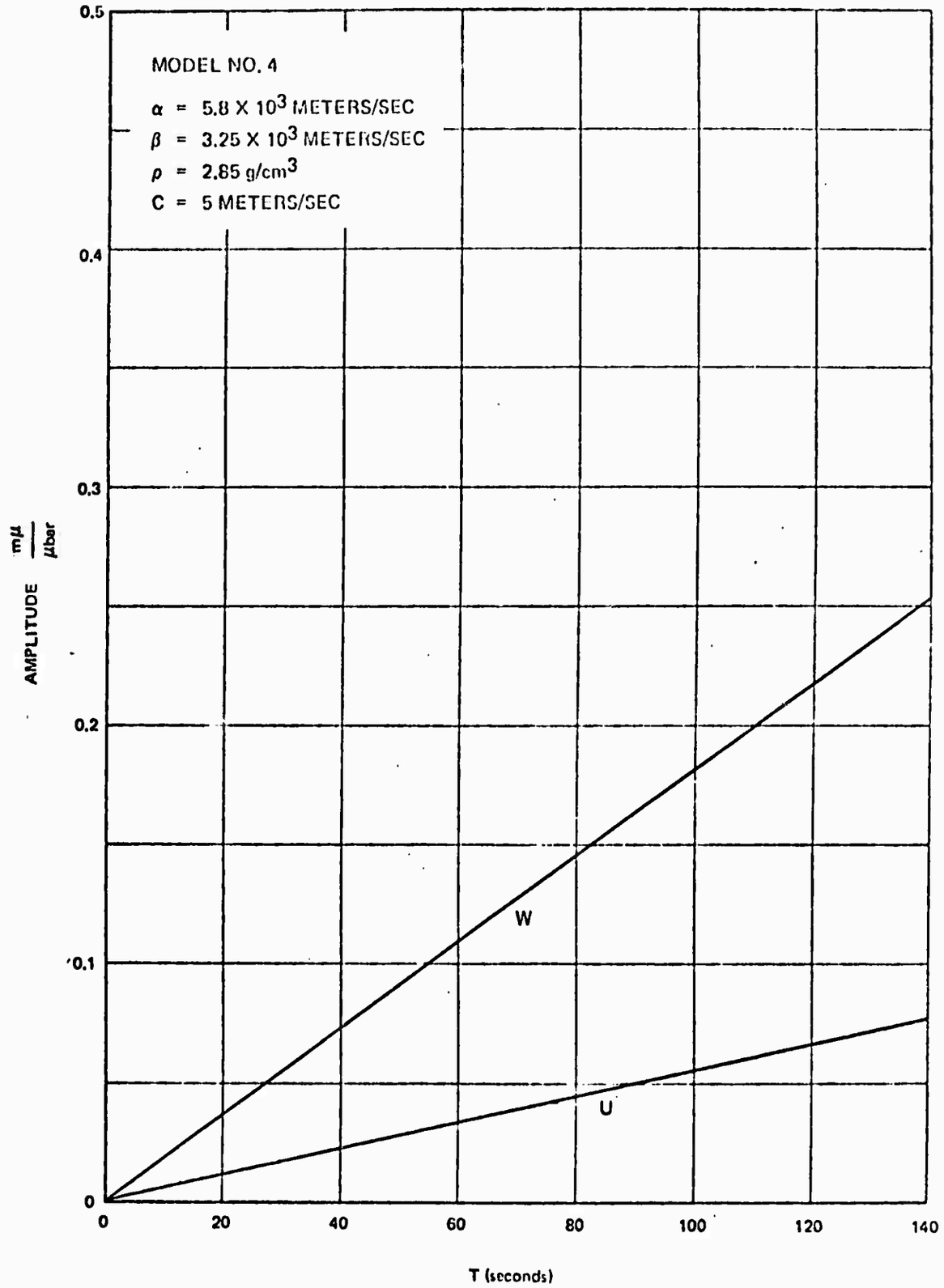

Figure 4. Surface displacement response for a granitic half space

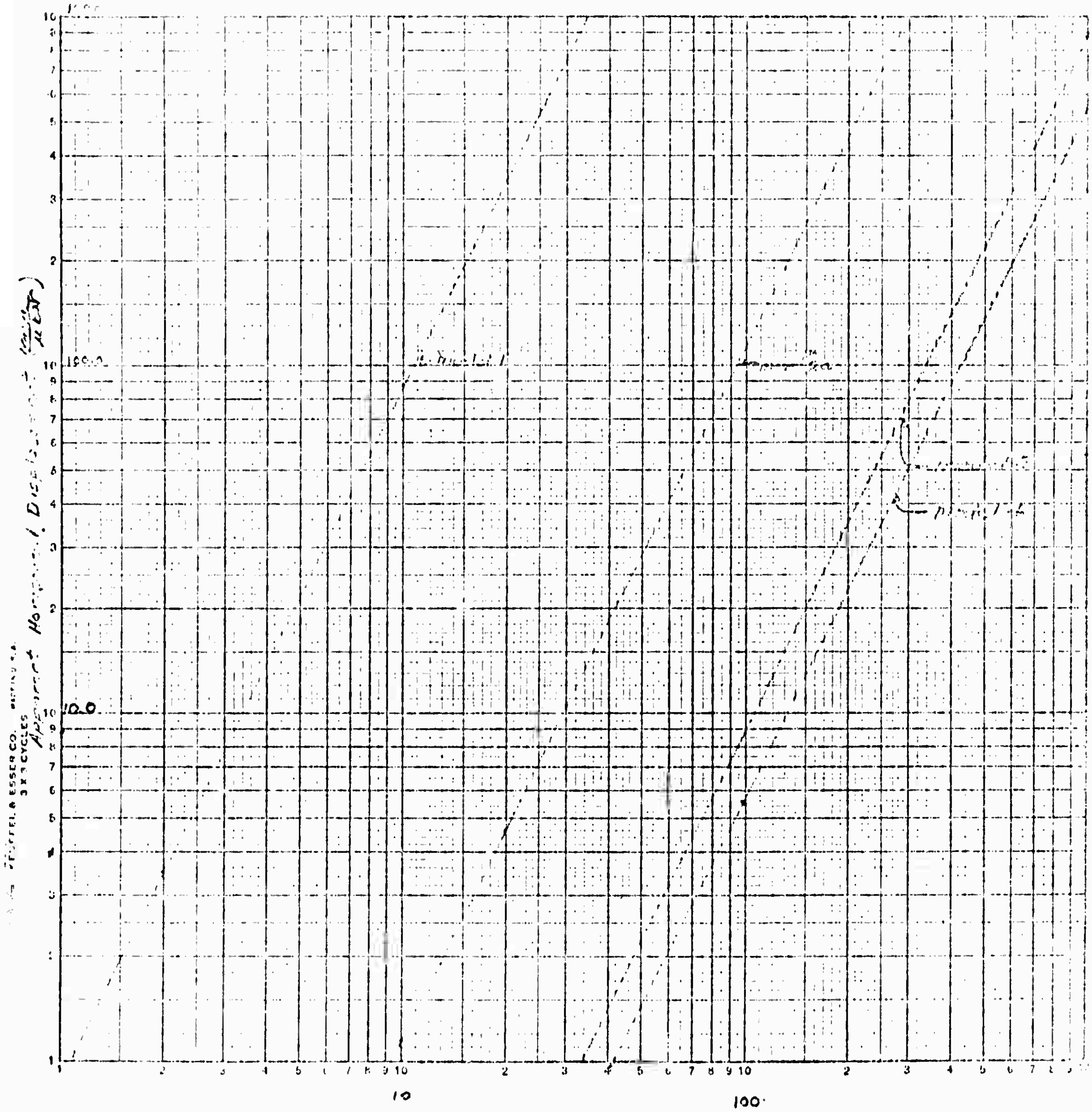

Fig. 5. Apparent Horizontal Displacement [illegible]

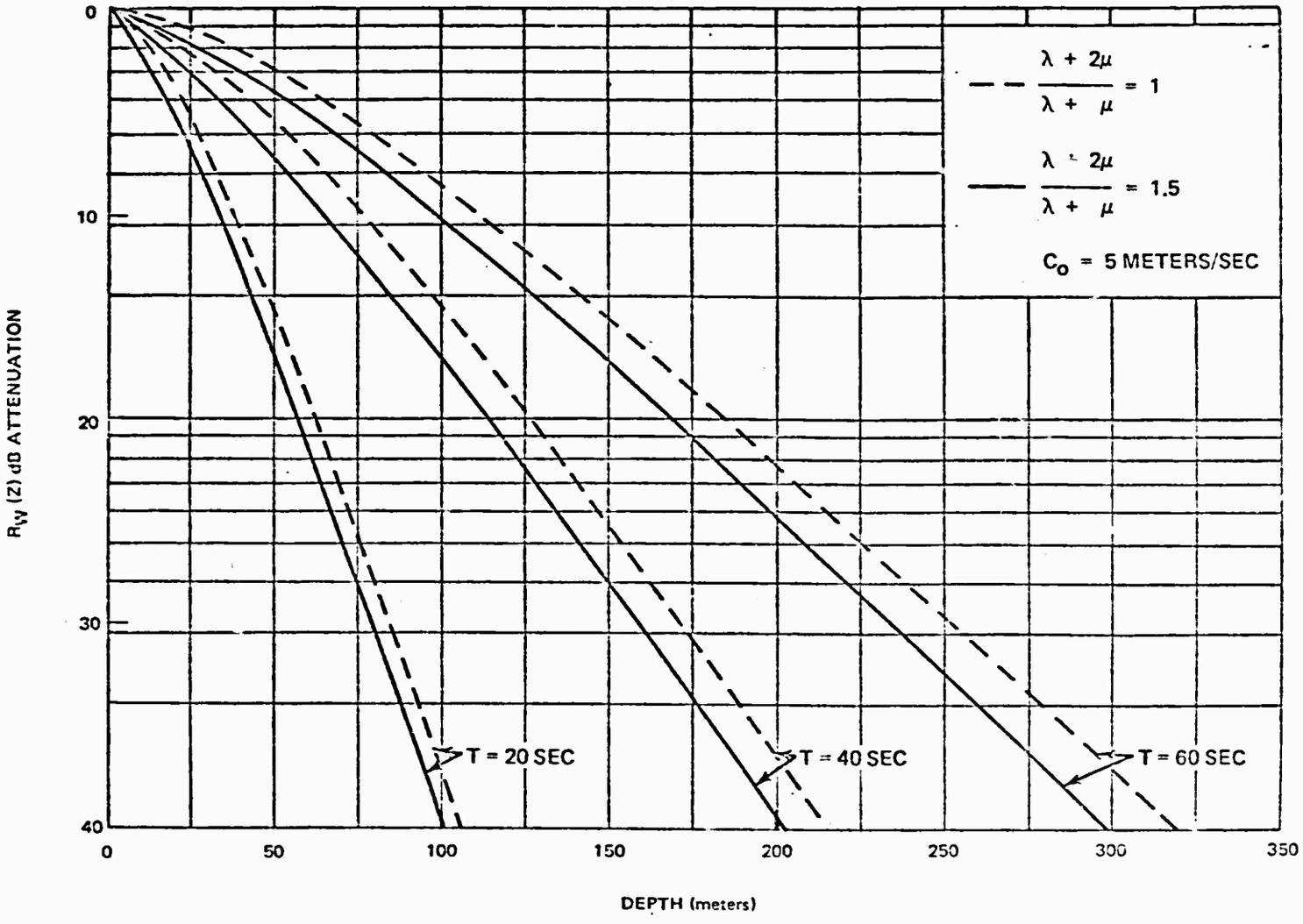

Figure 6. Attenuation of vertical displacements and tilts with depth

A DIGITAL SYSTEM FOR THE ACQUISITION AND PROCESSING OF GEOACOUSTIC DATA

Eugene Herrin

John A. McDonald

(In press, Geophysical Journal R. A. S.)

Dallas Geophysical Laboratory
Southern Methodist University
Dallas, Texas 75222

ABSTRACT

In the fall of 1969 we accepted delivery of three TC-200 digital data acquisition systems from Geotech-Teledyne. These systems can record up to 16 channels of long period, digital data with a specified sampling rate (currently 1 per sec) on magnetic tape in an "IBM compatible" format. Identifying headers are automatically written at the beginning of each file on tape and Universal Time is written each minute. The actual dynamic range of the recording system is about 70 dB, but an operating range of 120 dB is automatically assured by the use of binary, gain-ranging amplifiers. The systems have been tested and are now operating satisfactorily at Blacknest Laboratory near Reading in England, at the University of Alaska and at a field site east of Dallas, Texas.

INTRODUCTION

In 1969 we composed a set of specifications for a digital system expressly designed to acquire infrasonic and seismic data in a period range from 1 to 1000 sec. Three systems, trade-named TC-200, were designed and built by Geotech-Teledyne of Garland, Texas, and delivered for field tests in early 1970. All three are now in operation at a field site near Dallas (Canton Experiment), at the University of Alaska, and at Blacknest Laboratory (U.K.A.E.A.) near Reading in Berkshire, England.

The TC-200 system which we have operated at field sites east of Dallas has been very reliable and has provided data of superior quality. In fact, we cannot imagine how experiments which have been carried on at these sites during the last year could have been attempted without such a data acquisition system. While the hardware was being constructed and tested, software was being written for use in acquiring, quality controlling and processing the long period information. In March of 1970 field

testing was completed, and the system has operated routinely since that time. The following sections provide a general description the TC-200 geoacoustic data acquisition systems.

DATA ACQUISITION SYSTEM

Hardware: A block diagram of the TC-200 is shown in Figure 1 and a photograph of the system is shown in Figure 2. Sixteen inputs channels are available, and in the system we have used for our field studies, there are 8 FM and 8 analog input modules. The FM discriminators operate with a center frequency 1550 Hz and ± 45% deviation for a maximum output of ± 10 V. The dynamic range is 70 dB (peak to peak noise to 20 V p-p) from 0.001 Hz to 0.5 Hz, the passband required in our studies of infrasonics. The discriminators are followed by high-pass filters having a 3dB downpoint at 0.001 Hz and a rolloff of 6 dB/oct.

The direct analog input modules are balanced and have 10 Kohm nominal input impedance. Equival ent input noise is less than 15μ V rms in the passband of 0.01 Hz to 0.5 Hz. The input offset is adjustable to within ± 25μ V.

All 16 input modules are followed by anti-alias filters. These units are low pass filters with a 3 dB down point at 0.5 Hz and a roll-off of 30 dB/oct. Data sampled at a rate of 1 sample per sec may show significant aliasing at periods between 2 and 4 sec. At a sampling rate of 4 per sec, there should be no possible aliasing. With our currently available TC-200 software, we can

select sampling rates of 4, 2 or 1 per sec.

A TC-203 analog multiplexer follows the anti-alias filters. Upon command, this unit switches to any one of 16 channels and after a very short delay provides a channel-ready pulse to the anolog-to-digital converter. The command to switch and the channel code is provided by the Raytheon 703 Central Processing Unit (CPU). Analog voltages thus selected are converted to a 16 bit computer word which contains 4 bits of gain information and 11 bits, plus sign, of data. The details of this conversion process are described in the next paragraph.

Upon receipt of the channel ready pulse from the multiplexer, the binary gain amplifier (BGA) is set to unity gain and its output is tracked and held by the sample and hold amplifier (SHA). The voltage is then converted to digital form using 11 bits plus sign. The analog to digital converter (ADC) then resets the gain of the BGA such that its output will lie between 1/4 and 1/2 full scale (between 2.5 and 5.0 volts, positive or negative). The SHA again tracks and holds the BGA output and another conversion is made by the ADC. The computer input driver then transmits a 16 bit word consisting of a 4 bit gain character followed by 11 bits plus sign (twos complement) to the CPU. The central processer stores the word in core, readdresses the analog multiplexer

and, after the sampling cycle is complete, transmits the information to the tape unit. The sampling cycle is initiated by an interrupt pulse provided by the timing system interface unit.

The binary gain-ranged amplifier (TC-214) is a low-noise amplifier with eleven gain settings in binary steps from X1 to X1024. When the gain is set a binary gain word is provided along with the analog output voltage as illustrated below:

Gain Word	Gain Selected
0000	1
0001	2
0010	4
0011	8
⋮	⋮
1001	512
1010	1024

The maximum output voltage from the BGA is ± 5V for all gain settings except X1 for which ± 10V is allowed. When used with the 12 bit ADC, as is done in our TC-200, the actual dynamic range approaches 70 dB; however, the gain-ranging capability allows an operating range of about 120 dB. The 70dB data word is effectively positioned within this operating range on a sample by sample basis. All inputs to the TC-200 are conditioned so that the analog level at the multiplexer will not exceed ± 10V, thus

///

no gain adjustment are ever required, even for input levels less than a millivolt.

The sample and hold amplifier (TC-213) has an aperture time of less than 50 nanosec and will reacquire a voltage after switching from the hold mode in less than 10 μsec. The analog to digital converter (TC-201) is capable of 20,000 conversions per sec.

Recording is on a Peripheral Equipment Corporation (PEC) 7-track, 556 ips tape unit. The tape drive and controller has incremental-write and synchronous-read capability when used with the Raytheon 703 CPU. The recording format is "IBM compatible" and thus has standard inter-record gaps with longitudinal as well as horizontal parity check bits. Tapes generated by incremental recording in the field can therefore be read at any standard digital computer facility which employs 7-track tape drives.

Software: The data acquisition system is controled by a real-time monitor whose master clock is a timing system capable of maintaining Universal Time within approximately ± 10 msec. The monitor allows considerable flexibility in the selection of a data format and makes possible on-line calculations during the substantial periods of time when the CPU is not actually controlling

the sampling and recording of incoming data.

Data acquisition is initiated after a number of questions have been properly answered on the teletype. An improper answer is not accepted by the CPU; in this case the question is repeated. Parameters thus provided to the CPU include the numbers of the active channels, the sampling rate for each channel (currently 4, 2 or 1 sample per sec), the length of a tape record in real time (we now use 60 sec), a four-character tape identifier, and a "GO" command which initiates sampling precisely on the first second of the next minute as read on the timing system. A header is written containing the information provided to the CPU, and Universal Time is encoded on each record. Data acquisition continues until the operator has set a sense-switch on the CPU or the end-of-tape marker is sensed. In either case an end-of file is written and the tape is rewound.

We are currently sampling 14 channels, each at 1 sample per sec. With a 60 sec data-record, a 2400 ft. roll of computer tape will last for three days.

Reformating Routines: The header record at the beginning of each file recorded by the TC-200 is used for control in all future processing. All S.M.U. programs are required to read the header record and the information contained therein is always output with the processed data. Thus, there can never by any confusion as to either the origin of a tape or of the period covered by the data or of the original channel allocations.

At the present time we are sampling all channels at a rate of 1 per second; thus a 60 sec output record has three time words followed by 60 scans of data. Each scan contains a 16 bit word for each channel selected and an error flag. At our computer laboratory the 16 bit words are reformated to 24 bit words for further processing. The twelve bits comprising the data and its sign are placed in the top half of the 24 bit word, and these data are then right shifted within the 24 bit word according to the gain information in the first four locations of the 16 bit word. Zeros are placed in any remaining location and the sign information expands to fill the beginning of the word.

A quality control program checks the header record information, the allocation of data channels and ~~checks for~~ parity and timing errors. In addition the program may be used to strip data from

a Raytheon field tape allowing a choice of channels and of start and stop times. The program also has an option for the removal of "glitches".

Routine quality control and all other programming is performed on an XDS 925 Computer. This computer has facilities for input from magnetic tape, paper tape, card reader or typewriter and can output to magnetic tape, line printer or Cal. Comp. plotter.

As data are stripped from a tape and rewritten they are blocked in a format called Tape IØ. The header record is written at the beginning of the tape and the channels are serially multiplexed in records 1025 words in length. The data take up 2^9 (1024) of these and the last word is used as an identification flag. The flag contains the channel number of the data block and the sequential number of the block within the present set of data. All subsequent S.M.U. programs check the flag for correct channel number and for the sequential numbering of the blocks.

Various routines are available which rewrite specified channels from the Tape IØ format, omit a specified number of points from each channel or test for dropouts. The basic plot routine for the Cal. Comp. plotter uses the Tape IØ format. The routine scans

the data for the maximum excursion along the ordinate and can remove any zero offset. All the data are then scaled to the maximum excursion for plotting, or, optionally, the data can be prescaled. One point is plotted on the abscissa every 0.01 inches, thus for an original sampling rate of 1 per second one inch on the abscissa represents 100 sec. Figure 3 is a typical plot of microbarograph data after it has been arranged in the Tape IØ format. The figures on the abscissa represent the ends of blocks of 1024 points, thus 3072 points or 3072 seconds (about 51 minutes) is shown in this figure.

Processing Routines: Various programs are available which perform routine analysis of data in the Tape IØ format. A digital filter can be computed which will high-pass, low-pass or band-pass the data as required. These filters form part of a program which will decimate the data by a given factor provided the information has been appropriately reblocked. The filtered and decimated data are then output in the Tape IØ format. Figure 4 shows microbarograph data from the three elements of a triangular array and the wind velocity and direction after decimation by a factor of 30. The abscissa now represents over 25 hours of data.

The more efficient methods of determining spectra and cross spectra of time series depend on the Fast Fourier transform algorithm (Cooley and Tukey, 1965). The data from any two time series are segmented, transformed into the frequency domain and then averaged (Welch 1967). The storage capability of the computer is not a limiting factor in this method and, thus, high resolution can be obtained with high confidence. The present program computes auto-and cross-spectra for any two of a number of channels and, as an option, an adjustment can be made for the frequency response of the system during the computation. Auto-power, cross-power, coherence and phase can be plotted if desired.

Array Processing Techniques: There are essentially two array processing techniques in use; one calculates frequency wave number spectra and the other forms beams for an array.

The first program calculates the wave number spectrum at a given frequency for multi-channel time series recorded by an array. The peak within the two-dimensional plot in wave number space is determined and from this the velocity and azimuth of the energy peak are calculated and output to the typewriter. A high resolution form of this program is available which reduce the side lobes of

the array response and sharpens the peaks in wave number space. A separate program computes the fast Fourier transform of the data.

The array beam steering program scans a sequence of azimuths for energy moving at a particular velocity by time shifting data from the elements of an array. If the energy in a beam is above a predetermined level a signal is said to have been detected. The use of a digital recursion filter (Shanks, 1968) allows the data to be "remembered" for a while and also reduces the computation time.

118

THE GRAND SALINE EXPERIMENT

As part of a cooperative project undertaken by Southern Methodist University and Geotech-Teledyne, a synoptic, seismic and infrasonic experiment was undertaken at the site of the Morton Salt Company's Grand Saline Mine about 60 miles east of Dallas. Infrasonic, long-period seismic and meteorological data were recorded on the TC-200 system and analyzed using the XDS 925 in the laboratory. Detailed results of this study are reported in Sorrells et al., (1971). The following paragraphs briefly describe the Grand Saline experiment which served as an extensive field test and a first practical application of the TC-200 data acquisition and processing system.

A 5km triangular geoacoustic array was established with the base station near the recording trailer at the Morton Salt Mine. The data from the two remote stations were transmitted by VHF-FM radio-telemetry and received at the recording trailer.

Two other microbarographs were placed so as to create an 0.3km triangular array. A sixth microbarograph was placed in the mine near three long period seismometers.

The microbarographs used in the experiments are NBS model N3 designed by the National Bureau of Standards and built by NBS

and by Geotech. These microphones measure pressure variations with reference to a known volume that is connected to the atmosphere by an acoustical resistance, a combination which determines the long period response of the microbarograph. The short period response is controlled by an acoustical capacitance, a fore-volume which is fixed, and an acoustical input resistance which can be varied. In these experiments the short period 3db point was placed at about 2 sec.

The remote microbarographs were housed in small trailers along with the VHF transmitting equipment. Use of a short hose allowed pressure fluctuations to be sampled outside the trailer. Those microbarographs close to the recording trailer were buried to increase the thermal stability of the backing and fore-volumes, and a 50 ft. piece of garden hose was connected to them in order to place the sampling point away from the microphone body.

An anemometer and a weather vane installed at a height of 4 m above the recording trailer provided a continuous monitor of the wind speed and direction.

The seismograph systems used in these experiments were designed, built and maintained by Geotech-Teledyne. They consisted of a seismometer with a free period of 20 seconds and a photo

tube amplifier using a galvonameter with a free period of 30 seconds. A combination of a 200 sec high-pass filter, a 60 sec low-pass filter and an operational amplifier effectly boosted the long period end of the response of the seismographs.

Considerable care was exercised in the installation of the seismometer systems to ensure that buoyancy and temperature effects were at a minimum. Both the vertical and horizontal seismometers were housed in steel cases which, in the case of the vertical seismometers, were tightly sealed. These cases acted as low pass acoustic filters which, according to the manufacturer's specifications, had a time constant of about 4 hours. The cases for the horizontal seismometers were left unsealed in order to avoid spurious tilts. The atmospheric pressure fluctuations were additionally attenuated by enclosing the seismometers in sealed 10 gauge steel tank vaults. The space between the instrument and the vault was filled with fiberglass. After sealing, the time constants of the vaults were found to be between 10 and 26 hours. A time constant of 10 hours indicates that at periods of less than 200 sec the pressure variations inside the vaults should be at least 3 orders of magnitude lower than the ambient pressure fluctuations.

/2/

During the first half of the Grand Saline operation electrical power was provided by the mining company. Later we changed to commercial power in order to improve recording reliability; any momentary loss of power caused the data acquisition system to halt until the program could be manually restarted. Overall, we were on site in an operational configuration for 200 days. Satisfacotry digital recordings were obtained for 80% of this period with the largest cause of dropouts being power failures. During the last 30 days of operation we visited the site only two or three times each week and had no backup in case of power loss or system component failure. In this period satisfactory records were obtained for 90% of the total time.

127

FUTURE DEVELOPMENT OF THE SYSTEM

We are in the process of adding multiply/divide electronics, a high-speed paper tape punch and reader, and an additional 4K, 16 bit words of core memory to the TC-200 acquistion sytem now located near Canton in East Texas. This new hardware will allow the development and testing of on-line, real-time programs which can significantly expedite the processing of infrasonic data. We expect to be able to run beam-steer program for an array on the Raytheon 703 while we are acquiring data. In addition, we can record on tape, in place of one of the 16 input channels, processed output which might be an array beam in a preset direction or in the direction in which the on-line, beam-steer routine last detected a significant amount of coherent energy crossing the array. Programs which may run in real time while the TC-200 is acquiring data are currently being simulated and tested on our XDS 925.

ACKNOWLEDGEMENTS

John L. Lobdell and Nancy Cunningham were responsible for the systems programming and for developing the Fortran programs described in this paper, and Karl D. Thomason was the engineer responsible for the field installation.

Five of the microbarographs are on loan from the National Bureau of Standards.

This research was supported by the Air Force Office of Scientific Research under Contract No. AFOSR F44620-68-C-0086-P002.

REFERENCES

Cooley, J. S. and J. W. Tukey, An algorithm for machine calculation of complex Fourier series, Math. Computation, 19, 297-301, 1965.

Shanks, J. L., Recursion filters for digital processing, Geophysics, 32, 1, 33-51, 1967.

Sorrells, G. G., J. A. McDonald, Z. A. Der and E. Herrin, Earth motions caused by local atmospheric pressure changes, this edition of Geophysical Journal.

Welch, P. D., The use of fast Fourier transforms for the estimation of power spectra: a method based on time averageing over short modified periodograms, Trans. IEEE, AU-15, 2, 70-73, 1967.

FIGURES

1. Block diagram of the TC-200 data acquisition system.

2. Photograph of the TC-200 data acquisition system.

3. An example of microbarograph data blocked in the Tape IØ format.

4. Three channel microbarograph and wind data after decimation by a factor of 30.

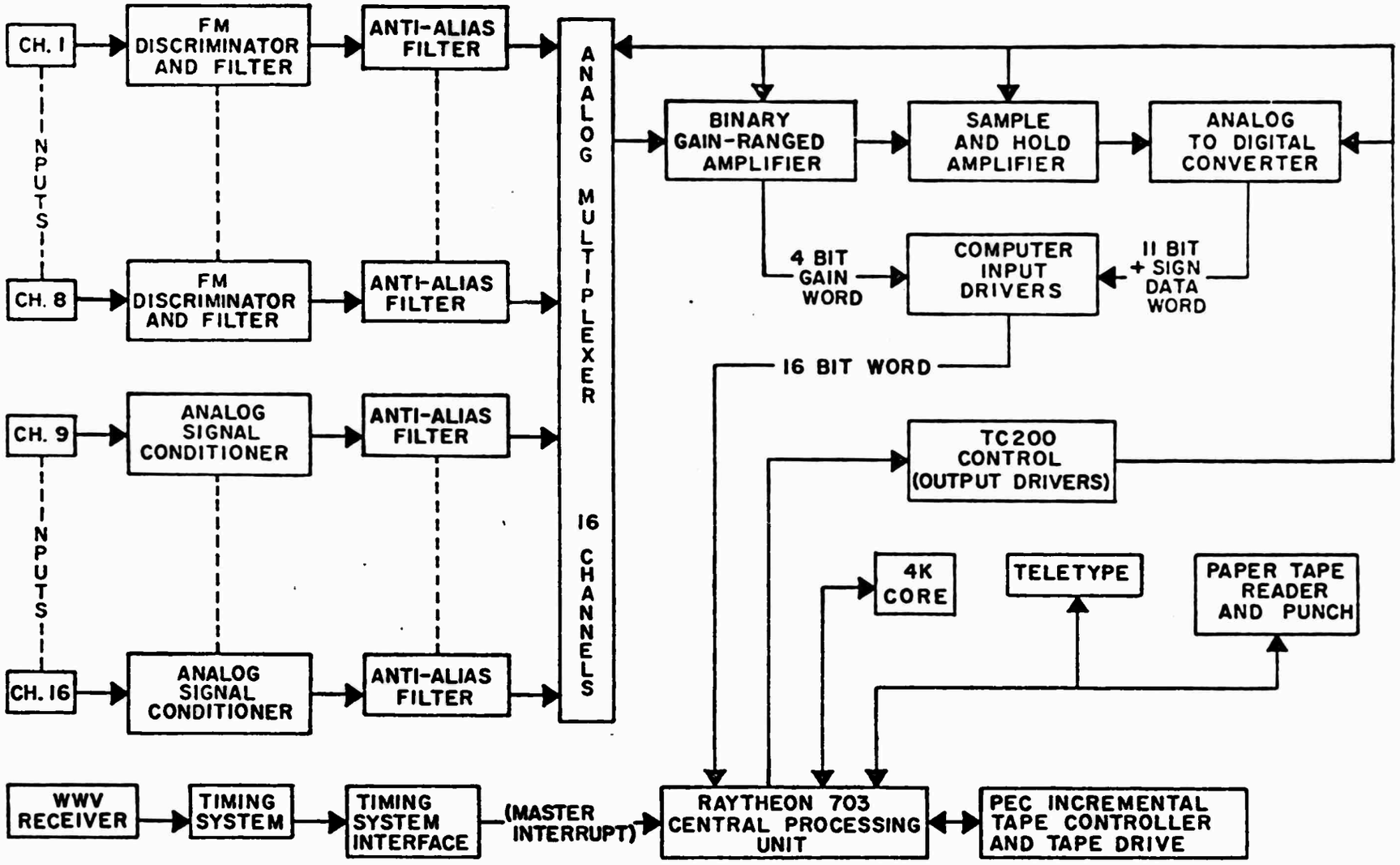

BLOCK DIAGRAM OF TC 200 DATA ACQUISITION SYSTEM

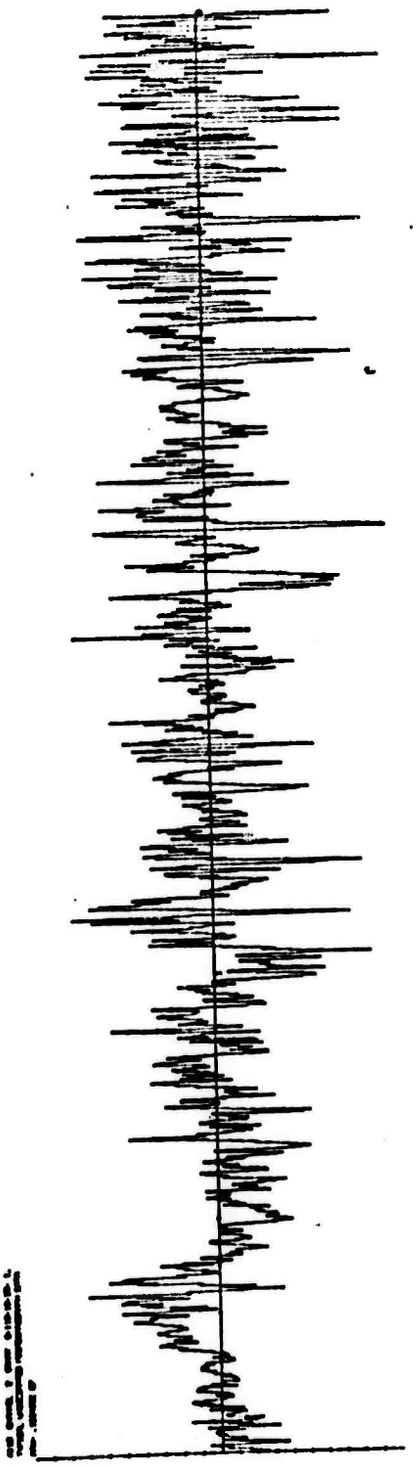

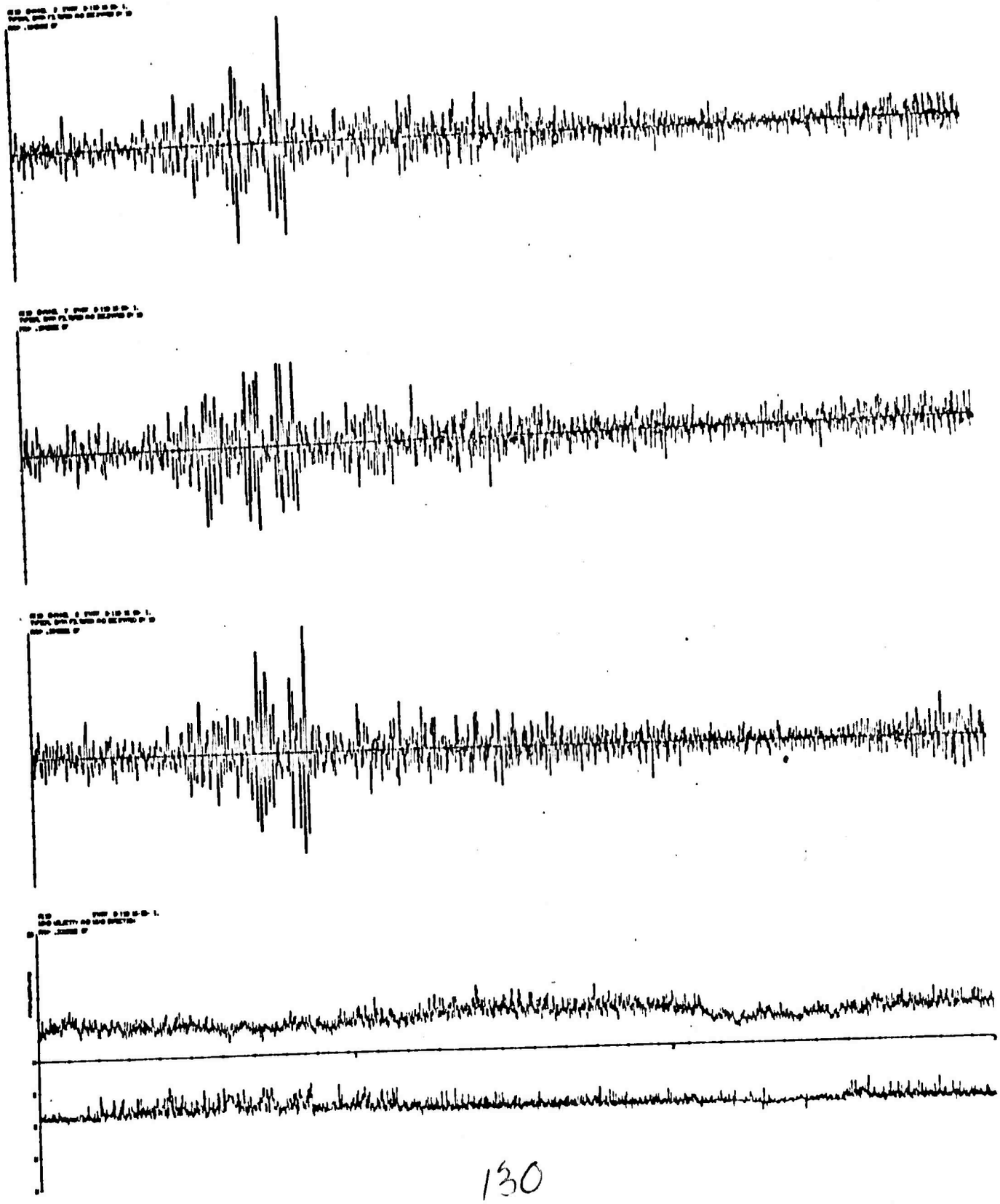

EARTH MOTION CAUDED BY LOCAL ATMOSPHERIC PRESSURE CHANGES

*G. G. Sorrells

*John A. McDonald

†Z. A. Der

*Eugene Herrin

(In press, Geophysical Journal R. A. S.)

January 1971

*Dallas Geophysical Laboratory
Southern Methodist University
Dallas, Texas 75222

†Teledyne-Geotech
3401 Shiloh Road
Garland, Texas 75040

ABSTRACT

Observations have been made of the local atmospheric pressure field and the long period seismic noise fields both on the surface of the earth and in a mine at a depth of 183 meters. The observations show that during windy intervals and in the period range 20-100 seconds there is a strong correlation between local atmospheric pressure changes and the noise recorded by a vertical seismograph located on the surface. In contrast over the same range of periods there is no correlation between the seismic noise recorded in the mine and local atmospheric pressure changes except during the passage of acoustic waves. It is shown that the noise in this pass band is not due to the buoyant response of the seismograph, but it is caused by the motion of the earth responding to atmospheric pressure changes.

INTRODUCTION

Since the earth is not a perfectly rigid body it must deform in response to atmospheric pressure changes. Theoretical studies (Khorosheva, 1958, Sorrells, 1971) indicate that given certain geological and meteorological conditions this deformation can constitute a significant fraction of the seismic noise power recorded with periods greater than 20 seconds. However, experimental evidence demonstrating that changes in the local atmospheric load can generate earth motion is sparse. Haubrich and MacKenzie (1965) have reported noise with periods greater than 100 seconds which they tentatively identify as earth motion caused by atmospheric gravity waves. More recently Capon (1969) found that the long period seismic noise field recorded at the Montana LASA often contains a non-propagating component which is apparently related to local atmospheric pressure variations. In the period range 20 to 40 seconds this component was responsible for 40% of the noise power 50% of the time. Unfortunately on the basis of the available evidence it was not possible to determine whether this noise was true earth motion or caused by buoyant effects within the seismograph. Observations by Sorrells and Der (1970) suffer from the same defect.

The purpose of this paper is to report the results of an experiment to measure the response of the earth to local changes in the atmospheric load. This experiment was performed at the Morton Salt Company mine near Grand Saline, Texas. Seismic and microbarometric data were recorded at a temporary observatory operated jointly by Southern Methodist University and Teledyne Geotech from May to mid August, 1970. The seismic data were recorded by two 3 component sets of long period seismographs installed at the surface and in the Morton Salt Co. mine. The vertical and horizontal distance between the two installations is shown in figure 1. Also shown in this figure are the relative positions of the microbarographs, the anemometer and the recording trailer. Data from the sensing systems were transmitted to a digital acquisition system housed in the recording trailer which sampled the observations at one second intervals, then recorded the results on magnetic tape. Details regarding the digital acquisition system, the microbarographs, and the seismographs are given by Herrin et al (1971). The average frequency response of the microbarographs and seismographs are shown in figure 2.

EXPERIMENTAL RESULTS

The results presented in this section are power spectral density and coherence estimates calculated from data recorded by the surface and mine vertical seismographs and the base microbarograph. The sample records used in the calculation are free of obvious earthquake signals. They were chosen to illustrate the noise levels observed during system noise tests, during calm and turbulent atmospheric conditions, and during the passage of an acoustic wave. All records are approximately 170 minutes long with the exception of those obtained during the passage of the acoustic wave which were 120 minutes long. The power spectral density estimates shown in the subsequent figures have been corrected for system response. They were calculated using a block averaging technique described by Welch (1967). Their stability at the 90% confidence level is ± 1.4 db for 170 minute records and ± 1.8 db for the 120 minute records. Squares of the estimated coherence which exceed 0.06 for the 170 minute records and 0.09 for the 120 minute records are significant at the 95% confidence level.

System noise: In figure 3-a we compare power spectral density estimates of the noise recorded in the mine during calm and

and windy periods with that observed during an interval when the seismometer was replaced by an equivalent resistance. This comparison demonstrates that sources within the system do not contribute significantly to the spectrum of the noise at periods less than about 200 seconds.

A similar comparison for data recorded at the surface is made in figure 3-b. The prominent difference between the noise levels observed during calm and windy periods will be discussed in some detail in the following paragraphs. The intent of this particular illustration is to demonstrate that even though the surface system noise is almost 12 dB greater than that observed in the mine its contribution to the total noise recorded at the surface can generally be neglected in a period range extending from about 5 to 150 seconds. It should also be pointed out that both system noise spectra were found to remain relatively constant despite extreme changes in meteorological conditions and the level of mining activity.

Calm Period: The results shown in figures 4-a through 4-d were calculated from data recorded during an interval when the mean wind speed was 3.1 meters/sec. As shown by the power

spectral density estimate plotted in figure 4-a the local atmospheric pressure field was relatively stable during this interval. In the period range 20-100 seconds the RMS amplitude of the pressure changes was found to be only 0.7 ubars. The spectral estimates of the seismic noise recorded at the surface and in the mine during this period are compared in figure 4-b. These results demonstrate that provided that the fluctuations in the local atmospheric pressure field are low, practically identical noise levels will be recorded at both locations. A prominent gap in the spectrum of the noise is observed to occur between the periods of 20 and 100 seconds. Within this range the RMS amplitude of the noise was found to be approximately 17 mu. It has been demonstrated by Molnar et al (1969) that the existence of this gap can have important implications with regard to the detection and identification of surface waves generated by low magnitude earthquakes and underground nuclear explosions.

The square of the estimated coherence between the noise recorded at the surface and in the mine is shown in figure 4-c. The strong coherence at 8 and 16 seconds is not surprising since most of the noise at these periods consists of fundamental mode

Rayleigh waves with wavelengths much greater than the distance separating the two seismographs. Note, however, that a significant degree of coherence is observed to exist out to periods on the order of 150 seconds. The source of the greater part of the noise beyond 20 seconds is unknown; however, estimates of the coherence between the data recorded by the base microbarograph and the two vertical seismographs which are shown in figure 4-d, suggest that a small fraction may be caused by local atmospheric pressure changes.

Windy Period: Power spectral density and coherence estimates calculated from data recorded during an interval when the mean wind speed was 7.8 meters/sec. are presented in figures 5-a through 5-d. Comparison of the spectral estimate shown in figure 5-a with that shown in figure 4-a shows that as the wind blows across the surface of the earth it creates relatively large fluctuations in the local atmospheric pressure field. In the period range 20-100 seconds the RMS amplitude of the pressure fluctuations was found to be 12 ubars or about 24 dB greater than that observed during calm periods. As shown in figure 5-b the increase in pressure variations is accompanied by an increase in the seismic noise observed at the surface relative to that observed in the mine. In

the period range 20-100 seconds it was found that during this interval the RMS amplitude of the noise recorded at the surface had increased to 54 mu while that observed in the mine remained at 1.7 mu. This amounts to a difference of about 10 dB between the noise levels recorded at the two locations. Comparison of the data displayed in figure 5-c with that shown in figure 4-c shows that during windy periods the coherence between the seismic noise recorded at the two locations is significantly reduced particularly in the period range 20-100 seconds. This result coupled with those shown in figure 5-b implies that during windy periods noise is added to the surface spectrum but not to the mine spectrum. The primary source of this noise may be inferred from the coherences between the base microbarograph and the two vertical seismographs which are shown in figure 5-d. Note that in the period range 20-100 seconds the seismic noise recorded at the surface is strongly coherent with variations in the local atmospheric pressure. In this passband 48% of the noise power is directly related to local pressure fluctuations and thus accounts for about 7dB of the 10dB increase in the surface noise level. In contrast there is no significant relationship between the seismic noise recorded in the mine and pressure variations at the surface.

Acoustic Waves: Spectral density and coherence estimates calculated from data recorded during the passage of an acoustic wave are shown in figures 6-a through 6-c. As shown in figure 6-a the fluctuations in the local atmospheric pressure field during this interval are larger than those observed during a calm period but are considerably smaller than those recorded during the windy period. The RMS amplitudes of the pressure variations in the period range 20-100 seconds during this interval was 2.4 ubars. Despite the relatively small fluctuations in atmospheric pressure it can be seen from the spectral estimates shown in figure 6-c that the seismic noise is quite high not only at the surface but in the mine as well. The RMS amplitude of the noise was found to be 73 mu at the surface and 52 mu in the mine. Estimates of the square of the coherence between local atmospheric pressure changes and the seismic noise recorded at both locations are shown in figure 6-c. These particular results were presented recently by Sorrells et al (1971) as evidence for earth movement accompanying acoustic waves. It can be shown with these data that within the period range 20-100 seconds 35% of the surface noise power and 62% of mine noise power is caused

by local atmospheric pressure changes. Thus the pressure fluctuations associated with the passage of an acoustic wave, despite their relatively small amplitudes, contribute significantly to the seismic noise recorded at both locations.

141

DISCUSSION OF RESULTS

From the results presented in the preceding section it is evident that during periods of atmospheric turbulence a pressure related component contributes significant energy to the seismograph system in the period range 20-100 seconds. The two most likely explanations for this phenomena are that either the vertical seismometer is responding buoyantly to pressure changes acting directly on the mass or the earth motion caused by local atmospheric pressure changes is large enough to be observed against the background of noise from other sources.

Buoyancy: It has been known for some time that vertical long period seismometers exposed to the atmosphere are quite sensitive to local pressure changes. This effect was described by Crary and Ewing (1952) who showed that the apparent vertical earth displacement W_a, caused by a sinusoidal pressure change of amplitude δp and frequency ω acting on the mass of the seismometer could be expressed by

$$W_a(\omega) = \frac{\rho_o g}{\rho_m p_o} \frac{\delta p}{\omega^2} \qquad (1)$$

where ρ_o is the density of the air, p_o is the ambient pressure, g is the local value of gravity and ρ_m is the density of the seismometer mass. The apparent earth motion in mu/ubar predicted by

this equation were calculated using parameters appropriate to our system and are listed as a function of increasing period in table 1, column 2. Notice that in the period range 20-100 seconds the apparent displacements increase from about 16 to 400 mu/ubar. Thus, unless steps are taken to isolate the vertical seismometer from the atmospheric pressure field, buoyant motion of the mass can be the primary source of noise in this period range.

In order to reduce possible buoyant effects the vertical seismometers used in the present experiment were placed in tightly sealed rigid steel cases which were then enclosed in sealed steel vaults. The time constant of the low pass acoustic filter formed by the seismometer case according to manufacturer tests was 14 hours. The time constants of the vaults were measured after the seismometers had been sealed inside; the minimum was found to be about 8 hours. The apparent displacement that an external pressure change would cause in a system consisting of a sealed vault and a sealed seismometer case is given by

$$|\bar{W}_a| = |R_v||R_c|\,W_a \qquad (2)$$

where $|R_v|$ and $|R_c|$ are the frequency responses of the acoustic filters formed, respectively, by the vault and the seismometer case. Both responses are of the form

$$|R(\omega)| = \left[1 + \left(\frac{\omega\tau}{2\pi}\right)^2\right]^{-1/2}$$

where τ is the time constant of the filter. In order to determine the direct contributions that external pressure fluctuations could make on the data recorded by the surface vertical seismograph, Eq 2 was used to predict the amplitudes for a system consisting of a vault with an 8 hour time constant and a case with a two hour time constant. The results are listed in column 3 of table 1. Observe that at periods less than 100 seconds the anticipated contribution is less than about 0.02 mu/ubar. The time constant of the vault containing the mine vertical seismograph was found to be approximately 24 hours. In addition, the mine itself acts as a low pass filter. At periods less than 100 seconds the pressure variations recorded in the mine were found to be greater than 20 dB below those observed at the surface. Thus, the direct effects of surface pressure variations on the mine vertical seismograph should be at least a factor of 30 below those anticipated for the surface system.

Theoretical studies of the response of the earth to the wind generated pressure field indicate that for rocks similar to those found at Grand Saline the vertical displacements should be of the order of a mu/ubar in the period range 20-100 seconds (Sorrells, 1971). Therefore, if the observed time constants accurately describe the pressure attenuateion characteristics of the vertical seismometer cases and vaults, the results listed in column 3, table 1, indicate that at periods less than 100 seconds the buoyancy contribution should be negligible in comparison to the anticipated earth motion caused by the wind generated pressure changes.

There is a more direct line of evidence bearing upon the buoyancy question. Suppose $|H(\omega)|$ is the frequency response of the unknown operator which relates local atmospheric pressure changes to one of the inputs to the

seismograph and suppose all other inputs are uncorrelated with local pressure changes then an estimate of the frequency response function may be obtained from

$$|\hat{H}(\omega)| = \frac{|\hat{R}_m(\omega)| \; |\hat{G}_{zm}(\omega)|}{|\hat{R}_z(\omega)| \; \hat{G}_m(\omega)} \tag{4}$$

where $|\hat{R}_m|$ and $|\hat{R}_z|$ are respectively the estimated frequency response functions of the microbarograph and the vertical seismograph; $\hat{G}_{zm}$ is the cross spectral density estimate between the outputs of the two systems and $\hat{G}_m$ is the power spectral density estimate of the output of the microbarograph. Eq 4 has been used to calculate $|\hat{H}(\omega)|$ from data recorded by the surface vertical seismograph and the base microbarograph. Examples of the responses calculated from data recorded during a windy period and during the passage of an acoustic wave are listed together with their respective 95% confidence limits in table 2. These results assume no errors in the estimated frequency response functions of the base microbarograph and the surface vertical seismograph. In order to account for errors of this type it is necessary to multiply both the estimated response and its confidence limits by the factor

$$\frac{1 + \epsilon_z}{1 + \epsilon_m} \tag{5}$$

where

$$\epsilon_z = \frac{|R_z| - |\hat{R}_z|}{|R_z|}$$

and

$$\epsilon_m = \frac{|R_m| - |\hat{R}_m|}{|R_m|} \tag{6}$$

Now generally speaking in the period range 20 to 100 seconds ϵ_z and ϵ_m probably do not exceed $\pm$ 0.1. Thus the actual values could be as much as

1.23 (+ 1.8 dB) times greater or 0.823 (- 1.8 dB) times less than those listed in table 2. In figure 7 we compare the experimentally determined functions with the buoyant responses of open and closed systems which were listed in table 1. It can be seen that the open system buoyant response lies well above the upper 95 percent confidence limits of both observed functions. From this, it may be inferred that at least one of the time constants is greatly in excess of 100 seconds. Therefore, if the observed functions are caused by the buoyant response of the vertical seismographs they should be increasing with increasing period at a rate of at least 18 dB/octave throughout the entire range of observation. However, a brief inspection of the experimental data is sufficient to demonstrate that a line with an 18 dB/octave slope cannot be fitted to either observed response and still remain within the 95% confidence limits for an appreciable range of values. This result strongly indicates that buoyancy does not contribute significantly to the observed results at periods less than 100 seconds. Finally, it can be seen that the response to atmospheric pressure changes caused by the acoustic wave is significantly greater than the response to pressure changes generated by the wind, at least over the period range from about 30-100 seconds. Even if we assume combined errors in the estimated instrument responses of -1.8 dB for the acoustic data and +1.8 dB for the windy period data there will still be no overlap of their respective 95% confidence regions in the period range 40-100 seconds. This observation is completely at odds with the buoyancy hypothesis since the response of a vertical seismometer to a pressure change acting directly on the mass must be same regardless of the cause of the pressure change. Therefore,

on the basis of the results presented in this section we conclude that the pressure related seismic disturbances observed during windy periods and during the passage of acoustic waves are not caused by the buoyant response of the vertical seismograph.

Elastic Deformation: Considerable experimental evidence exists which indicates that the pressure field created by the wind is spatially organized and tends to propagate at the mean wind speed (McDonald et al., 1971, Priestley, 1966, Cook and Young, 1962). On the strength of this evidence Sorrells (1971) suggested that, to a first approximation, the wind generated pressure field could be considered to be a plane wave propagating at the mean wind speed. Using this source an approximate solution was derived for the displacement frequency response of a homogeneous, elastic half space. An interesting property of the solution is that the dynamic response may be obtained from the static response by substituting $\frac{\omega}{c}$ for the static wave number k, where c is the speed of the pressure wave. This approximation is valid as long as

$$\omega z << \frac{2\beta^2}{c} \tag{5}$$

where z is the depth of observation and β is the shear wave velocity of the medium. A method for computing the static response of a

layered elastic solid is given in the Appendix. It has been used to obtain the displacement frequency response to a plane pressure wave using the substitution given above. Theoretical responses have been calculated for two models which approximate the geologic structure at and around the Grand Saline salt dome. The vertical distribution of velocities and densities assumed for the dome are shown in figure 8-a. The densities and layer thicknesses were taken from Peters and Dugan (1945). The velocities in the semi infinite layer are typical values reported for rock salt (Anderson and Liebermann, 1966). The compressional and shear wave velocities in the second layer, which approximates the limestone and anhydrite cap, were assumed to be 4.7 and 2.7 km/sec. The velocities in the upper layer are poorly determined. Data from a sonic log taken in a nearby well showed the compressional wave velocity to be 1.9 km/sec. at a depth of 183 meters and it is reasonable to assume that it is somewhat lower in the uppermost 78 meters. Cores from test wells at the mine indicate that this layer consists primarily of sandy clay with interbedded sand lenses. Measurements reported by Press (1966) show that the compressional velocity could be as low as 900 meters/sec for such a medium. We have assumed a compressional velocity of 1.4

km/sec and a shear wave velocity of 0.475 meters/sec for the upper layer. The apparently high value of Poisson's ratio (0.43) has been observed in similar rock types (Press, 1966).

The vertical distribution of seismic velocities and densities in the earth surrounding the dome are approximated by the model shown in figure 8-b. The structure down to 88 meters is the same as that shown in figure 8-a. Below that depth down to 4000 meters, the compressional velocities and thicknesses were determined from a sonic log taken some 5 miles from the recording site. The shear wave velocities were calculated from the compressional wave velocities under the assumption that Poisson's ratio was 0.33. Likewise the densities were calculated from the compressional wave velocities assuming a linear relationship between the two quantities. The compressional and shear wave velocities used for the semi infinite layer below 4000 meters were 6.2 km/sec and 3.56 km/sec. The corresponding density was assumed to be 2.65 g/cm^3.

In figure 8-c, we compare the windy period response listed in table 2 with theoretical responses calculated for the two models. The mean wind speed during the interval of observation was 8.0 meters/sec.

Note that the response for the salt dome model (figure 8-a) agrees quite well with the experimental results particularly at the longer periods. The response at the shorter periods is controlled by the structure above the cap rock. The difference between the observed and calculated values suggests that the structure in this region is considerably more complex than was assumed in the construction of the model. It should also be noted this model predicts that the earth displacements created by the pressure changes will be substantially reduced at a depth of 183 meters. At a period of 100 seconds the earth motion should be 26 dB below that observed at the surface. At the shorter periods the attenuation is seen to be even greater reaching a value of about 50 dB at a period of 20 seconds. This phenomenon accounts for the absence of a pressure related component in the noise recorded in the mine during windy periods.

In figure 8-d we compare experimental frequency responses estimated from acoustic wave data with theoretical responses calculated from the well log model assuming a velocity of 330 meters/sec. The theoretical responses are seen to provide a relatively good fit to the observed data at periods greater than 40 seconds.

The response calculated from seismic data recorded at the surface runs consistently lower than its theoretical counterpart, but at periods greater than 40 seconds the maximum difference amounts to only 3db. This could be caused by an error in the estimated gain of the vertical seismograph. At periods less than 40 seconds both observed frequency responses depart systematically from the theoretical responses. The cause of this departure is not known at the present time.

The close agreement between observed and calculated frequency responses shown in figures 8-c and 8-d lead us to conclude that most of the noise observed during windy periods and during the passage of acoustic waves is earth motion in response to slowly propagating pressure waves.

CONCLUSIONS

It can be concluded from the results presented in the previous sections that during windy intervals earth motion caused by the turbulent pressure field can contribute substantially to the noise recorded at the surface within the period range 20-100 seconds. Most of this noise can be eliminated by placing the detector several hundred meters below the surface. Acoustic waves and, by inference, other relatively fast moving atmospheric disturbances can also generate earth motion which will contribute significantly to the noise in this pass band even though the perturbations they produce in the local atmospheric pressure field are relatively small. The attenuation of earth noise from these sources is potentially a more serious problem because it will not decay rapidly with depth. However, disturbances of this type with periods on the order of 20-100 seconds may not occur often enough to constitute a major noise source. More study in this particular area is obviously required.

APPENDIX

METHÓD OF COMPUTATION OF TWO-DIMENSIONAL DEFORMATION CAUSED BY SINUSOIDAL LINE LOADS

The theory is based on the extension of results described by Sneddon (1951) for two-dimensional deformation of elastic solids, the Fourier transform G of the Airy stress function with respect to the horizontal coordinate x_1 is satisfied by the equation

$$\left(\frac{d^2}{dx_3^2} - k^2 \right)^2 G = 0 \qquad (1)$$

where k is the horizontal wave number, x_3 is the vertical co-ordinate. This equation has the general solution

$$G = (A + Bx_3)e^{-|k|x_3} + (C + Dx_3)e^{|k|x_3} \qquad (2)$$

The Fourier transforms of t'e stresses and displacements can be derived from this equation the following way

$$U = \frac{1+\sigma}{E}\left[\frac{\sigma-1}{k^2}\frac{d^3G}{dx_3^3} - (2-\sigma)\frac{dG}{dx_3} \right]$$

$$V = i\frac{1+\sigma}{E}\left[(1-\sigma)\frac{d^2G}{dx_3^2} + \sigma k^2 G \right]\frac{1}{k} \qquad (3)$$

$$\tau_{33} = -k^2 G$$

$$\tau_{13} = ik\frac{dG}{dx_3}$$

where u, v, t_{33}, t_{13} are the vertical and horizontal displacements, normal and shear stresses at the surface, respectively, os is the Poisson ratio, E is the Young's modulus of the elastic media.

For a layered medium consisting of homogenous isotropic layers the solution (2) can be propagated by the Thompson-Haskell matrix method where A, B, C, and D take the place of the sums and differences of constants A'_m, A''_m, Δ'_m, Δ''_m in Haskell's paper. The matrix which is equivalent of Haskell's D_m for this boundary value problem can be obtained by substituting 2 into 3. It takes the form, D_m =

$$\begin{vmatrix} \frac{1+\sigma_m}{} & 0 & 0 & 0 \\ 0 & i\frac{1+\sigma_m}{E_m} & 0 & 0 \\ 0 & 0 & 1 & 0 \\ 0 & 0 & 0 & 1 \end{vmatrix} \begin{vmatrix} |k| & 1+|k|d_m-2\sigma_m & -|k| & i-kd_m-2\sigma_m \\ -|k| & k^d_m+2\sigma_m-2 & |k| & |k|^d_m-2\sigma_m+2 \\ -k^2 & -k^2d_m & -k^2 & -k^2d_m \\ -k^2 & |k|(1-|k|d_m) & k^2 & -|k|(1-|k|d_m) \end{vmatrix} \begin{vmatrix} e^{-kd_m} & 0 & 0 & 0 \\ 0 & e^{-kd_m} & 0 & 0 \\ 0 & 0 & e^{kd_m} & 0 \\ 0 & 0 & 0 & e^{kd_m} \end{vmatrix}$$

155

where d_m is the layer thickness, E_m and σ_m are the elastic constants for layer m.

This matrix relates the vector of displacements and stresses to the vector of displacements and stresses to the vector of coefficients A, B, C and D in the following way in layer m

$$(u_m, v_m, {}_m\tau_{33}, {}_m\tau_{13}) = D_m (A_m, B_m, C_m, D_m)$$

In the halfspace below the layers C and D must vanish in order to have decreasing displacements and stresses with depth. The rest of the algebra is analogous to that given by Haskell, (1953).

Many other algorithms for the computation of static deformation in layered solids with more general geometric distribution of stresses are given in the literature (Kuo, 1969, Ben Menahem, and Singh, 1968).

A computer program LOAD 2 has been written for the calculation of the displacements and tilts. The program computes the responses of the layered medium to sinusoidal stresses at the surface as functions of wavelength and depth. Both normal and shear stresses can be applied. The program reads the densities, the stresses and seismic velocities of the layers, and the range of horizontal wave numbers at the surface. It is a simple matter to

use the program to compute the static deformation of the layered medium due to stresses of arbitrary shape by Fourier synthesis of sinusoidal loads. The same program can be used to compute strains due to surface stresses at any depth.

In case of random pressure fields the power spectrum of the tilt response and the cross spectrum between the tilt and the pressure variations can be estimated by integrating the output of this program in the plane of the horizontal wavenumbers k_1 and k_2.

Some numerical problems can arise if the displacements are computed for greater depths using large wave numbers; after reading the value near zero at a certain depth the displacements start to increase without bound with increasing depth. The problem is purely numerical and is similar in nature to that encountered in surface wave calculations (Dunkin 1965). It can be remedied by double precision calculations or the elimination of the large (and obviously erroneous) displacement values below a certain depth.

The matrix algebra is analogous to that presented by Haskell (1953). The program has been checked out against formulas derived by Sorrells (1971) and several other examples in the literature.

ACKNOWLEDGEMENTS

The authors would like to thank S. Montoya and H. Gautreaux of Teledyne Geotech for their valuable assistance during this project. The success of the experiment was, largely, due to their continuous and careful efforts to keep the seismographs operating at peak efficiency. Karl D. Thomason provided valuable engineering assistance and John L. Lobdell and Nancy Cunningham were responsible for most of the systems programming.

The research would not have been possible without the help and cooperation of the management and staff of the Morton Salt Company. We would like to thank Ray Rucker and Joe Clements of the management in particular.

Five of the microbarographs were on loan from the National Bureau of Standards.

The research was carried out during the tenure of a National Aeronautics and Space Administration Traineeship by one of us (J. A. M.), and was supported by the Air Force Office of Scientific Reasearch under Contract No. 67-041-14C.

REFERENCES

Anderson, O. L. and R. C. Liebermann, 1966, Sound velocities in rocks and minerals, VESIAC State-of-the-Art Report 7885-4-x, Willow Run Laboratories, Inst. of Science and Technology, Univ. of Michigan, Ann Arbor, Michigan, 182 p.

Ben Menahem, A. and S. T. Singh, 1968, Multipolar elastic fields in a layered half space: Bull. Seis. Soc. Am., Vol. 58, p. 1519-1572.

Capon, J., 1969, Investigation of long period noise at the large aperture seismic array: Jour. Geophys. Res., Vol. 74 pp. 3812-3194.

Cook, R. K. and J. M. Young, 1962, Strange sounds in the atmosphere: Part II, Sound, Vol. 1, p. 25-33.

Crary, A. P. and M. Ewing, 1952, On a barometric disturbance recorded on a long period seismograph: Trans. A.G.U., Vol. 33, p. 499-502.

Dunkin, J. W., 1965, Computation of modal solutions in layered elastic media at high frequencies: Bull. Seis. Soc. Am., Vol. 55, p. 335-358.

Haskell, N. A., 1953, The dispersion of surface waves on multilayered media: Bull. Seis. Soc. Am., Vol. 43, p. 17-43.

Haubrich, R. A. and G. S. MacKenzie, 1965, Earth noise 5-500 millicycles per second. 2 Reaction of the earth to oceans and the atmosphere: Jour. Geophys. Res., Vol. 70, p. 1429-1440.

Herrin, E. T., G. G. Sorrells and J. A. McDonald, 1971, a digital acquisition system for geophysical data and some preliminary results: (in preparation).

Khorosheva, V. V., 1958, Effect of the atmospheric pressure on the tilting of the earth's surface; Izv. Akad. Nauk SSR Ser. Geofiz. No. 1, p. 77-79.

Kuo, J. T., 1969, Static response of a multilayered medium under inclined surface loads: Jour. Geophys. Res., Vol. 74, p. 3195-3207.

McDonald, J. A., E. J. Douze, and E. Herrin, 1971, The structure of atmospheric turbulence and its application to the design of pipe arrays (submitted to Geophys. Jour. Royal Astron. Soc.).

Molnar, P., J. Savino, L. Sykes, R. Liebermann, G. Hade, P. Pomeroy, 1969, Small earthquakes and explosions in western North America recorded by new high gain long period seismographs: Nature, Vol. 224, p. 1268-1273.

Peters, J. W. and A. F. Dugan, 1945, Gravity and magnetic observations at the Grand Saline salt dome, Van Zandt Co., Texas: Geophysics, Vol. 10, p. 376-393.

Press, F., 1966, Seismic velocities in Handbook of Physical Constants Geol. Soc. Am. mem. 97, edited by S. P. Clark, Jr., p. 195-218.

Priestley, J. T., 1966, Correlation studies of pressure fluctuations on the surface beneath a turbulent boundary layer, N.B.S. Rept. 8942, U.S. Dept of Commerce, National Bureau of Standards.

Sneddon, I. N., 1951, Fourier transforms: McGraw-Hill, New York, p. 402-406.

Sorrells, G. G., 1971, A preliminary investigation into the relationship between long period seismic noise and local fluctuations in the atmospheric pressure field, Geophys. Jour. Royal Astron. Soc. (in press).

Sorrells, G. G. and Z. A. Der, 1970, Long period seismic noise and atmospheric pressure variations: Tech. Rept. 70-12, Teledyne Geotech, Garland, Texas, 61 p.

Sorrells, G. G., J. A. McDonald and E. Herrin, 1971, Ground motions associated with acoustic waves: Nature (in press).

Welch, P. D., 1967, The use of fast Fourier transforms for the estimation of power spectra: a method based on time averaging over short modified periodograms: Trans. I.E.E.E. AU-12, Vol. 2, p. 70-73.

160

FIGURE CAPTIONS

1. The microbarograph and seismograph installations at the Morton Salt Co. mine near Grand Saline, Texas.

2. The average frequency responses of the microbarograph and seismograph systems. For the digital system used in this experiment there are 0.838×10^6 counts per volt into a 10k ohm input impedance.

3. A comparison of the power spectral density estimates calculated from data recorded during calm and windy periods, and during equivalent resistance tests. (a) Data recorded in the mine. (b) Data recorded at the surface. The small vertical bar appearing in the lower right hand corner of these and subsequent figures indicates the expected spread of the estimates at the 90% confidence level.

4. Data recorded during a calm interval; wind speed 3 m/sec or less (a) Power spectral density estimate of the noise recorded by the base microbarograph. (b) A comparison of the power spectral density estimates of the noise recorded by the two vertical seismographs. (c) The square of the estimated coherence between the noise recorded by the two vertical seismographs. (d) The square of the estimated coherence between the base microbarograph and each seismograph.

5. Data recorded during a windy period; mean wind speed 7.8 m/sec. (a) Power spectral density estimate of the noise recorded by the base microbarograph. (b) A comparison of the power spectral density estimates of the noise recorded by the two vertical seismographs. (c) The square of the estimated coherence between the noise recorded by the two vertical seismographs. (d) The square of the estimated coherence between the base microbarograph and each seismograph.

6. Data recorded during the passage of an acoustic wave (a) Power spectral density estimate of the noise recorded by the

base microbarograph. (b) A comparison of the power spectral density estimates of the noise recorded by the two vertical seismographs. (c) The square of the estimated coherence between the base microbarograph and each seismograph.

7. A comparison of predicted buoyant frequency responses with experimentally determined responses calculated from data recorded during a windy interval and during the passage of an acoustic wave. The open system buoyant response is proportional to the square of the period. The closed system buoyant response in the period range shown is proportional to the 4th power of the period.

8. (a) The estimated velocity and density structure of the Grand Saline salt dome. (b) The estimated velocity and density structure of the sediments surrounding the Grand Saline salt dome. (c) A comparison of observed and calculated frequency responses for a windy period. The solid dots represent the estimated frequency response. The solid lines are theoretical displacement frequency responses of the models shown in figures 9a and 9b to a plane pressure wave propagating at a speed of 8 m/sec. (d) Comparison of observed and calculated frequency responses for period characterized by the passage of an acoustic wave. The speed of the wave is assumed to be 330 m/sec.

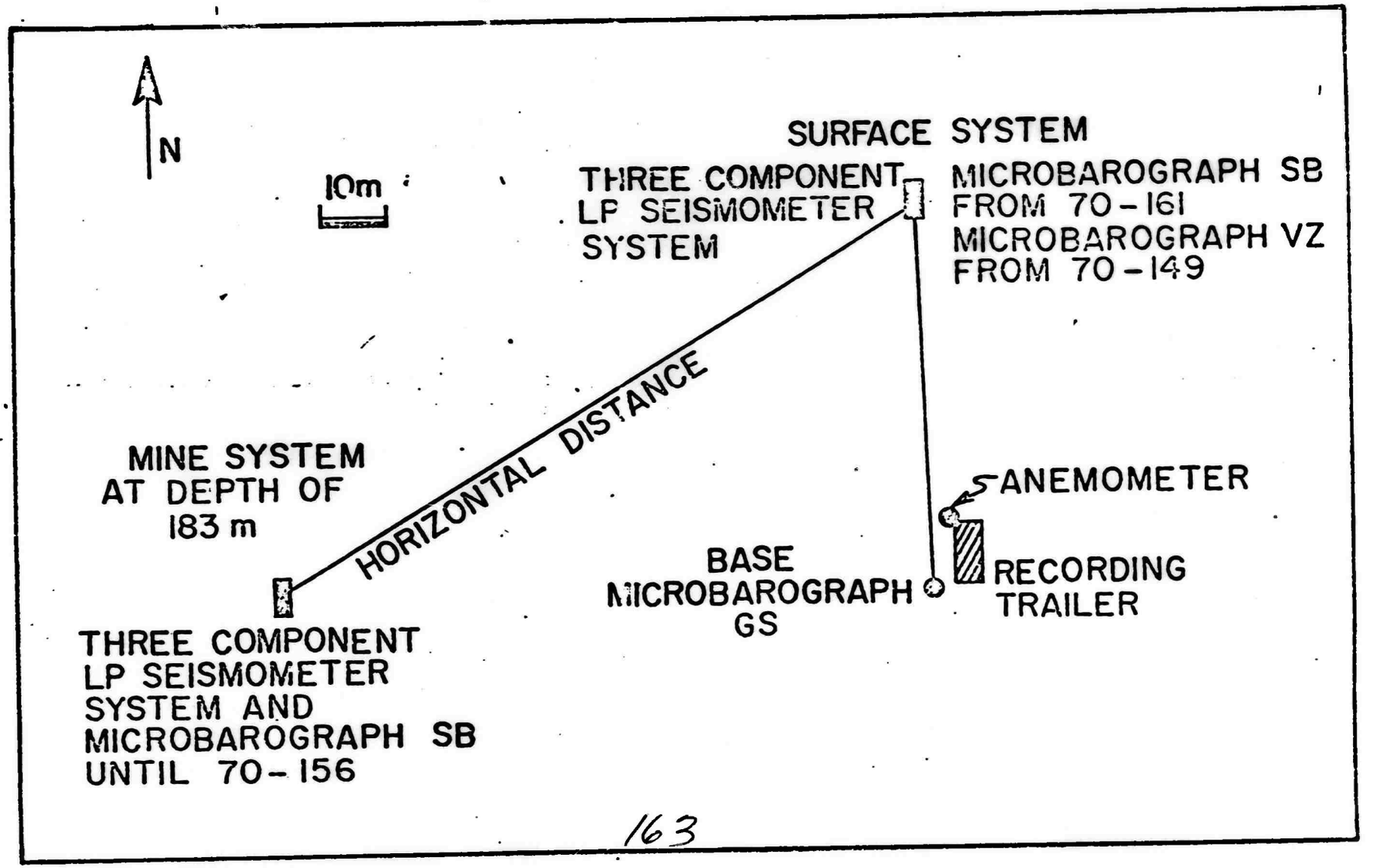
N
10m
SURFACE SYSTEM
THREE COMPONENT
LP SEISMOMETER
SYSTEM
MICROBAROGRAPH SB
FROM 70-161
MICROBAROGRAPH VZ
FROM 70-149
HORIZONTAL DISTANCE
MINE SYSTEM
AT DEPTH OF
183 m
ANEMOMETER
BASE
MICROBAROGRAPH
GS
RECORDING
TRAILER
THREE COMPONENT
LP SEISMOMETER
SYSTEM AND
MICROBAROGRAPH SB
UNTIL 70-156

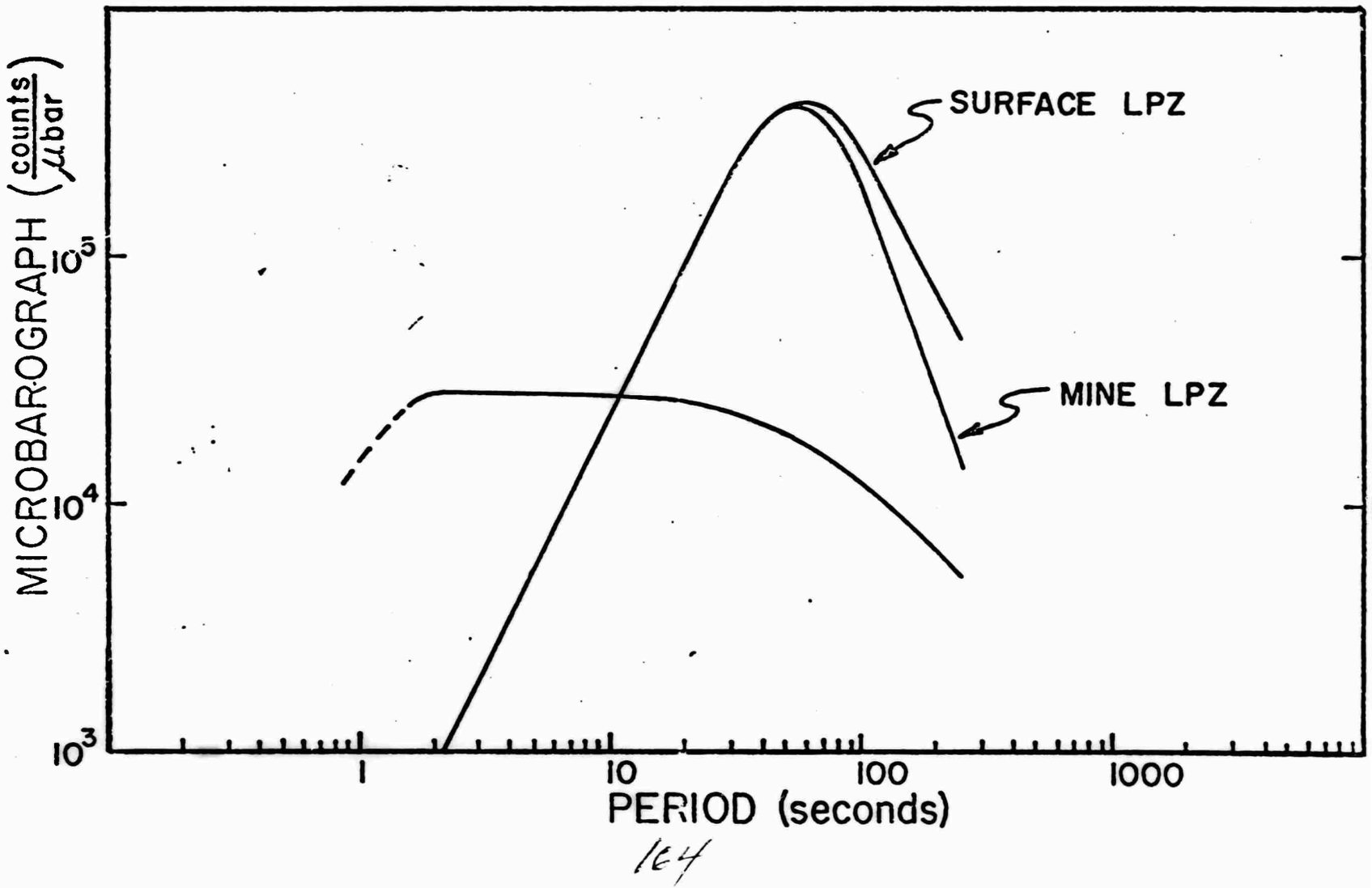
MICROBAROGRAPH (counts/μbar)
10^5
10^4
10^3
SURFACE LPZ
MINE LPZ
1
10
100
1000
PERIOD (seconds)

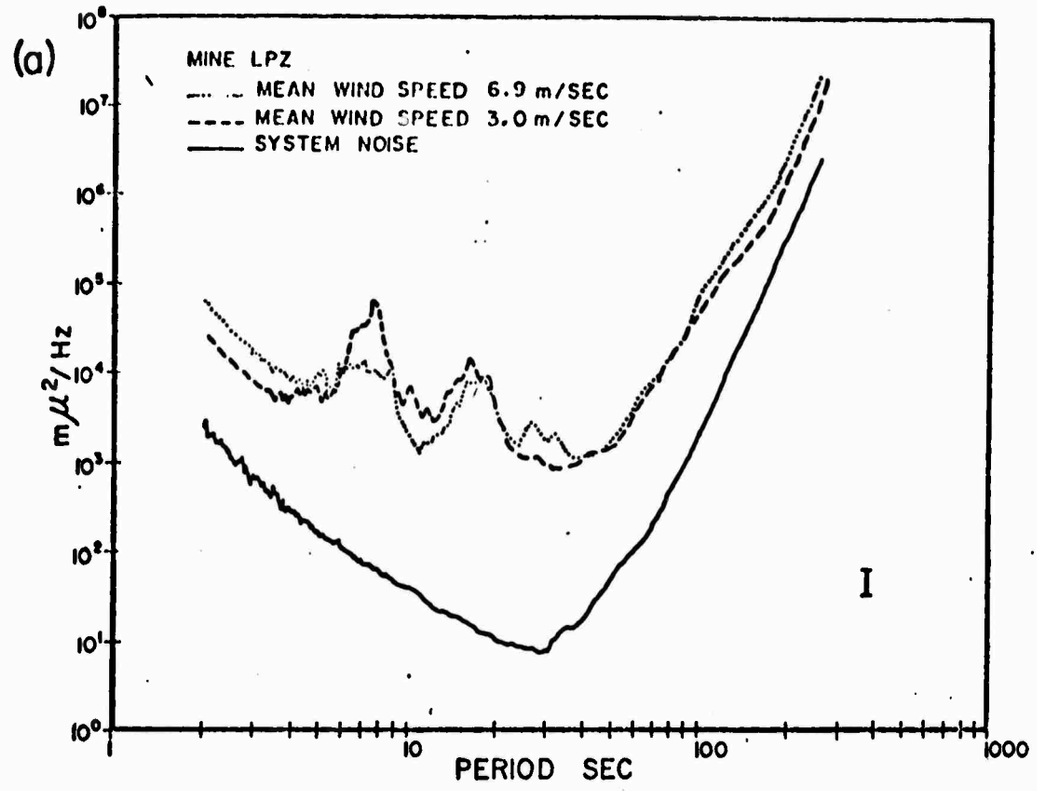
(a)
MINE LPZ
MEAN WIND SPEED 6.9 m/SEC
MEAN WIND SPEED 3.0 m/SEC
SYSTEM NOISE
$m\mu^2/Hz$
10^8
10^7
10^6
10^5
10^4
10^3
10^2
10^1
10^0
I
1
10
100
1000
PERIOD SEC

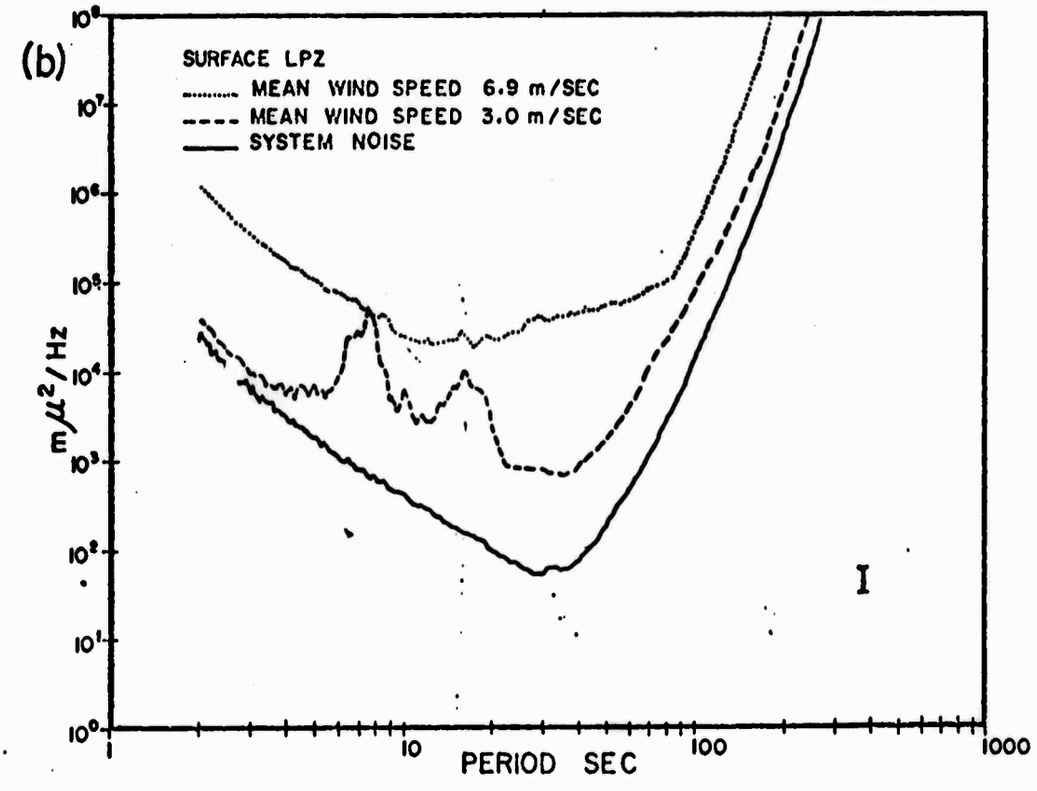
(b)
SURFACE LPZ
MEAN WIND SPEED 6.9 m/SEC
MEAN WIND SPEED 3.0 m/SEC
SYSTEM NOISE
$m\mu^2/Hz$
10^8
10^7
10^6
10^5
10^4
10^3
10^2
10^1
10^0
I
1
10
100
1000
PERIOD SEC

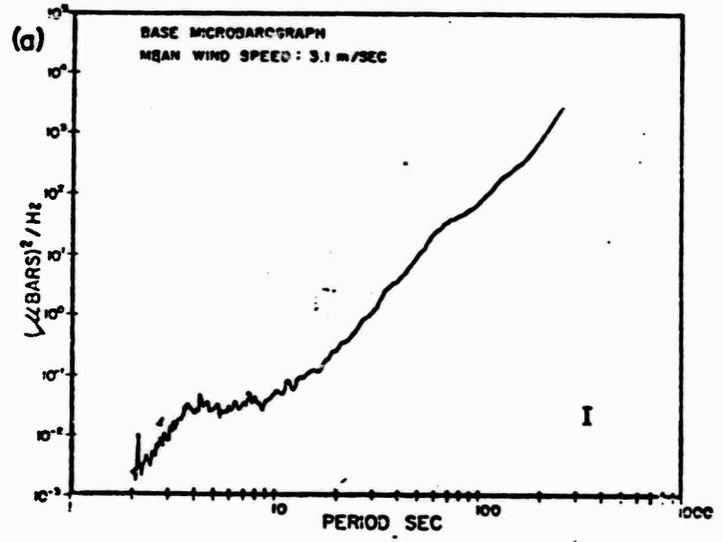
(a)
BASE MICROBAROGRAPH
MEAN WIND SPEED : 3.1 m/SEC
(μBARS)² / Hz
PERIOD SEC
I

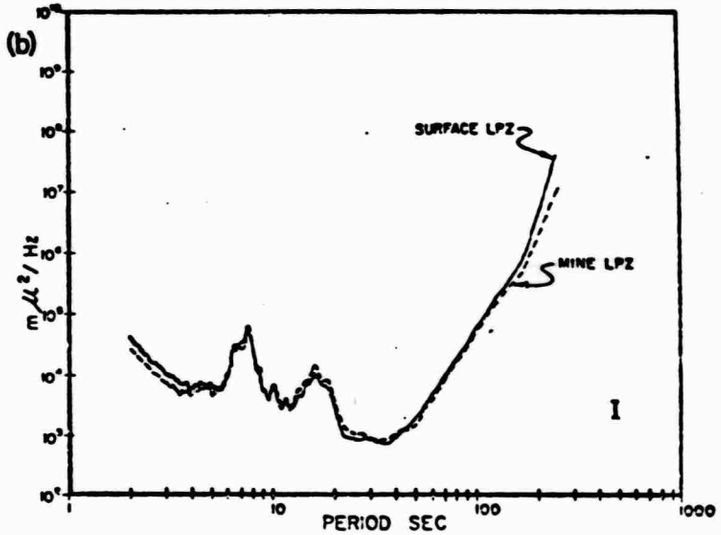
(b)
SURFACE LPZ
MINE LPZ
mμ² / Hz
PERIOD SEC
I

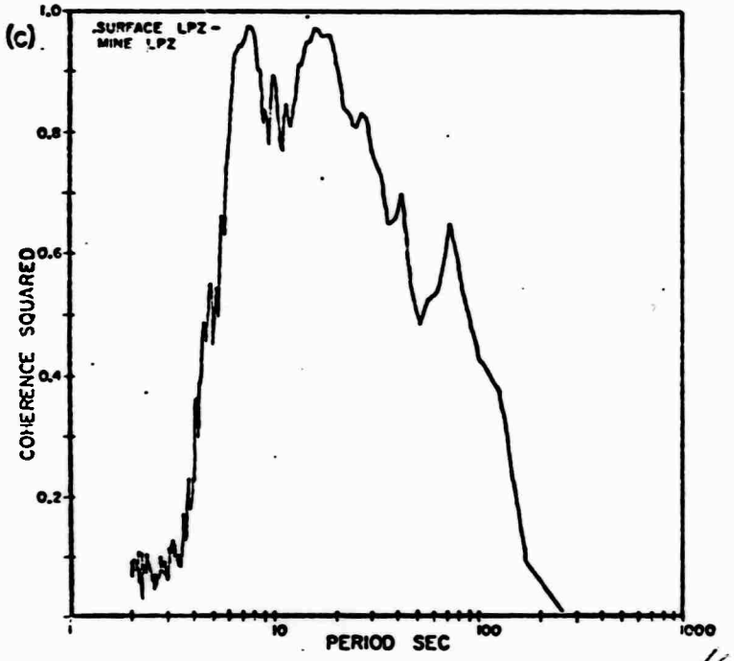
(c)
SURFACE LPZ -
MINE LPZ
COHERENCE SQUARED
PERIOD SEC

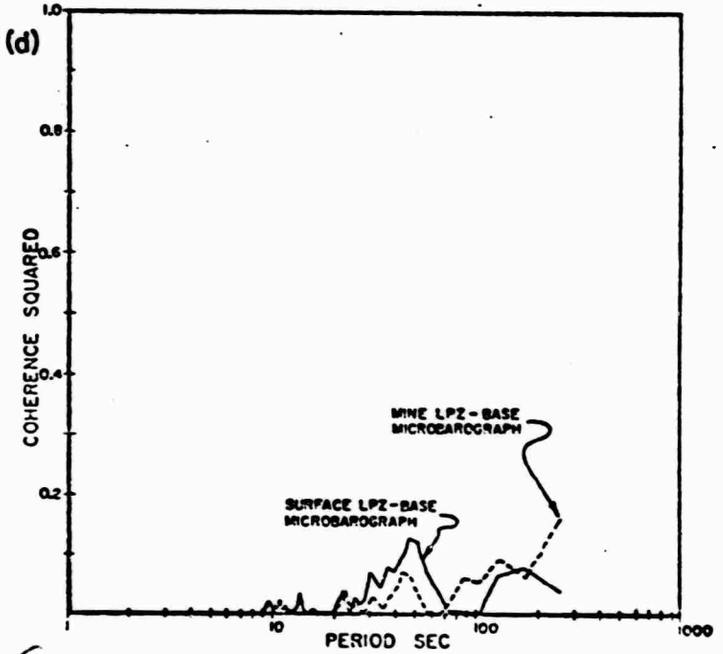
(d)
MINE LPZ - BASE
MICROBAROGRAPH
SURFACE LPZ - BASE
MICROBAROGRAPH
COHERENCE SQUARED
PERIOD SEC

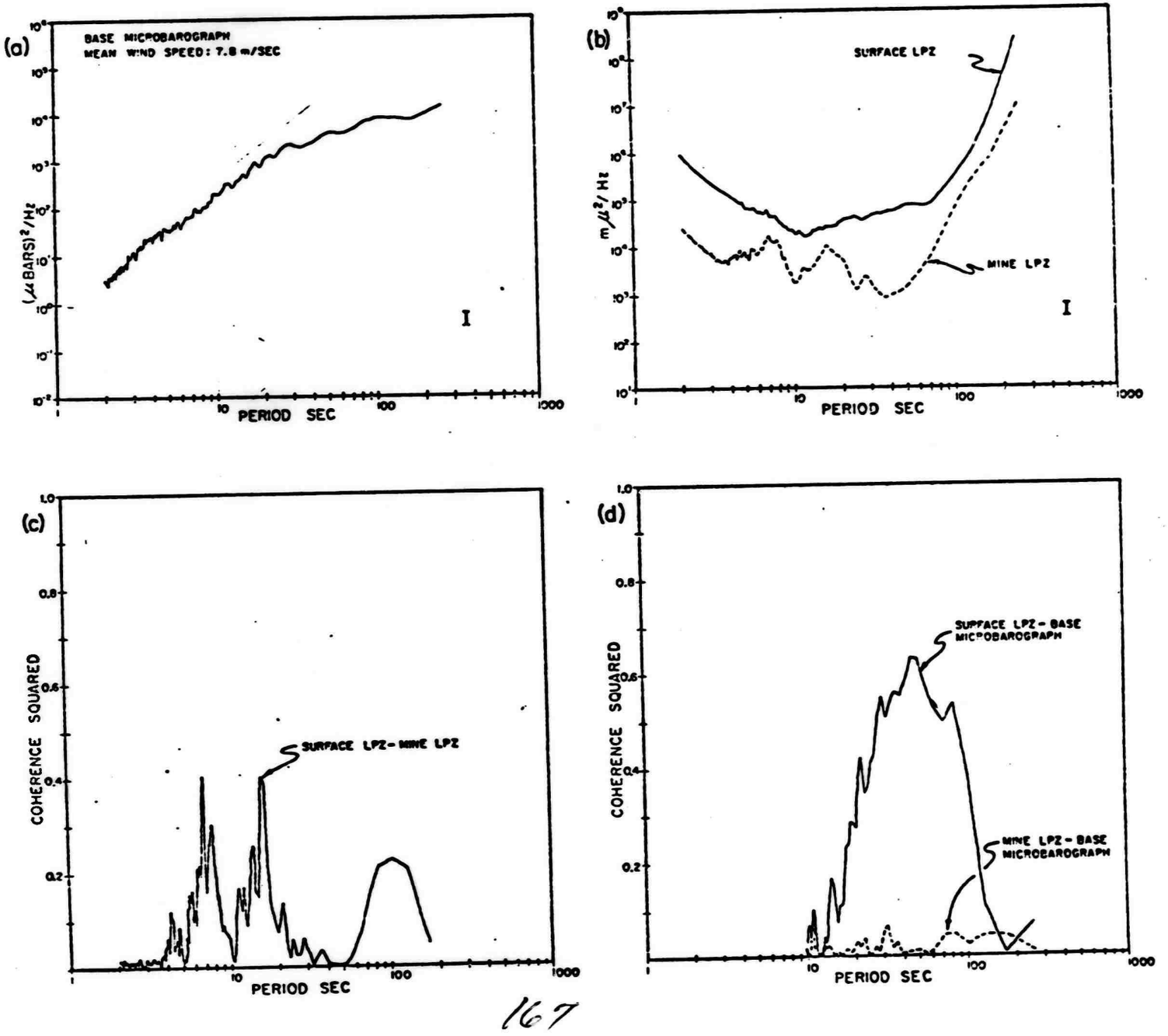
(a)
BASE MICROBAROGRAPH
MEAN WIND SPEED: 7.8 m/SEC
(μBARS)²/Hz
PERIOD SEC
I
(b)
SURFACE LPZ
MINE LPZ
m/μ²/Hz
PERIOD SEC
I
(c)
COHERENCE SQUARED
SURFACE LPZ - MINE LPZ
PERIOD SEC
(d)
COHERENCE SQUARED
SURFACE LPZ - BASE MICROBAROGRAPH
MINE LPZ - BASE MICROBAROGRAPH
PERIOD SEC

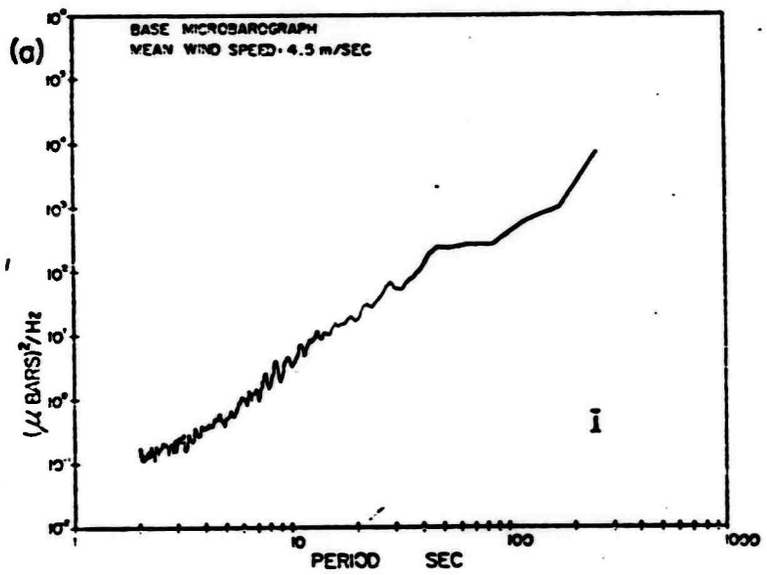
(a)
BASE MICROBAROGRAPH
MEAN WIND SPEED - 4.5 m/SEC
(μ BARS)²/Hz
PERIOD SEC
1
10
100
1000

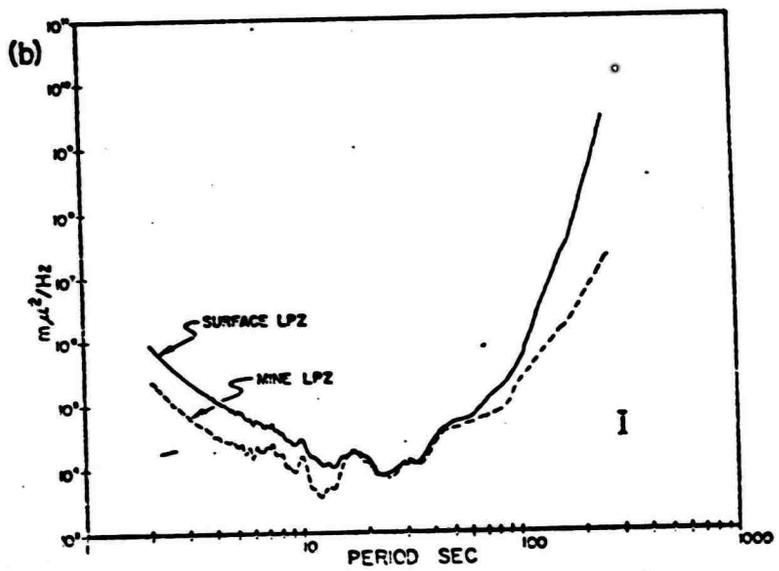
(b)
SURFACE LPZ
MINE LPZ
mμ²/Hz
PERIOD SEC
1
10
100
1000

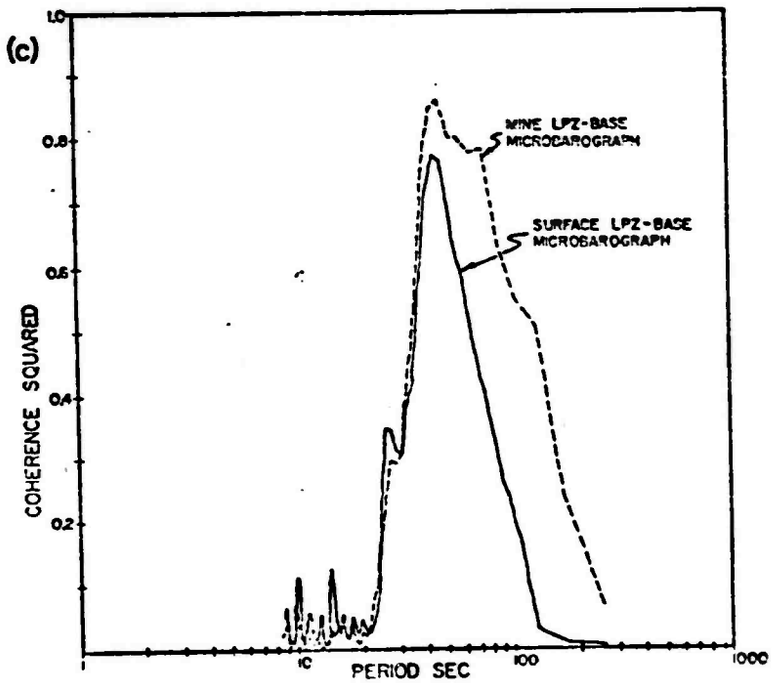
(c)
MINE LPZ-BASE MICROBAROGRAPH
SURFACE LPZ-BASE MICROBAROGRAPH
COHERENCE SQUARED
0.2
0.4
0.6
0.8
1.0
PERIOD SEC
1
10
100
1000

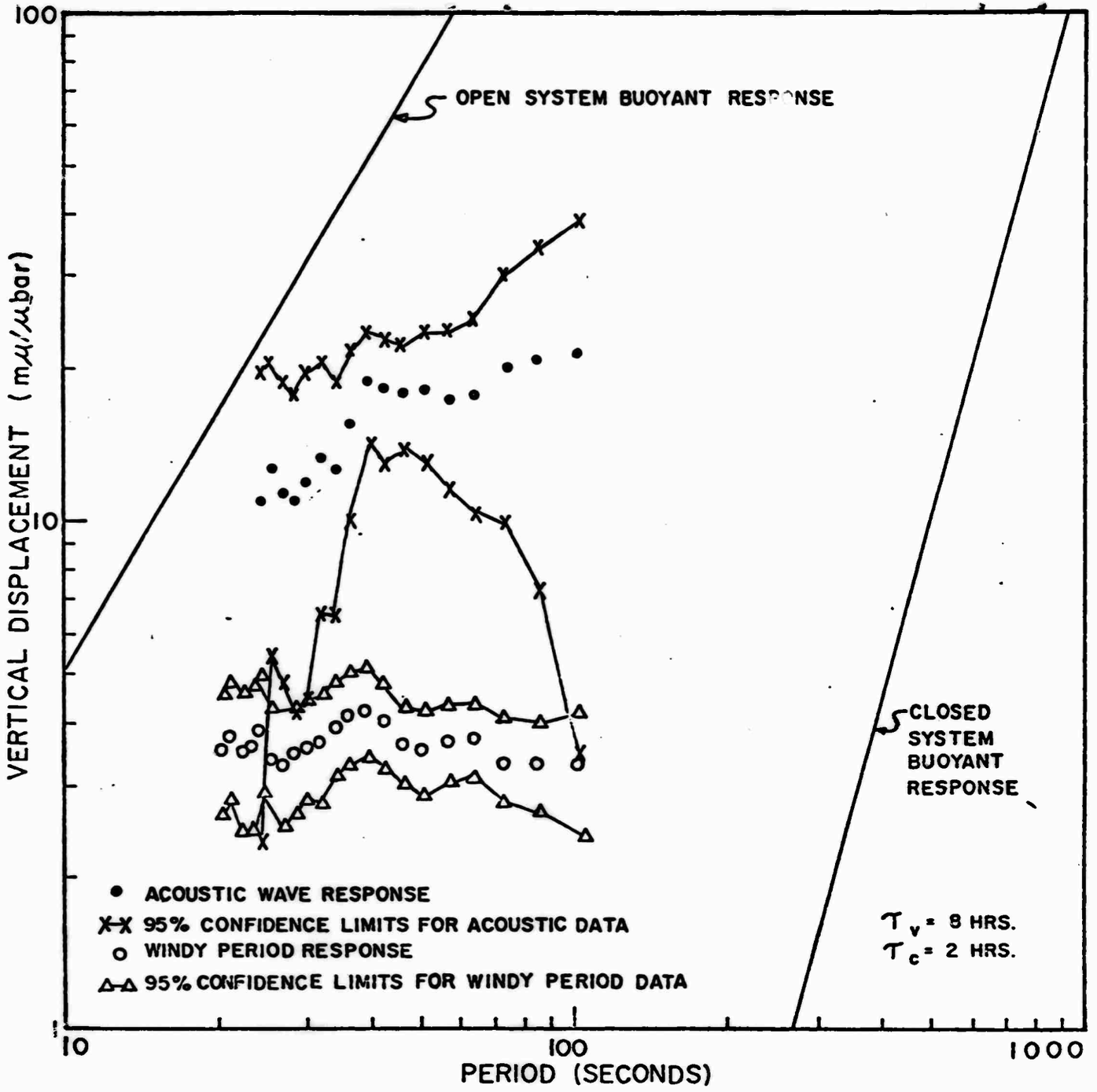
100
10
1
VERTICAL DISPLACEMENT (mμ/μbar)
OPEN SYSTEM BUOYANT RESPONSE
CLOSED SYSTEM BUOYANT RESPONSE
ACOUSTIC WAVE RESPONSE
95% CONFIDENCE LIMITS FOR ACOUSTIC DATA
WINDY PERIOD RESPONSE
95% CONFIDENCE LIMITS FOR WINDY PERIOD DATA
τ_v = 8 HRS.
τ_c = 2 HRS.
10
100
1000
PERIOD (SECONDS)

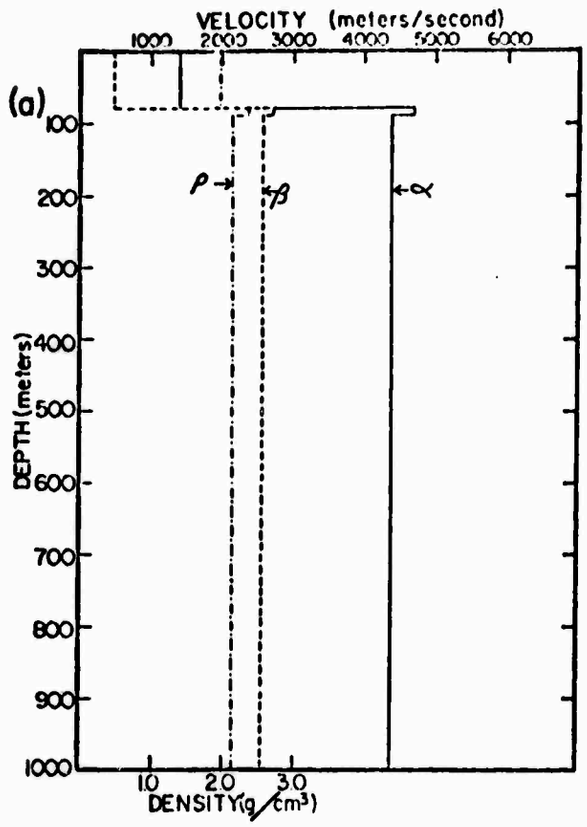
(a)
VELOCITY (meters/second)
1000 2000 3000 4000 5000 6000
DEPTH (meters)
100 200 300 400 500 600 700 800 900 1000
ρ
β
α
1.0 2.0 3.0
DENSITY (g/cm³)

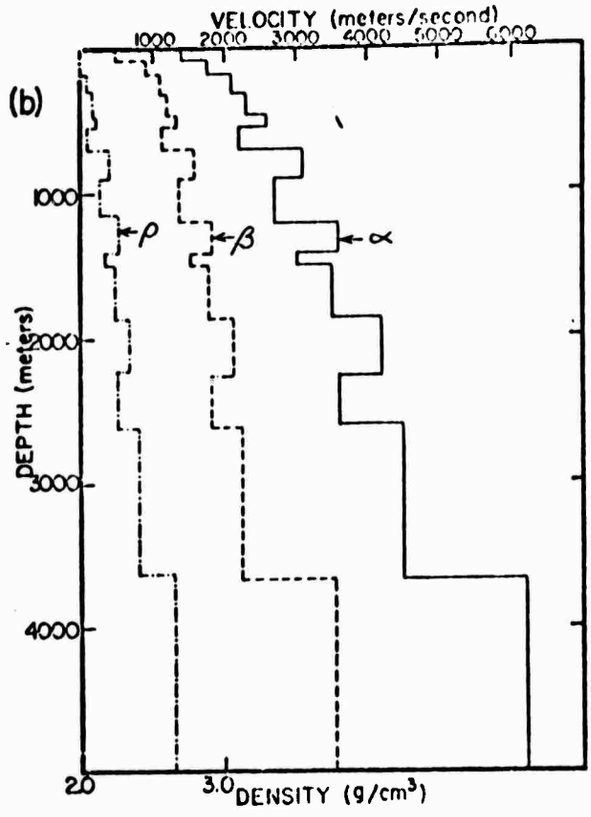
(b)
VELOCITY (meters/second)
1000 2000 3000 4000 5000 6000
DEPTH (meters)
1000 2000 3000 4000
ρ
β
α
2.0 3.0
DENSITY (g/cm³)

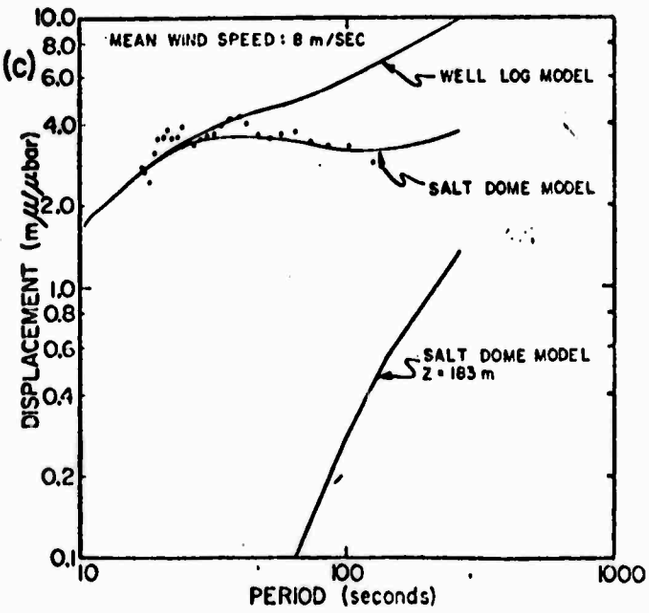
(c)
MEAN WIND SPEED: 8 m/SEC
WELL LOG MODEL
SALT DOME MODEL
SALT DOME MODEL Z = 183 m
DISPLACEMENT (mμ/μbar)
10.0 8.0 6.0 4.0 2.0 1.0 0.8 0.6 0.4 0.2 0.1
10 100 1000
PERIOD (seconds)

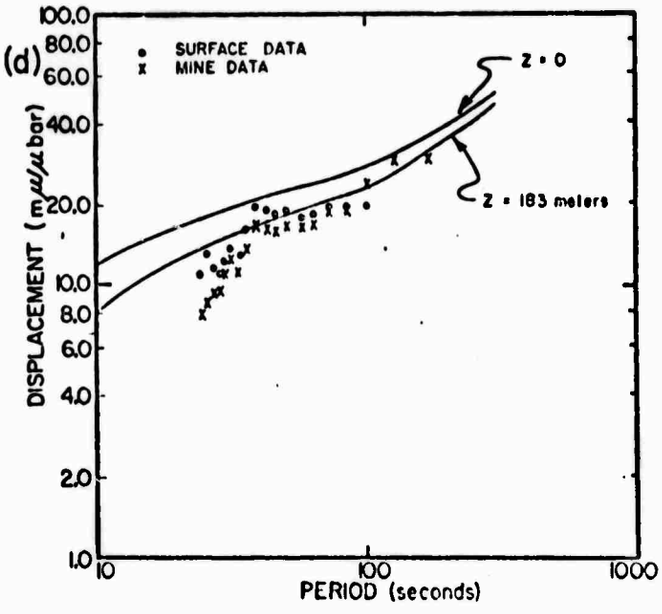
(d)
SURFACE DATA
MINE DATA
Z = 0
Z = 183 meters
DISPLACEMENT (mμ/μbar)
100.0 80.0 60.0 40.0 20.0 10.0 8.0 6.0 4.0 2.0 1.0
10 100 1000
PERIOD (seconds)

Table 1. The buoyant response of a vertical seismograph

Period (seconds)	Buoyant Response Open system mμ/μbar	*Closed system mμ/μbar
10	3.92	1.89×10^{-6}
20	15.68	3.02×10^{-5}
30	35.28	1.53×10^{-4}
40	62.72	4.84×10^{-4}
50	98.00	1.18×10^{-3}
60	141.12	2.45×10^{-3}
70	192.08	4.54×10^{-3}
80	250.88	7.74×10^{-3}
90	317.52	1.24×10^{-2}
100	392.00	1.89×10^{-2}
120	564.48	3.92×10^{-2}
140	768.32	7.26×10^{-2}
160	1003.52	1.24×10^{-1}
180	1270.08	1.98×10^{-1}
200	1568.00	3.02×10^{-1}

* The closed system response is calculated under the assumption that the seismometer is enclosed in a sealed case and vault which have time constants of 2 and 8 hours, respectively.

Table 2. Estimated Frequency Response

A Windy Period Data*

Period (Seconds)	Estimated response mu/ubar	95% Confidence Interval	
		Upper limit mu/ubar	Lower limit mu/ubar
20.5	3.59	4.65	2.56
21.3	3.86	4.89	2.83
22.3	3.56	4.66	2.46
23.3	3.62	4.76	2.48
24.4	3.96	5.00	2.92
25.6	3.48	4.39	2.57
26.9	3.38	4.25	2.51
28.4	3.56	4.41	2.71
30.1	3.66	4.51	2.81
32.0	3.70	4.62	2.78
34.1	4.00	4.88	3.12
36.6	4.18	5.03	3.33
39.4	4.30	5.17	3.43
42.7	4.06	4.83	3.29
46.5	3.70	4.37	3.03
51.2	3.60	4.29	2.91
56.9	3.73	4.39	3.07
64.0	3.78	4.40	3.14
73.1	3.47	4.13	2.81
85.3	3.36	4.05	2.67
102.4	3.34	4.26	2.42

* The estimated response given above was calculated from 9 hours of data recorded at 3 hour intervals when the mean wind speed was 8.0 ± 0.2 meters/sec. The equivalent degrees of freedom for the calculation are 168.

Table 2. (Continued)

B Acoustic Wave Data*

Period (Seconds)	Estimated response mu/ubar	95% Interval	
		Upper limit mu/ubar	Lower Limit mu/ubar
20.5	0.0+	-	-
2.3	0.0+	-	-
22.3	0.0+	-	-
23.3	0.0+	-	-
24.4	11.0	19.7	2.3
25.6	13.0	20.5	5.5
26.9	11.5	18.2	4.8
28.4	11.0	17.8	4.2
30.1	12.1	19.7	4.5
32.0	13.5	20.6	6.4
34.1	12.7	18.9	6.5
36.6	15.8	21.6	10.0
39.4	19.1	23.4	14.5
42.7	18.6	22.8	14.4
46.5	18.1	22.3	13.9
51.2	18.5	24.0	13.0
56.9	17.5	23.5	11.0
64.0	17.9	25.4	10.4
73.1	20.4	30.8	10.0
85.3	21.1	34.8	7.4
102.4	21.5	39.5	3.5

* The estimated response given above was calculated from 2 hrs of data. The equivalent degrees of freedom for the calculation are 39.

+ Not significantly different from zero at the 95% confidence level.